

The Network for the Detection of Atmospheric Composition Change at 35 Years: Achievements and Future Strategy.

Irina Petropavlovskikh^{1,2}, Martine De Mazière³, Anne M. Thompson^{4,5}, Jeannette D. Wild^{6,7}, James W. Hannigan⁸, Henry B. Selkirk⁹, Reem A. Hannun¹⁰, Wolfgang Steinbrecht¹¹, Jean-Christopher Lambert³, Roeland Van Malderen¹², Elizabeth Asher^{1,2}, Raul R. Cordero^{13,14}, Sophie Godin-Beekmann¹⁵, Daan Hubert³, Sergey Khaykin¹⁵, Karin Kreher¹⁶, Thierry Leblanc¹⁷, Emmanuel Mahieu¹⁸, Eliane Maillard Barras¹⁹, Glen McConville^{1,2}, Gerald Nedoluha²⁰, Ivan Ortega⁸, Alberto Redondas Marrero²¹, Gunther Seckmeyer²², Ryan M. Stauffer⁴, Sarah A. Strode^{4,23}, Kim Strong²⁴, Takafumi Sugita²⁵, Michel Van Roozendael³, Voltaire Velazco¹¹, Corinne Vigouroux³, Bärbel Vogel²⁶

¹CIRES, University of Colorado, Boulder, CO USA

²NOAA, Global Monitoring Lab, Boulder, CO, USA

³Royal Belgian Institute for Space Aeronomy (BIRA-IASB), Brussels, Belgium

⁴Atmospheric Chemistry and Dynamics Laboratory, NASA Goddard Space Flight Center, Greenbelt, MD, USA

⁵University of Maryland, Baltimore County, Baltimore, MD, USA

⁶Earth System Science Interdisciplinary Center (ESSIC/CISESS), University of Maryland, College Park, MD, USA

⁷NOAA/NESDIS/Center for Satellite Applications and Research (STAR), College Park, MD, USA

⁸National Center for Atmospheric Research, Boulder, CO, USA

⁹Agile Decision Support, NASA Headquarters, Washington, DC USA

¹⁰Atmospheric Science Branch, NASA Ames Research Center, Moffett Field, CA USA

¹¹Deutscher Wetterdienst - German Weather Service, Hohenpeissenberg, Germany

¹²Royal Meteorological Institute of Belgium, Solar-Terrestrial Centre of Excellence, Uccle, Belgium

¹³RUG, University of Groningen, Wirdumerdijk 34, 8911 CE Leeuwarden, The Netherlands

¹⁴USACH, Universidad de Santiago de Chile. Av. Bernardo O'Higgins 3363, 9170022 Santiago, Chile.

¹⁵LATMOS/IPSL, CNRS, Sorbonne Université, UVSQ, Paris, France

¹⁶BK Scientific GmbH, Mainz, 55130, Germany

¹⁷Jet Propulsion Laboratory, California Institute of Technology, Wrightwood, California, USA

¹⁸Department of Astrophysics, Geophysics and Oceanography, UR SPHERES, University of Liège, Liège, Belgium

¹⁹Federal Office of Meteorology and Climatology MeteoSwiss, Payerne, Switzerland

²⁰Remote Sensing Division, Naval Research Laboratory, Washington, DC, USA

²¹Izaña Atmospheric Research Center, Agencia Estatal de Meteorología, 38001 Santa Cruz, Tenerife, Spain

²²Leibniz University of Hannover/Institute of Meteorology, 30419 Hannover, Germany

²³Morgan State University, GESTAR-II, Baltimore, MD, USA

²⁴Department of Physics, University of Toronto, Toronto, ON, Canada

²⁵National Institute for Environmental Studies (NIES), Tsukuba, Ibaraki, Japan

²⁶Institute of Climate and Energy Systems (ICE-4), Forschungszentrum Jülich, Jülich, Germany

Correspondence to Irina Petropavlovskikh (irina.petropavlovskikh@colorado.edu), Anne Thompson (amt16@psu.edu), Martine DeMaziere (martinedemazi@gmail.com)

Abstract. Since 1991, continuous, consistently calibrated and openly archived ground-based measurements from the Network for the Detection of Atmospheric Composition Change (NDACC) have been collected to investigate processes

45 responsible for decadal-scale changes, anomalies in atmospheric composition, and to validate satellite observations and
46 model simulations. These measurements, from nearly 120 stations, support fundamental research in the area of
47 stratospheric and tropospheric processes impacting ozone chemistry, greenhouse gases, atmospheric radiative forcing,
48 air quality, and interactions with solar radiation and the entire Earth system. NDACC data are supplemented by
49 observations from eleven global Cooperating Networks. The operational principles of Cooperating Networks are well
50 aligned with NDACC objectives and protocols, focusing on data that (a) are high-quality, uniformly processed and
51 traceable to reference standards; and (b) capture short-term (daily to interannual) anomalies and long-term trends. This
52 paper summarizes the NDACC organizational structure. We also review the major accomplishments of NDACC since
53 De Mazière et al. (2018), collaborative research with Cooperating Networks, and interactions with the satellite and
54 modeling communities. Ground-based atmospheric composition monitoring is at a crossroads. Challenges include
55 sustainability of human and financial resources required for complex and intensive data collection, technical issues
56 including aging instrumentation, requirements for FAIR (findable, accessible, interoperable, reusable) data, and lack of
57 data over large parts of Asia, Africa and South America. NDACC is well-positioned to adopt a three-pronged strategy
58 going forward: protecting and modernizing existing stations; promoting the growing use of NDACC data; expanding the
59 number of measured species and network coverage in under-sampled or under-reporting regions.

60

61 **1 Introduction**

62 As an integral part of the global observing system, the overriding goal of the Network for Detection of Atmospheric
63 Composition Change (NDACC) has been to collect and maintain high-quality ground-based data – both remote-sensing
64 and *in situ* – in order to detect changes and trends in atmospheric composition and to understand the impacts of these
65 changes on the mesosphere, stratosphere, and troposphere. NDACC first emerged as the Network for Detection of
66 Stratospheric Change (NDSC) in the late 1980s and became operational in 1991 (Kurylo et al, 2016). The network was
67 given its present title in 2006, reflecting research support beyond the stratosphere. The network extended selected
68 measurements into the mesosphere to understand its chemical and physical state as well as into the troposphere to study
69 processes impacting air quality and the climate.

70 As the network extended its vertical domain, NDACC’s objectives expanded and are currently:

- 71 ● Establish long-term databases to detect changes and trends in atmospheric composition and to understand their
72 impacts on mesosphere, stratosphere and troposphere;
- 73 ● Establish scientific links and feedbacks among changes in atmospheric composition, climate, and air quality;
- 74 ● Validate and merge atmospheric measurements from other platforms (i.e., satellites, aircraft and ground-based
75 platforms);
- 76 ● Provide critical data sets to help fill gaps in satellite observations;
- 77 ● Provide collaborative support to scientific field campaigns and to other chemistry and climate-observing networks;
- 78 ● Provide validation and development support for atmospheric models;
- 79 ● Contribute to assessments of the state of the atmosphere (WMO/UNEP, IGAC, IPCC, etc.).

80 The last objective was added in 2024, following the recognition of its importance as a fundamental contribution to the
81 NDACC since its establishment.

82 De Mazière et al. (2018) provided a brief history of the network, reviewed major accomplishments during its first 25
83 years of operation, and discussed recent developments and challenges. Their paper emphasized that NDACC must update
84 its capabilities as new data needs arise. They highlighted developments that could enable NDACC to meet its objectives
85 going forward. In the eight years since *De Mazière et al. (2018)* the need for the network enhancements has become
86 urgent. *Salawitch et al. (2025)* described a train of unexpected geophysical events, both natural and human-induced, that
87 have led to substantial anomalies in stratospheric composition. They point out that our understanding of the scale, extent,
88 and timing of these disturbances was made possible by robust, comprehensive global-scale observations by the
89 Microwave Limb Sounder (MLS) on the Aura satellite and the Atmospheric Chemistry Experiment-Fourier Transform
90 Spectrometer (ACE-FTS) on SCISAT since the early 2000s. However, our global scale capability to observe upper
91 atmospheric composition will be drastically reduced when the NASA Aura satellite ceases operations in the next year or
92 two. It will take five years or more before new satellites are launched to recover some of that lost capability. Meanwhile
93 the climate system will evolve apace with impacts on ozone recovery and air quality. Significant human-induced changes
94 in atmospheric composition may emerge from experiments referred to as Solar Radiation Management (SRM) and from
95 a projected increase in low-Earth orbit (LEO) satellite and re-entry debris.

96 The following science questions provide a focus for the work of NDACC in the coming years:

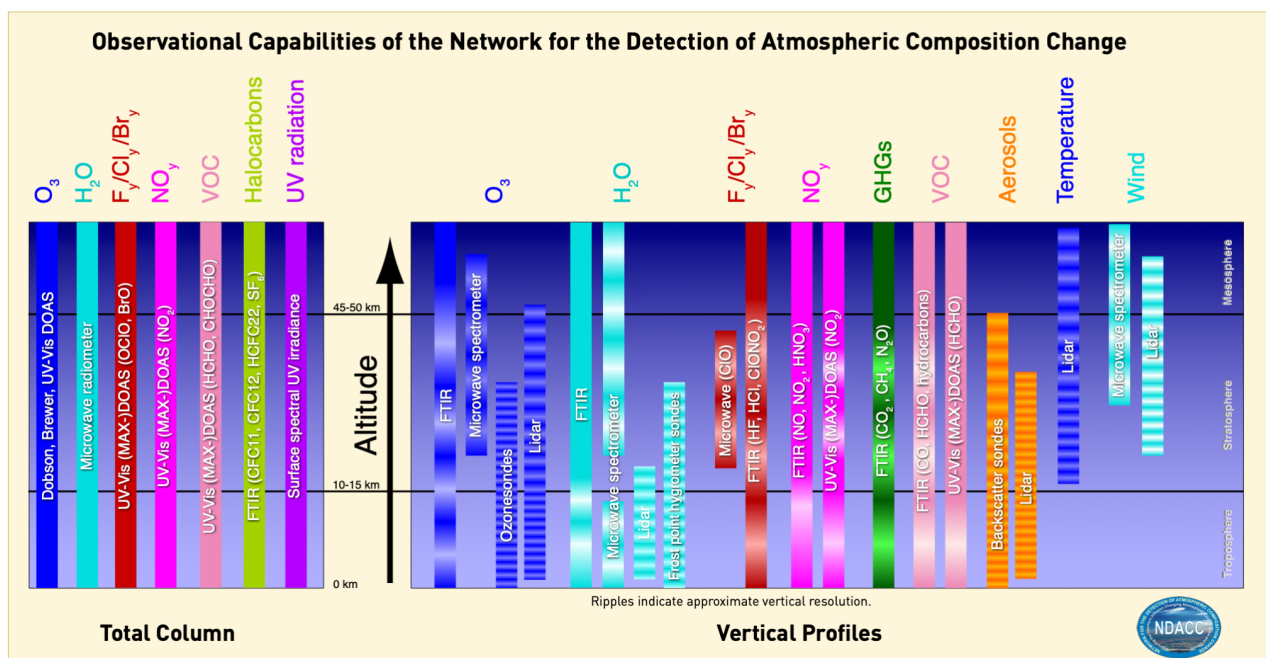
- 97 ● Which ozone-depleting substances, regulated by the Montreal Protocol or otherwise, will most influence the
98 ongoing stratospheric ozone recovery?
- 99 ● What are the processes driving atmospheric composition changes in the “Global South”?
- 100 ● What new stratospheric species require monitoring following atmospheric injections from volcanic eruptions (e.g.,
101 Hunga Tonga) and strong wildfires?
- 102 ● For which atmospheric species and in which regions are enhanced measurement capabilities and precision required
103 for better trend detection and reference data?
- 104 ● What are the most important factors driving changes in air quality?
- 105 ● What are the impacts of climate change and extremes on atmospheric composition and vice versa?

106 NDACC has succeeded for more than three decades because it has leveraged the scarce resources that support its member
107 stations as well as its archival facilities. It is exemplary in channeling technological improvements to meet changing
108 measurement and data requirements. As we enter a period of substantially reduced satellite monitoring of the upper
109 atmosphere – the “data desert” of *Salawitch et al. (2025)* – the scientific community will increasingly rely on the ground-
110 based measurements of NDACC and its Cooperating Networks to bridge data gaps or replace observational methods for
111 some atmospheric species. This challenge is compounded by the prospect of new modalities of atmospheric composition
112 change that require innovative measurement strategies.

113 This paper reviews NDACC achievements since the publication of *De Mazière et al. (2018)* and serves as an introduction
114 to the special issue “Achievements and perspectives of the Network for the Detection of Atmospheric Composition
115 Change after 35 years of operation”. These are discussed in the light of the seven NDACC cardinal objectives and

116 optimization of its strategy to best address the science questions above. The paper is organized into six sections. Section
 117 2 describes the organization of the network. Section 3 describes NDACC's partnerships and stakeholders. Section 4
 118 summarizes NDACC's achievements in recent years. Section 5 describes technical and scientific challenges facing
 119 NDACC. Section 6 looks ahead to prospects for the coming decade and beyond.

120 **2 The organization of NDACC**



121
 122 **Figure 1: Chart of NDACC observational capabilities is color-coded by observed atmospheric species and parameters with**
 123 **chemical formulas listed at the top. The altitude range of profiles illustrates approximate vertical resolution associated with**
 124 **each measurement technique (light horizontal stripes on vertical columns). Two horizontal dashed lines define approximate**
 125 **levels of tropopause and stratopause.**

126 NDACC collects atmospheric composition data at 118 globally distributed stations with over 170 active instruments. For
 127 an interactive map of NDACC stations see <https://ndacc.org>. Figure 1 shows NDACC's portfolio of long-term and
 128 campaign-based measured species and parameters. These include aerosol, BrO, C₂H₂, C₂H₄, C₂H₆, CCl₂F₂, CCl₃F,
 129 CH₃OH, CH₄, CHF₂Cl, chlorine, ClONO₂, CO, CO₂, COF₂, H₂CO, H₂O and isotopologues, HCHO, HCl, HCN, HCOOH,
 130 HF, HNO₃, HONO, N₂O, NH₃, NO, NO₂, OCIO, OCS, O₃, PAN, SF₆, temperature, spectral UV irradiance, and wind.
 131 NDACC refocuses its objectives as measurement priorities evolve, maintaining high data quality, quick archiving and
 132 rapid open data access in compliance with FAIR (Findable, Accessible, Interoperable, and Reusable) data principles.
 133 More information about FAIR can be found at e.g. GOFAIR (<https://www.go-fair.org/>).

134 Instrument Working Groups (Dobson, Brewer, FTIR, Lidar, Microwave, Sonde, UV/Vis, Spectral UV) oversee
 135 instrument and algorithm quality, providing expertise and resources for teams developing new instruments interested in
 136 NDACC affiliation. The Satellite Working Group fosters collaboration between NDACC and satellite missions and

137 provides meteorological data to the NDACC database via NOAA/NCEP. The Theory and Analysis Working Group
138 promotes NDACC data use and supplies model output to aid interpretation of observations.

139 NDACC recognizes the value of collaboration with external measurement and analysis networks that operate
140 independently. To foster this partnership, the NDACC offers a "Cooperating Network" (CN) designation. This allows
141 for mutual data access and network representation in the annual meetings while maintaining each network's integrity.
142 Further details on agreements with Cooperating Networks appear in Section 3.

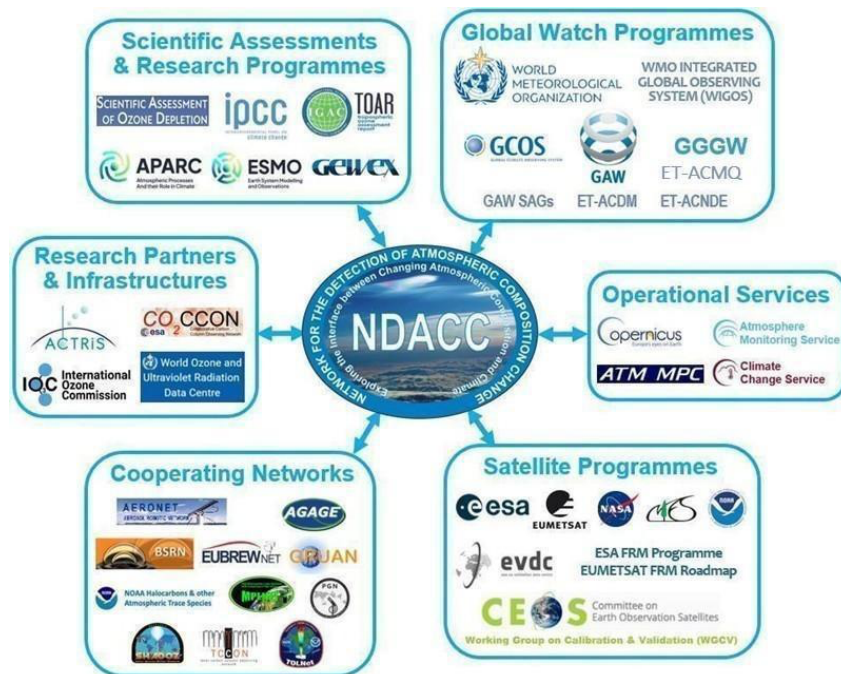
143 The NDACC Steering Committee is the organizational backbone of the network (see Fig. A1 in Appendix A, and the
144 most up-to-date version in www.ndacc.org > ABOUT > Organizational Structure). Established in 1989, the Steering
145 Committee (SC) includes all NDACC components. In addition to the Co-Chairs, it is composed of representatives from
146 each Instrument Working Group (IWG), the Theory and Analysis Working Group, and the Satellite Working Group.
147 Each CN has representatives on the NDACC SC. The IWGs promote exchange of expertise among NDACC members
148 and the CN and support for establishing new measurement sites or new instrumentation at existing sites. Functional and
149 Ex-Officio SC positions are used for tasking and/or reviewing of specific science matters and for addressing special
150 NDACC-related issues; they ensure that international organizational interests are represented. Emeritus SC
151 Representatives also provide expertise on measurements and science, including historical perspectives on evolving
152 NDACC needs. SC member terms are finite but renewable. The list of current SC members is available on the NDACC
153 webpage (ndacc.org).

154 NDACC organizational structure includes the Data Host Facility (DHF) where the observational and support datasets
155 are archived and made publicly available. The NDACC website provides an easy interface to the DHF and promotes
156 news and information about the network.

157 The procedures and data quality requirements for affiliating instruments with NDACC are defined in dedicated NDACC
158 Protocols that specify expectations for existing NDACC instrument types and for proposing new techniques. Other
159 protocols stipulate NDACC structure and operating procedures. All protocols are regularly updated to maintain best
160 practices.

161 **3 NDACC partners and stakeholders**

162 Since its inception, NDACC has been endorsed by international agencies and other stakeholders, including United
163 Nations Environment Program (UNEP), the International Ozone Commission (IO3C) of International Association of
164 Meteorology and Atmospheric Sciences (IAMAS) and the Global Atmosphere Watch (GAW) Program of the World
165 Meteorological Organization (WMO). The current landscape of NDACC stakeholders is presented in Fig. 2, grouped in
166 categories: global watch programs, scientific assessments and research programs, cooperating networks, satellite
167 programs, research partners and infrastructures, and operational services. Exchanges with the stakeholders occur through
168 their SC delegates and reciprocally through the participation of NDACC delegates in stakeholder committees or creation
169 of formal agreements.



170

171 **Figure 2. Overview of NDACC stakeholders.**

172 **3.1 Engagement with international environmental programs**

173 NDACC data are essential to the global atmosphere watch program data centers operated under the auspices of the WMO,
 174 UNEP and the UN Framework Convention on Climate Change (UNFCCC). NDACC contributes most of the atmospheric
 175 composition Essential Climate Variables (ECVs) required by GCOS (Global Climate Observing System) and plays an
 176 essential role in WMO’s Global Greenhouse Gas Watch (GGGW) approved in May 2023. NDACC delegates serve on
 177 several GAW Expert Teams and participate in WMO’s Rolling Review of Requirements process in support of the WMO
 178 Integrated Global Observing System (WIGOS). Its responsibilities as a Contributing Network to GAW were laid out in
 179 a formal agreement between both Parties in 2022.

180 **3.2 Engagement with scientific assessments and research programs**

181 NDACC is a major contributor to the following assessments: the quadrennial WMO/UNEP Scientific Assessment of
 182 Ozone Depletion; the Tropospheric Ozone Assessment Reports (TOAR) under the umbrella of International Global
 183 Atmospheric Chemistry (IGAC); Intergovernmental Panel on Climate Change (IPCC) assessments. NDACC also
 184 contributes to research programs aimed at understanding links among changes in atmospheric composition, dynamics
 185 and transport, and the evolution of air quality and climate. Joint activities include the Atmospheric Processes And their
 186 Role in Climate (APARC, formerly known as Stratospheric Processes And their Role in Climate, SPARC) and Global
 187 Energy and Water Exchanges (GEWEX) projects sponsored by the World Climate Research Program. The Long-term
 188 Ozone Trends and Uncertainties in the Stratosphere (LOTUS-1 and -2) and Observed Composition Trends And
 189 Variability in the Upper Troposphere and Lower Stratosphere (OCTAV-UTLS) projects rely on NDACC observations
 190 to assess ozone and atmospheric composition trends and their uncertainties. NDACC data serve as a reference for

191 climate model development and evaluation in the WCRP core project Earth System Modelling and Observations
192 (ESMO).

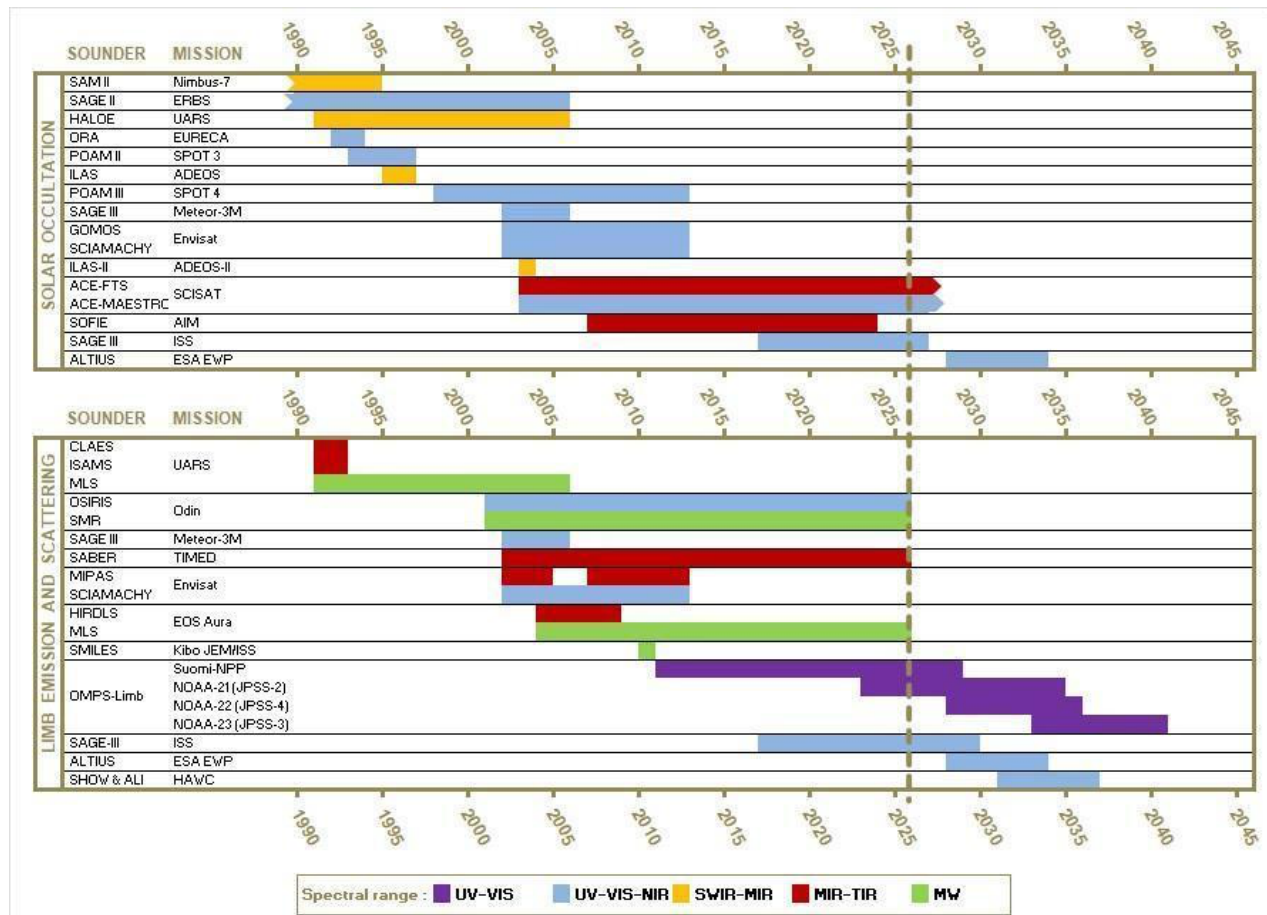
193 **3.3 Engagement with Cooperating Networks, research partners and infrastructures and operational services**

194 To widen its scope and foster collaboration on complementary measurements, NDACC has long had agreements with
195 Cooperating Networks (CN, see Figure 2). A list showing colocation of NDACC long-term measurement stations with
196 those of Cooperating Networks (referenced in the table) is available in the ‘Site List’ of the ‘Measurements and Analyses
197 Directory’ in the DATA Tab of the NDACC website (ndacc.org). CN agreements since 2018 have been established with
198 the European Brewer Network (EUBREWNET), the Pandonia Global Network (PGN), and the Tropospheric Ozone
199 Lidar Network (TOLNet). The European Research Infrastructure for Aerosols, Clouds and Trace Gases (ACTRIS),
200 established as a European Research Infrastructure Consortium in 2023 (Laj et al., 2024) supports and shares scientific
201 objectives and user communities with NDACC. To avoid discrepancies among instrument, measurement, and data
202 protocols related to common products, a Memorandum of Understanding between NDACC and ACTRIS defines how
203 the Parties operate to maximize benefits to users through exchange of data and expertise. For example, the ACTRIS
204 Centre for Reactive Trace Gases Remote Sensing (CREGARS) will serve the NDACC community through the
205 maintenance of central data processing units (Section 4.4.2), and the provision of training and consultancy for compliance
206 with ACTRIS/NDACC requirements; the ACTRIS Data Portal (formerly GEOmon data portal) is a gateway to
207 complementary data and services.

208 Agreements with the Copernicus Atmosphere Monitoring Service (CAMS) facilitate the use of NDACC reference data
209 for independent evaluation of CAMS global and regional data products and reanalysis, and with the Copernicus Climate
210 Change Service to deliver NDACC Climate Data Records of ECVs to the Climate Data Store (CDS). Whereas the
211 NDACC Protocol for Data Providers requires consolidated data archiving in the DHF for public availability within one
212 year after acquisition, a majority of NDACC PIs have moved to faster delivery of controlled quality data, for example,
213 meeting timeliness and quality requirements specific to CAMS Rapid Delivery.

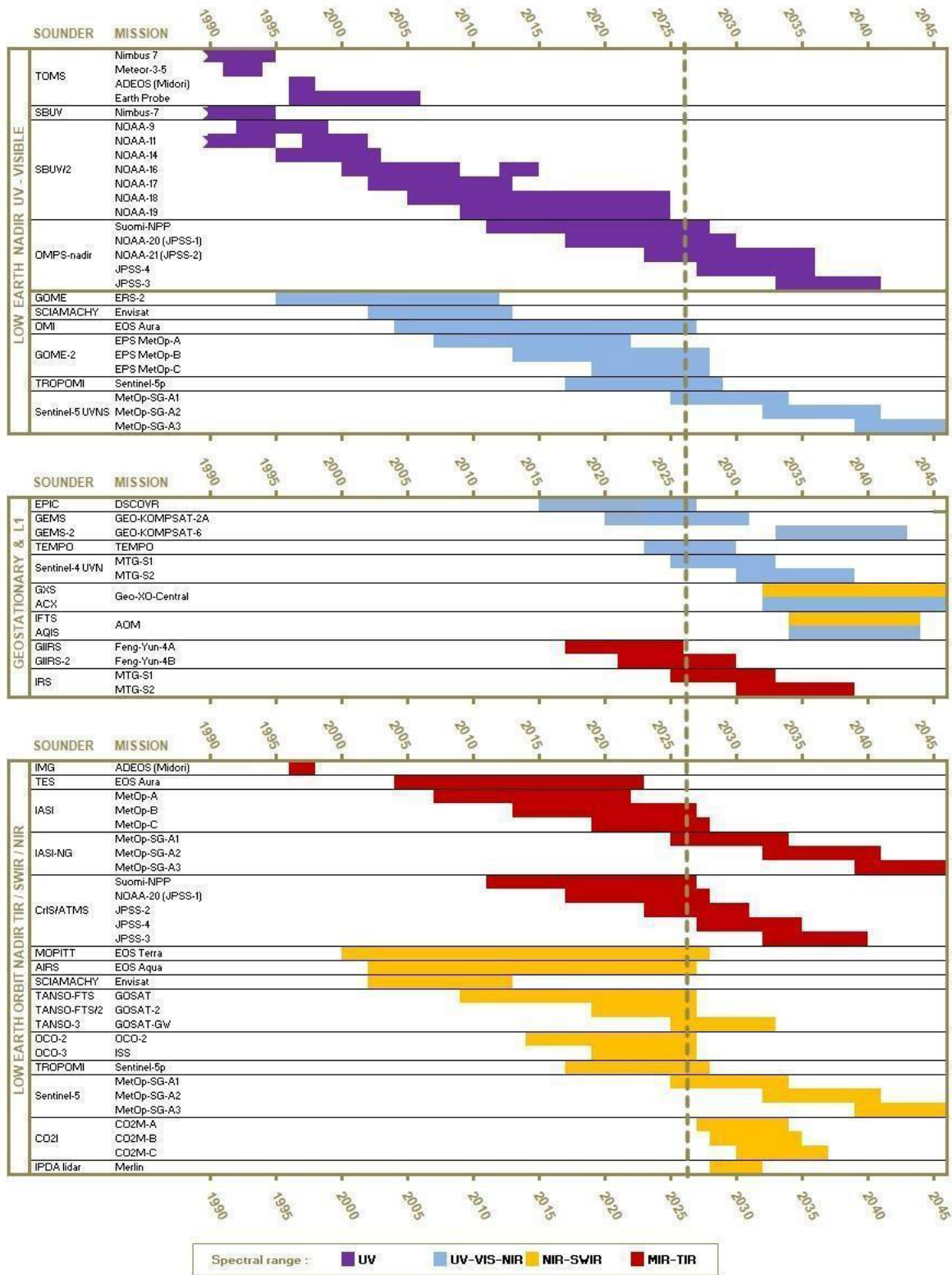
214 **3.4 Engagement with satellite observations**

215 A primary objective of NDACC remains the provision of high-quality reference measurements to support geophysical
216 validation and evolution of satellite atmospheric composition products. The network helps validate various data
217 reprocessing phases for a vast array of atmospheric composition satellite missions ranging from limb solar occultation
218 and emission sensors (see Fig. 3) to nadir-viewing platforms (see Fig. 4) across the UV-VIS and infrared spectrum.



219
 220
 221
 222

Figure 3. Timelines for limb solar occultation (upper panel) and limb emission (lower panel) satellite sensors that have been, are, or will be supported by NDACC observations.



224

225

226

227

Figure 4. As in Fig. 3 but for nadir-viewing satellite sensors: LEO UV-VIS (upper panel), GEO (geostationary) and L1 (middle panel), and LEO SWIR (Sort Wavelength InfraRed), NIR (near InfraRed) or TIR (Thermal InfraRed) (lower panel).

228 NDACC collaborative efforts are formalized through the representation of several space agencies on the NDACC
229 Steering Committee and Satellite Working Group (WG). Enhanced cooperation with space agencies in support of a
230 Fiducial Reference Measurements (FRM) framework has allowed NDACC to meet increasingly stringent satellite
231 validation requirements for data quality, traceability, uncertainty assessment, cross-network harmonization and
232 timeliness of data access (Goryl et al., 2023). Close links exist with the European Satellite Agency (ESA) Validation
233 Data Centre (EVDC) hosted at the Norwegian Institute for Air Research (NILU) and with NASA's Aura Validation Data
234 Center (AVDC) which both mirror NDACC data to facilitate seamless access for the satellite community.

235 At the inter-agency level, NDACC promotes exchange of data by contributing to the Committee on Earth Observation
236 Satellites (CEOS) through the Atmospheric Composition Subgroup of the Working Group on Calibration and Validation
237 (WGCV). By advancing the FAIRness of its data, NDACC serves as a reference for the mutual consistency of the
238 satellites, such as CEOS Atmospheric Composition Virtual Constellation (AC-VC) for air quality, for greenhouse gases
239 and for ozone. NDACC up-to-date involvement in developing satellite validation protocols and strategic planning
240 documents, ensures that validation frameworks, such as the Quality Assurance Framework for Earth Observation
241 (QA4EO) and FRM principles and maturity matrix, remain fit-for-purpose for evolving global constellations.

242 Operational satellites feeding numerical weather prediction and environmental services require a fast response to
243 validation needs. NDACC currently supports several operational systems, including NOAA's Products Validation
244 System (NPROVS) and the ESA/ Copernicus Validation Data Analysis Facility (VDAF). As new operational missions
245 (e.g. Copernicus Sentinel-4 and -5 or the upcoming Anthropogenic Carbon Dioxide Monitoring constellation), come
246 online, NDACC is evolving its data delivery mechanisms to provide near-real-time (NRT) data on a contractual basis.
247 This evolution is essential for informed international efforts to control emissions of atmospheric pollutants, thus
248 positioning NDACC for an important role to play in support of modern satellite remote sensing operations.

249 **4 Highlights of NDACC scientific achievements**

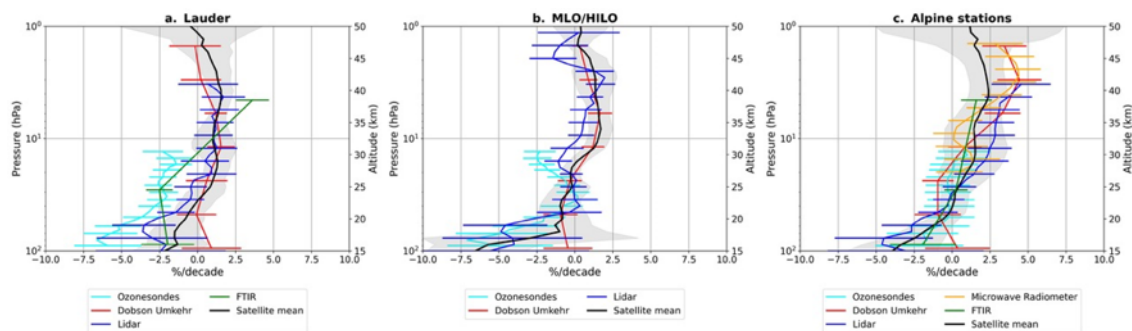
250 Selected recent achievements are described in this section. These include discoveries related to both stratosphere and
251 troposphere, synergistic collaboration with satellite observations, and advances in network infrastructure. In all
252 endeavors, NDACC's temporal coverage and adherence to standardized instruments, data-processing methods and
253 protocols, have been essential in creating the high-quality data required for quantifying chemical composition changes
254 and achieving network science goals. Nearly 500 publications since 2018 attest to NDACC's scientific contribution,
255 (<https://ndacc.org/publications>). Highlights of stratospheric and tropospheric research appear in Sections 4.1 and Section
256 4.2 respectively. Section 4.3 discusses satellite collaborations. Section 4.4 illustrates NDACC's advances in
257 instrumentation, technology and archiving infrastructure.

259 **4.1 NDACC stratospheric composition observations**

260 As a remote sensing network, the NDSC began with a primary focus on stratospheric composition: ozone, ozone-
261 depleting substances, and water vapor, and that commitment remains to the present.

262 4.1.1 Stratospheric Ozone Trends.

263 Section 3.2 described how NDACC is an integral component in SPARC/APARC research focus areas and the
264 quadrennial WMO/UNEP Scientific Assessments of Ozone Depletion. Within APARC/LOTUS, statistical multi-linear
265 regression models were used to detect linear decadal trends in the ground-based (i.e., NDACC, WMO GAW, SHADOZ)
266 and satellite ozone records (Godin-Beekmann et al., 2022) over the 2000–2020 period. The study confirmed significant
267 ozone increase in the upper stratosphere using satellite records averaged in three broad latitude bands, varying from 1.6
268 to 2.2 % per decade (Godin-Beekmann et al. 2022; 2022 WMO Ozone assessment). Fig. 5 shows longitudinally resolved
269 merged satellite records compared to ground-based data, i.e., from lidars, ozonesondes, Dobson Umkehr, microwave
270 radiometers and FTIR, that confirm the satellite trends. Non-linear behavior in the decline of lower stratospheric ozone
271 (60°S-60°N, below 24 km) during the post-2000 period was first reported by Ball et al. (2018). By applying dynamical
272 linear modeling (DLM) to the Arosa/Davos homogenized Dobson Umkehr record, Maillard Barras et al. (2022) showed
273 that upper stratospheric trends only became significantly positive after 2004, at 0.2-0.5% per year; negative trends persist
274 in the middle stratosphere and were more significant in the lower stratosphere from 2008 to 2018.
275



276
277 **Figure 5. Ozone profile trends post-2000 from selected ground-based NDACC stations: (a) Lauder, Southern Hemisphere**
278 **station, (b) tropical Mauna Loa and Hilo (ozonesonde) stations, (c) combined Alpine North Hemisphere stations. From Sofieva**
279 **et al. in review.**

280
281 APARC OCTAV-UTLS utilizes a dynamical coordinate system (i.e. tropopause, equivalent latitude, etc. derived from
282 MERRA-2 reanalyses) for binning the high-resolution ozone records to separate transport, chemical, and mixing
283 processes in the UTLS region. The method was implemented using several NDACC ozonesonde and lidar high-
284 resolution profiles, aircraft (Civil Aircraft for the Regular Investigation of the atmosphere Based on an Instrument
285 Container) and satellite (Aura/MLS and ACE-FTS) observing systems (Millan et al., 2023). The result is reduced
286 sampling bias among records, with ground-based and satellite data both revealing patterns of changing atmospheric
287 dynamics (Millan et al, 2024) and a reduction of uncertainties in fitted trends (Millan et al, 2025).

288 Investigation of the Arctic stratospheric ozone depletion during an unusually strong and stable polar vortex in 2019/2020
289 winter (Bognar et al. 2021) relied on long-term observations by NDACC UV-VIS, FTIR, ozonesondes and Brewer
290 instruments located at the Polar Environment Atmospheric Research Laboratory in Eureka, Canada (80°N, 86°W).
291 Cooperating network observations (PGN, Système D'Analyse par Observations Zénithales or SAOZ), non-NDACC lidar

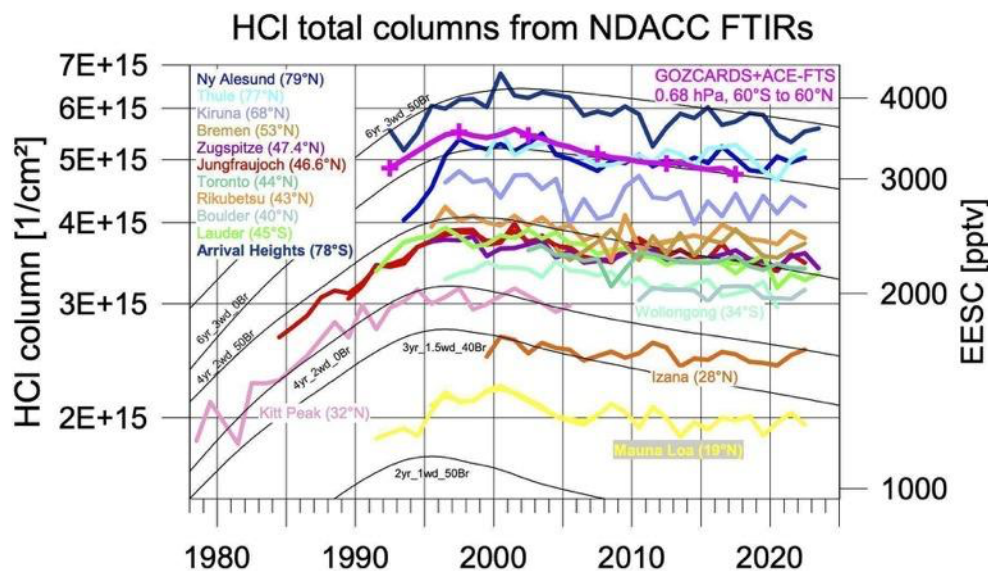
292 and the SLIMCAT model simulations were used to quantify ozone loss. The paper highlighted the importance of
293 combining NDACC measurements with models for attribution of ozone loss processes for predicting ozone recovery.

294 4.1.2 Ozone-depleting substances, halogenated stratospheric reservoir species and stratospheric circulation

295 NDACC data were crucial in detecting the unexpected slow decrease of CCl₄, forcing a re-evaluation of missing sources,
296 sinks and atmospheric lifetime (SPARC, 2016; Chipperfield et al., 2016). NDACC data confirmed the unexpected
297 emissions of CFC-11 (CCl₃F) after 2012 (Montzka et al., 2018, Chipperfield et al., 2021, Pardo-Campos et al., 2022),
298 which resulted in a slowing of its atmospheric decay, potentially delaying ozone recovery.

299
300 In the 2022 Ozone Assessment, trends in the Jungfraujoch FTIR time series of CFC-11, CFC-12, HCFC-22, HCFC-
301 142b, CCl₄, CF₄ and SF₆ support and bridge the trends observed in the high precision in situ data and upper troposphere
302 observations from satellites where available (Laube et al., 2022; Chapter 1 in WMO 2022). Work continues with CFC-
303 11, CFC-12, HCFC-22 (Polyakov et al., 2021) and HFC-23 (Takeda et al., 2021) using innovative retrieval approaches
304 and water vapor continuum models. A study using data from 16 NDACC FTIR stations quantified decreases in the
305 growth rate of atmospheric HCFC-22 columns derived from harmonized retrievals (Zhou et al, 2024).

306
307 Transport of source ODSs to the stratosphere maintains halogen reservoir species. The most abundant chlorine- and
308 fluorine-bearing reservoirs, HCl, ClONO₂, HF, and COF₂, are standard NDACC data products. Fig. 6 shows the evolution
309 of total column HCl from several NDACC stations and the evolution of 60°S – 60°N lower stratospheric HCl from Global
310 OZone Chemistry And Related trace gas Data records for the Stratosphere (GOZCARDS) and ACE-FTS observations.
311 Because only second-order reservoirs are missing, the weighted combination of the respective time series represent
312 budgets of stratospheric inorganic chlorine and fluorine.



313
314 Fig. 6. Total column HCl, the predominant reservoir of Cl, time series from a subset of the NDACC stations representing
315 latitudes from 78°S to 79°N, Included is the aggregate satellite time series for 60°S-60°N GOZCARDS, augmented with ACE-

316 **FTS HCl and Equivalent effective stratospheric chlorine (EESC) model (solid curves represent ODS lifetime and Br efficiency,**
317 **https://ozonewatch.gsfc.nasa.gov/facts/eesc_SH.html).**

318 NDACC data answer questions about atmospheric change that would otherwise remain speculative. Minganti et. al.
319 (2022) used multi-decade satellite and NDACC data to evaluate WACCM modeled N₂O trends to better understand
320 changes in the Brewer-Dobson circulation. Strahan et al. (2020) used MLS HCl and HNO₃ data, model output from GMI
321 (NASA’s Global Modeling Initiative) and measurements from 9 globally dispersed NDACC stations to find (i) a decrease
322 in the age of air of the southern hemisphere lower stratosphere relative to the north by about 1 month/decade and (ii) a
323 5-7 y variability in both HCl and HNO₃ total columns. The 1994–2018 NDACC record provided more conclusive
324 evidence as it spans 3-plus Solar cycles (11+ years) not available in a single satellite record. The analysis generally
325 supports the finding that the Solar cycle confounds statistical trend regression on the QBO (quasi-biennial oscillation) if
326 not accounted for. Alternatively, N₂O records from the NDACC FTIR stations helped validate the ACE-FTS satellite
327 hemispheric data and global model simulated changes in Brewer Dobson global circulation (Minganti et al, 2022).

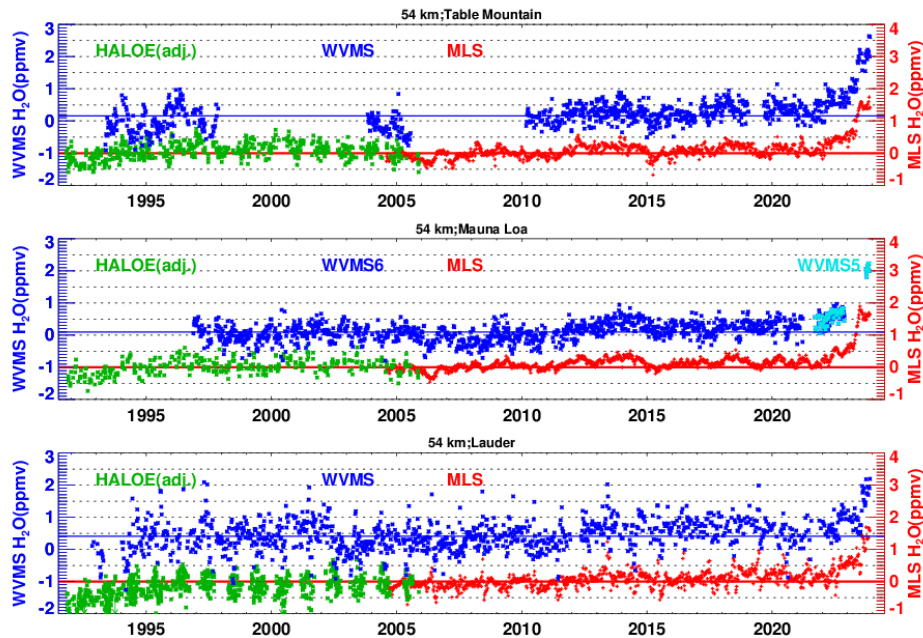
328 **4.1.3 Water vapor observations**

329 Detection of small water vapor trends in the upper troposphere, stratosphere and mesosphere is hampered by differences
330 among instruments and sites, as well as natural variability in the troposphere and the large 2022 volcanic water vapor
331 injection into the middle stratosphere. The APARC Water Vapor Assessment II intercomparison of satellite and ground-
332 based microwave measurements, thoroughly investigated trends in water vapor between pressures of 3 hPa and 0.03 hPa
333 (Nedoluha et al, 2017). Agreement between satellite retrievals and ground-based microwave instruments was generally
334 within ±10%. This assessment also included an intercomparison of relative humidity from 19 limb-viewing satellites and
335 the Vaisala RS92 radiosonde coincident with frost point instruments from NDACC (and other) sites between pressures
336 of 300-100 hPa (Read et al., 2022). Agreement of relative humidity in the upper troposphere measured by space-based
337 and frost-point instruments was on average within ±30%, with an additional 30% variability; the Vaisala R92 radiosonde
338 was not recommended for use at pressures below 200 hPa.

339 **4.1.4 Hunga volcanic eruption**

340 On 15 January 2022 the eruption of the Hunga undersea volcano at 20° S injected ~140-150 Tg of water vapor (H₂O)
341 into the atmosphere (Millan et al., 2022; Nedoluha et al., 2024). The bulk of the injection was in the lower stratosphere
342 where it was measured by balloon-borne sondes (Vömel et al. 2022). Not only was the plume injection observed from
343 NDACC stations, a rapid-response team deployed to Réunion Island within one week to make sonde observations (Evan
344 et al., 2023; Asher et al., 2023; Baron et al., 2023). Water vapor from the Hunga plume moved equatorward from its
345 original injection site, where it was first measured in the mid-stratosphere by ground-based microwave instruments at
346 the NDACC station at Mauna Loa, Hawaii (19.5° N) in April 2022 (Nedoluha et al., 2023a). Fig. 7 shows water vapor
347 anomalies at 54 km (just above the stratopause) measured by ground-based microwave instruments at Mauna Loa;
348 Lauder, New Zealand (45.0° S); and Table Mountain, California (34.4° N). In 2022, water vapor mixing ratios at all three
349 sites were unusually large, partly due to dynamical conditions (Nedoluha et al., 2023b). In 2023 water vapor at Table
350 Mountain and Mauna Loa was significantly higher than ever observed in 30+ years of measurements at these (Nedoluha
351 et al., 2024). Lauder showed record-breaking mixing ratios, but short-term weekly anomalies of similar magnitudes can

352 occur during certain seasons due to dynamical variations. Finally, in late 2023/early 2024, ~2 years after the eruption,
353 maximum water vapor anomalies were observed at all three sites at 54 km. These findings are described in more detail
354 in the APARC “The Hunga Volcanic Eruption Atmospheric Impacts Report” (APARC, 2025).
355

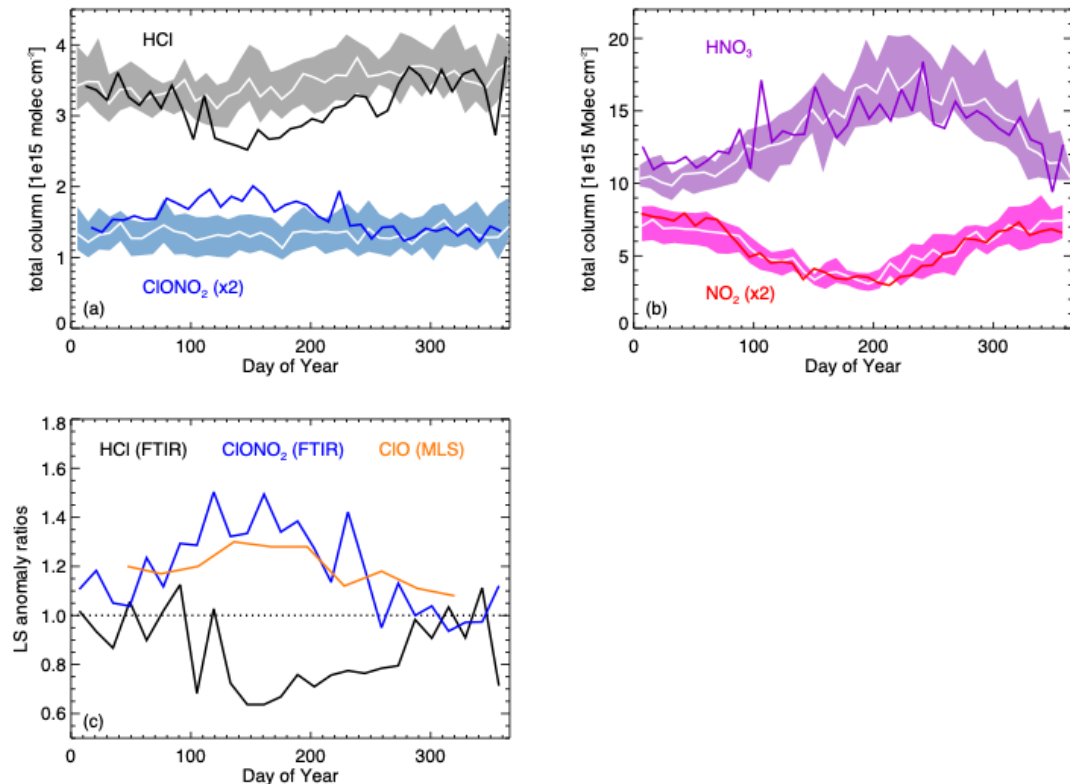


356
357 **Figure 7. Water vapor volume mixing ratio anomalies at 54 km from ~weekly ground-based microwave measurements at**
358 **Table Mountain, California (34.4°N, 242.3°E), Mauna Loa, Hawaii (19.5°N, 204.4°E) and Lauder, New Zealand (45.04°S,**
359 **169.68°E). The anomaly is calculated relative to a climatology based on Aura MLS measurements from 2004-2021. From**
360 **Nedoluha et al. (2024).**

361 4.1.5 Extreme Australian wildfires and stratospheric chemistry

362 In late December 2019 and early January 2020, Australian New Year wildfires injected record-breaking amounts of
363 smoke and aerosol into the southern hemisphere stratosphere. Aerosols were injected up to 32 km, resulting in a bimodal
364 size distribution as was observed in sonde flights launched at Lauder, New Zealand (Asher et al., 2024). Although
365 heterogeneous reactions on stratospheric aerosol surfaces have been known since early analyses of the Antarctic ozone
366 hole, less was known about reactions on black or brown carbon from biomass burning smoke. What NDACC and satellite
367 observations revealed in the post-fire months was unprecedented stratospheric chlorine partitioning (Fig. 8; Strahan et
368 al., 2022) which has important implications for predicting stratospheric ozone in a more wild-fire prone world. Satellite
369 observations of fire-perturbed HCl, ClONO₂, HF, O₃, N₂O and NO₂ by NDACC and H₂O, ClO and aerosol extinction
370 were reported by Santee et al. (2022) and Boone et al. (2020). Chemical simulations by Solomon et al. (2023) proposed
371 that chlorine partitioning was caused by oxidized organics and sulfates increasing hydrochloric acid solubility (and
372 associated heterogeneous reaction rates). This is supported by the observed enhanced ClONO₂ and decreased HCl,
373 although Strahan et al. (2022) pointed out that definitive ozone loss is not confirmed due to entangled chemistry/transport
374 effects. Ozone losses appear to peak in May-June.

375



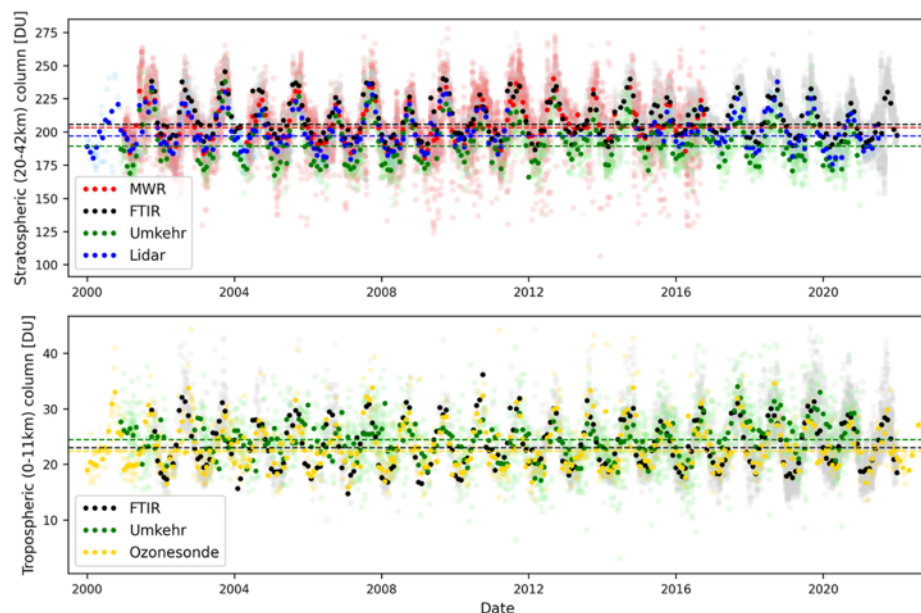
376
 377 **Figure 8.** (a) 2020 9-day average of Lauder FTIR total column HCl and CIONO₂ (scaled for clarity) along with associated
 378 2010-2019 mean (white) and 1 standard deviation (shaded). (b) Same as (a) but for HNO₃ and NO₂ (scaled for clarity). (c)
 379 Lower stratosphere column (LS, ~150-50 hPa, ~12-21 km) 2020 anomalies (9-day average, ratioed to 10-year means, 2009-
 380 2019) for HCl and ClO. Total column CIONO₂ anomalies are displayed because there is insufficient signal for a CIONO₂ LS
 381 column. Aura-MLS ClO observations are averaged over 40°-50°S. (after Strahan et al. 2022)

382 4.2 NDACC tropospheric composition observations

383 NDACC research in the 2000's has focused increasingly on tropospheric composition and radiation as described below.

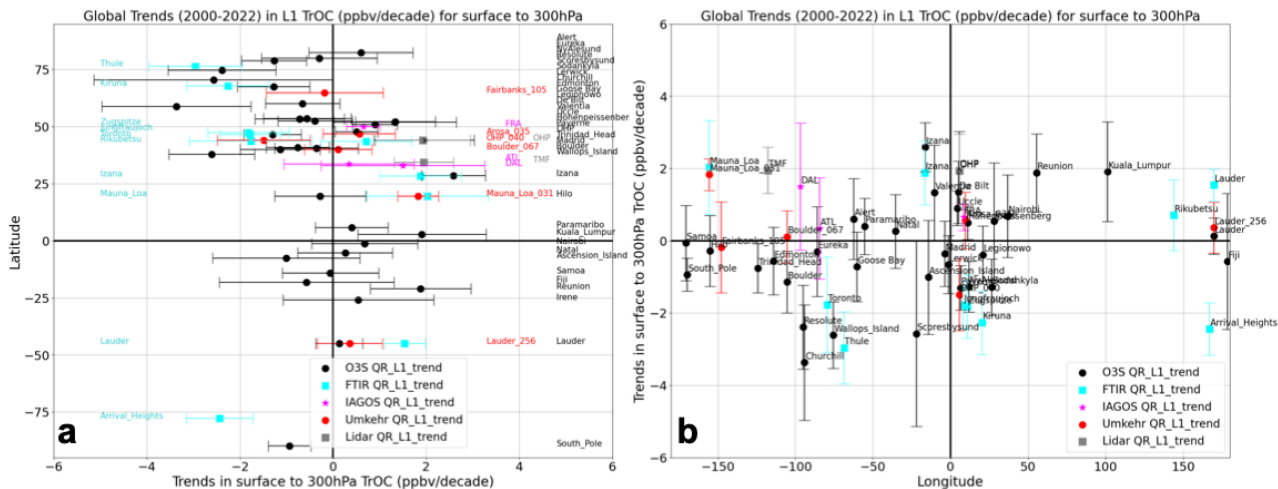
384 4.2.1 NDACC and the Tropospheric Ozone Assessment Report (TOAR)

385 NDACC played a major role in analyzing global tropospheric ozone trends in the second phase of IGAC's Tropospheric
 386 Ozone Assessment Report (TOAR II; see TOAR I reports by Gaudel et al., 2018; Tarasick et al. 2019). Within the
 387 HEGIFTOM working group (Harmonization and Evaluation of Ground-based Instruments for Free-Tropospheric Ozone
 388 Measurements), records from NDACC and other atmospheric measurement networks for four instruments – FTIR, Lidar,
 389 Brewer/Dobson Umkehr, ozonesonde – were reprocessed with absolute reference standards and archived to produce
 390 ozone column data with uniform formats with uncertainty estimates and quality flags (Van Malderen et al, 2025a). Fig.
 391 9 shows an intercomparison study at the multi-instrumented Lauder supersite (Björklund et al., 2024) for both
 392 stratospheric and tropospheric columns based on time-series for 2000-2022. More than 50 articles from TOAR II
 393 analyses, including those based on HEGIFTOM and other ground-based data, with satellite products, have been
 394 published in a TOAR II special collection (see https://bg.copernicus.org/articles/special_issue10_1256.html).



395
 396 **Figure 9. Upper: Time series (2000-2022) ozone columns (20-42 km) in Dobson Units (DU) from four remote sensing techniques**
 397 **at Lauder, New Zealand. Shaded points are all data, highlighted points are monthly means, dashed lines are median of all data**
 398 **by technique. Lower panel shows the tropospheric ozone column (defined as surface to 11km). After Björklund et al., (2024).**

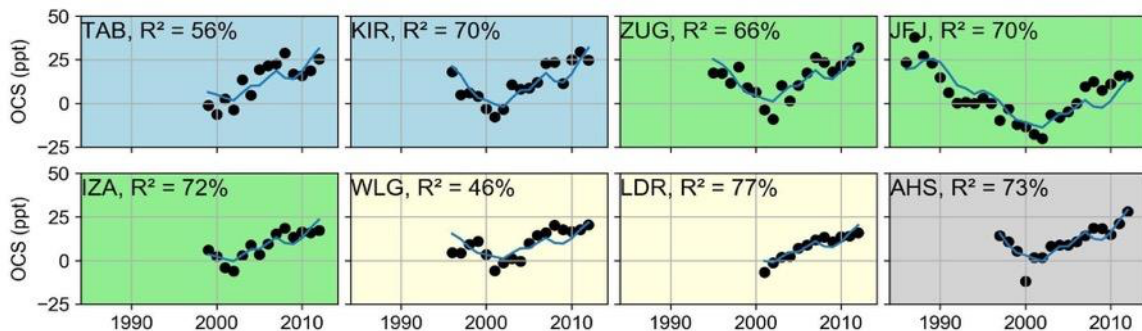
399 Trends for individual station HEGIFTOM/NDACC ozone columns, augmented by landing/takeoff profiles from the In-
 400 service Aircraft for a Global Observing System (IAGOS) airports, were calculated following TOAR-II guidelines on
 401 metrics, units, time range, and statistical trend model in a series of studies (e.g., Van Malderen et al., 2025a,b; Gaudel et
 402 al., 2024; Thompson et al., 2025). A summary of median trends for a tropospheric total column (TrOC, specified as
 403 surface to 300 hPa, for 2000 to 2022, based on the HEGIFTOM data, appears in Fig. 10. Trends are illustrated with 2- σ
 404 uncertainties for 55 sites (Van Malderen et al., 2025a) as a function of latitude (Fig. 10, left) and longitude (Fig. 10,
 405 right). The HEGIFTOM-derived trends mark a turning point for the tropospheric ozone community because it is the first
 406 time that a global picture of changes based on consistently processed observations from multiple ground-based
 407 instruments is available. The outcome is a definitive reference dataset for evaluating still-evolving satellite products,
 408 some of which cover fewer than 10 years (Hubert et al., TOAR-II Satellite Ozone Report, 2025). For ozone profile trends
 409 in the troposphere, there is no substitute for ozonesondes and aircraft data (Thompson et al., 2025; VanMalderen et al.,
 410 2025b).



411
 412 **Figure 10. Tropospheric column ozone (TrOC, surface to 300 hPa) trends in ppbv/decade, determined at three IAGOS airports**
 413 **and for four NDACC instruments: ozonesondes, FTIR, Umkehr, and Lidar. Calculation was made using all data (L1, 2000 to**
 414 **2022) by Quantile Regression. Uncertainties at $\pm 2\text{-}\sigma$. Most stations exhibit median trends within $\pm 3\text{ppbv/decade}$ (Van**
 415 **Malderen et al., 2025a). a) trends as function of latitude, b) trends as function of longitude.**

416 **4.2.2 Long-term trends in whole atmosphere carbonyl sulfide.**

417 Carbonyl sulfide (OCS), the reservoir sulfur species in the free troposphere, is a product of anthropogenic, biogenic and
 418 oceanic emissions, a tracer for CO_2 uptake by the biosphere and the largest source of sulfur transported to the stratosphere
 419 during periods of low volcanic emissions, helping maintain the lower stratospheric sulfate aerosol layer. Despite these
 420 important roles, it remains under-observed. NDACC FTIR OCS measurements are unique in having near-global coverage
 421 for 3+ decades. Hannigan et al. (2022) derived trends in the lower free troposphere and the lower stratosphere, showing
 422 distinct trends over discrete time periods since 1986. They showed that regression models using available geophysical
 423 proxies of varying time periods could not adequately explain the multi-decadal OCS variability. For the longest time
 424 series through to 2012 the highest correlations to the free tropospheric NDACC time series was with the gridded, bottom
 425 up anthropogenic emissions from Zumkehr et. al., 2018. Shown in Fig. 11, between 46% to 77% of the variability can
 426 be attributed to anthropogenic sources at stations between 76°N and 80°S.



427
 428

429 **Figure 11. Fit of the annual anthropogenic emissions inventory from Zumkehr et al. (2018) (blue line) to annually**
430 **averaged FTIR OCS data (black dot) from stations with the longest running data records. The emissions inventory**
431 **is interpolated to the station location. From Hannigan et al. (2022). TAB: Thule Air Base 76°N, KIR: Kiruna 67°N,**
432 **ZUG: Zugspitze 47°N, JFJ: Jungfraujoch 46°N, IZA: Izana 28°N, WLG: Wollongong 34°S, LDR: Lauder 45°S,**
433 **AHS: Arrival Heights 79°S.**

434 **4.2.3 Surface UV radiation: Monitoring, impacts, and research**

435 Surface UV radiation is a crucial indicator of atmospheric change, capturing the combined effects of aerosols, clouds,
436 ozone, and other atmospheric composition changes driven by natural and anthropogenic sources, transport and
437 atmospheric mixing. Its reach extends to public health, impacts on terrestrial and aquatic ecosystems and the degradation
438 of materials like plastics into microplastics. Regular high-precision NDACC spectral UV observations are conducted at
439 12 globally distributed stations, strategically located to cover diverse environments (polar, mid-latitude, tropical) to
440 ensure data collection across Earth's UV regimes. In Antarctica, continuous monitoring since 1990 has shown a slight
441 decline in overall UV exposure since the early 2000s (Bernhard & Stierle, 2020), consistent with ozone layer recovery.
442 However, ground-based measurements still record extremely high UV levels like persistent ozone holes (Cordero et al.,
443 2022). These observations have greatly advanced our knowledge of public health impacts from spatial and temporal
444 variability in UV doses (Brogniez et al., 2021). Cumulative, low-dose UV exposure has significant health implications,
445 leading to advocacy for a more nuanced understanding of UV benefits and risks (McKenzie & Lucas, 2018; McKenzie
446 et al., 2022).

447 **4.3 Satellite validation and collaboration**

448 There is considerable synergy between NDACC, with its focus on remote sensing measurements, and the satellite
449 observations community for initial validation of new space-based instrumentation, detection of long-term drifts, and
450 collaborative research. Selected highlights follow. More examples with publications appear in Table C1 in Appendix C.

451 **4.3.1 Detection and quantification of long-term satellite drifts**

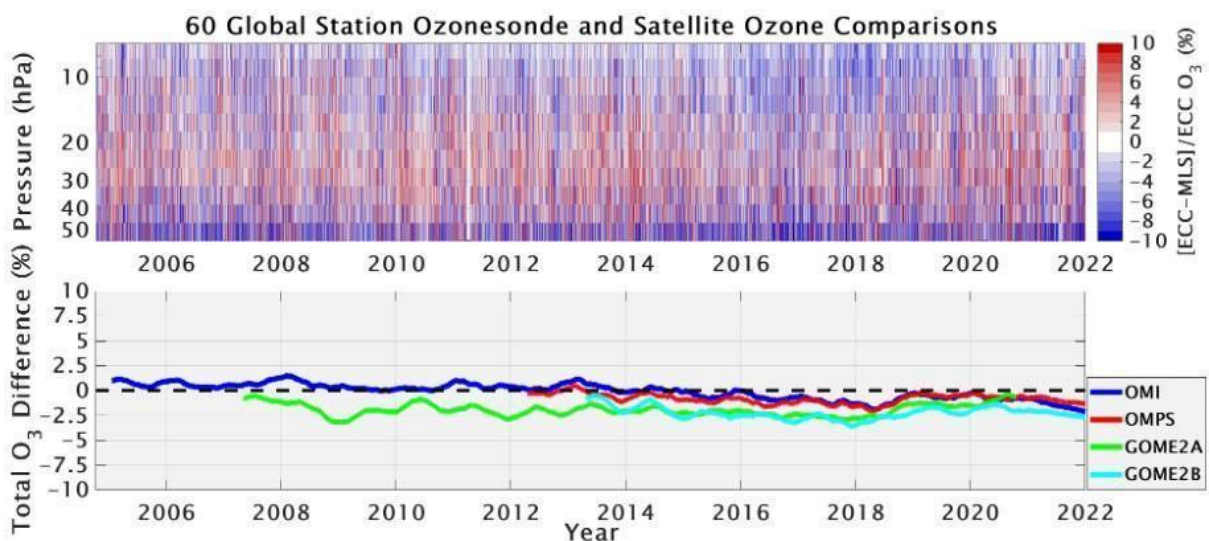
452 Without long-term ground-based observations, detection of drifts or steps in satellite data record is difficult. The
453 MOPITT instrument aboard NASA's EOS-Terra satellite launched in 2000 measuring near-global CO has exceeded
454 initial specifications. Buchholz et. al. (2017) used data from 14 latitudinally distributed NDACC FTIR stations to
455 determine drifts over the first 17 years. Co-located data carefully matched using the vertical sensitivity (averaging
456 kernels) to account for the respective response of each FTIR examined three MOPITT retrieval schemes. Mean bias for
457 all sites was determined to be 2.4 % for TIR-only, 5.1 % for TIR–NIR, and 6.5 % for NIR-only. The MOPITT long-term
458 bias drift is calculated to be within $\pm 0.5 \text{ \% yr}^{-1}$. Aura MLS has also operated past its programmed lifetime. NDACC
459 water vapor sonde data at Lauder, Hilo and Boulder were used to evaluate, determine and correct for drifts over 15 years,
460 2005 to 2020 (Livesey et. al., 2021).

461 Stability of ground-based records themselves can be compromised by instrumental artifacts, e.g. “drop-off” in
462 ozonesonde records due to manufacturing changes (Stauffer et al., 2020), which are often detected through calibration
463 and multi-instrument intercomparison activities (Thompson et al., 2019) and by adherence to NDACC observational

464 protocols. Processing satellite and ground-based (GB) data by identical statistical methods minimizes biases in trend
465 detection while illustrating potential inconsistencies among records (Petropavlovskikh et al, 2025).

466 Over the past 25 years, members of the NDACC ozonesonde community have been part of the WMO/GAW ASOPOS
467 (Assessment of Standard Operating Procedures for Ozonesondes) activity to optimize sonde data quality through
468 specification of standard operating procedures (SOP) including data processing (Smit et al., 2024). Roughly 2/3th of the
469 60 global sonde stations have reprocessed their records. For ozonesonde data since mid-2004, satellite measurements are
470 used to evaluate the sonde profiles as shown in Fig. 12. Total column and stratospheric ozone from the sondes were
471 compared to overpass readings from satellites (Aura OMI and MLS, S-NPP OMPS, GOME-2A and -2B) from mid-2004
472 through 2021 to determine stability in the sonde measurements. Overall, the ozonesonde data show remarkable agreement
473 compared to satellite instruments. Total column ozone derived from the sondes is on average within $\pm 2\%$ of the Aura
474 OMI over the last 18+ years (Fig. 12), and the ozone profiles match Aura MLS to within $\pm 5\%$ in the mid-stratosphere up
475 to 10 hPa (Stauffer et al., 2022). The excellent agreement is achieved even with a known instrumental bias at several
476 stations (Stauffer et al., 2020). These comparisons underscore the success of the ozonesonde data reprocessing and
477 homogenization effort (Smit et al., 2021). In the 1990s, ozonesonde data uncertainty was on the order of 20%, and biases
478 near 10% in total column ozone were common. Today, data uncertainties approach 5%, with total column ozone biases
479 $< 2\%$.

480



481 **4.3.2** Figure 12. Coincident ozonesonde and satellite comparisons (% difference) for 60 global ozonesonde
482 stations. (Top) Time series comparisons among all ozonesonde and Aura Microwave Limb Sounder (MLS) ozone
483 profiles ($[\text{ECC-MLS}/\text{ECC}]$) where ECC signifies the sonde value. Red (blue) colors indicate where the sonde ozone
484 is greater (less) than MLS. (Bottom) Ozonesonde and satellite total ozone comparisons in % difference ($[\text{ECC-}$
485 $\text{satellite}]/\text{ECC}$) for OMI (blue), S-NPP OMPS (red), GOME-2A (green), GOME-2B (cyan).

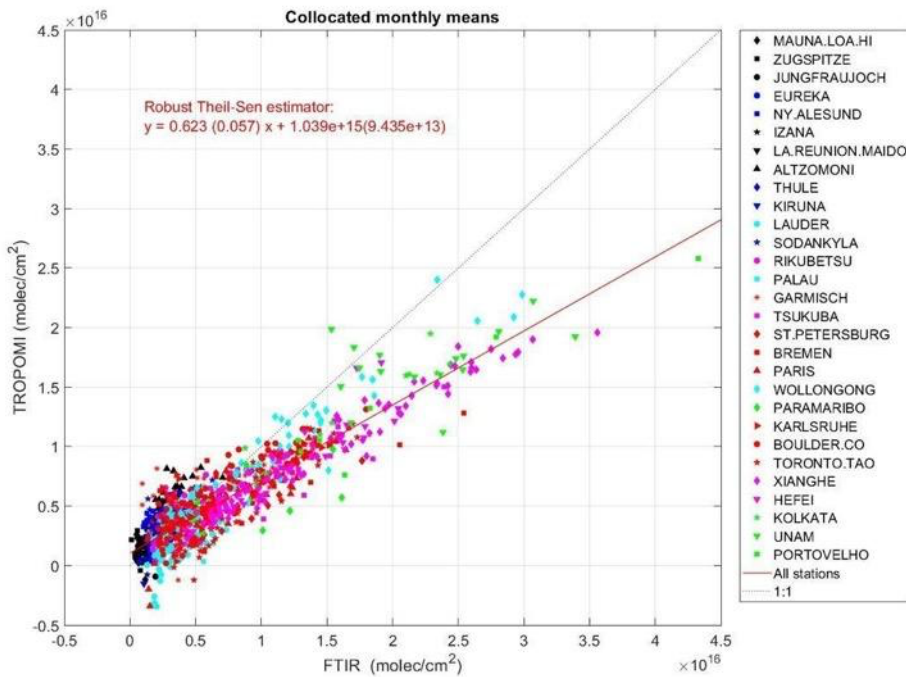
486 4.3.3 Operational validation of HCHO and NO₂ for Sentinel-5P

487 The operational validation service of Sentinel-5P TROPOMI relies on the fast delivery of correlative measurements
488 acquired by most of the NDACC sub-networks and several cooperating networks. Total and tropospheric ozone column

489 and profile data products are quality assessed by an operational validation server (<https://mpc-vdaf.tropomi.eu>) using
490 Brewer, Dobson, FTIR, lidar, ozonesonde and Zenith-Sky DOAS measurements acquired from pole to pole and under a
491 variety of measurement conditions and influencing parameters (Garane et al., 2019; Hubert et al., 2021; Keppens et al.,
492 2024).

493 The quality assessment of NO₂ total and partial columns relies on a holistic approach combining validation of TROPOMI
494 stratospheric NO₂ with respect to NDACC Zenith-Sky DOAS columns, tropospheric NO₂ with respect to MAX-DOAS
495 columns, total NO₂ with respect to PGN total columns (Verhoelst et al., 2021) and cloud parameters validation using the
496 ACTRIS-Cloudnet network of lidars and radars (Compernelle et al., 2021). Harmonization of NDACC FTIR NO₂
497 (Vigouroux et al., 2025), provides a new global dataset for TROPOMI validation (see S5P Quarterly Validation Reports
498 at <https://mpc-vdaf.tropomi.eu>). Stratospheric NO₂ columns measured by NDACC FTIR, Zenith-Sky DOAS and PGN
499 at pristine stations (i.e., without tropospheric NO₂ pollution) give mutually consistent validation results, showing e.g. a
500 similar station-to-station 1-sigma scatter of the bias with TROPOMI of ~5%.

501 Although not a standard NDACC product, harmonized HCHO FTIR data were produced by the network (Vigouroux et
502 al., 2018) and used for the first TROPOMI HCHO validation (Vigouroux et al. 2020). TROPOMI HCHO products were
503 shown to be biased high over clean regions by ~26% but underestimated by ~31% in polluted conditions. The robust
504 linear relationship between TROPOMI and NDACC data is shown in Fig. 13 across a range of HCHO concentrations.
505 These data are used in inverse modeling studies to correct TROPOMI and OMI products before inverting them (Oomen
506 et al., 2024; Müller et al., 2024). The high internal consistency of FTIR-based HCHO is illustrated; HCHO is now
507 archived as a standard NDACC species. The HCHO FTIR data set has been employed in other satellite validations (Lee
508 et al., 2024; Kwon et al., 2023; Ayazpour et al., 2025; Müller et al., 2024) and for characterizing errors in satellite-based
509 HCHO/NO₂ ratios (Souri et al., 2023) and for TEMPO validation over North America.



510

511 **Figure 13. Scatter plot of NDACC FTIR and TROPOMI HCHO data, after Vigouroux et al. (2020).**

512 Similarly, harmonization of NDACC FTIR NO₂ (Vigouroux et al., 2025), provides a global network dataset for
 513 TROPOMI validation (Quarterly Reports at <https://mpc-vdaf.tropomi.eu>). The NDACC FTIR and Zenith-Sky DOAS
 514 NO₂ columns are characterized by excellent internal consistency, showing a similar station-to-station 1-sigma scatter of
 515 biases with TROPOMI of ~5% (Verhoelst et al., 2021).

516 4.3.4 Correlative observations of new species

517 Some of the most exciting advances in satellite observations are due to advances in retrieval algorithms providing data
 518 products for new species. Species like methanol, ethane, ethene, ethyne and isoprene (CH₃OH, C₂H₆, C₂H₂, C₂H₄, C₃H₈
 519 respectively) have been observed with the Cross-track Infrared Sounder (CrIS) (Wells et al., 2022, Wells et al., 2024,
 520 Brewer et al., 2024). These species, primarily originating from biogenic and anthropogenic sources, are important as
 521 ozone precursors, traceable to emissions sources. NDACC has developed new retrievals for these species, in some cases
 522 providing the only validation data. The Infrared Atmospheric Sounding Interferometer (IASI) has produced a formic acid
 523 (HCOOH) data product that Franco et al. (2020) validated with global NDACC FTIR data. Other new species observed
 524 by NDACC are PAN (CH₃C(O)O₂NO₂) (Mahieu et. al., 2021, Wizenberg et. al., 2022) and ammonia (NH₃) (Dammers
 525 et al, 2015; Lutsch et. al., 2019, Yamanouchi et. al., 2021, Herrera et. al., 2022). See Table A1 (Appendix B) for the list
 526 of species validated by NDACC observations.

527 4.4 Advances in instrumentation, data processing and archiving infrastructure

528 Since its inception, the NDACC mission has been to observe the atmosphere with the precision and accuracy required to
 529 answer the key science questions of the day, hence the focus on state-of-the-art, calibrated, certified instrumentation.
 530 Instrumentation techniques, data acquisition, and signal-to-noise specifications have greatly improved over the last three

531 decades while data processing and analysis techniques have evolved to deliver larger, better characterized, versioned
532 datasets with improved uncertainty budgets. These complex and versatile datasets are used by a more diverse research
533 community. Simultaneously, the geographical, temporal, representativeness, precision requirements of the research and
534 monitoring communities have increased. Some examples of how NDACC has responded to this new environment follow.

535 **4.4.1 Instrumental: Automation, compactness, mobility**

536 The Jet Propulsion Laboratory (JPL) Atmospheric Lidar Team has developed a compact, more affordable class of
537 tropospheric ozone differential absorption lidar (DIAL) systems. The Small Mobile Ozone Lidar (SMOL) is compact
538 enough to be readily deployed for rapid air quality measurement campaigns at 10 to 50% the cost of most existing
539 tropospheric ozone lidars (Chouza et al., 2025). In June-August 2023 JPL deployed two SMOL instruments in the Los
540 Angeles Basin to participate in the NOAA-led AEROMMA-2023 campaign and in the NASA-led STAQS Mission for
541 the validation of TEMPO. By June 2024, two more SMOL instruments had been built, enabling unprecedented
542 deployment configurations for field campaigns, e.g., within a tight spatial grid for air quality studies, or at a larger,
543 synoptic scale to study long-range transport and stratospheric intrusions.

544 In 2024, a version optimized for stratospheric ozone (SMOL-X) was designed and successfully tested. SMOL-X can
545 measure vertical profiles of ozone between 5 km and 35 km altitude with a precision better than 10% for a 3-hour
546 averaging time. Because of its affordability and ease of deployment, this new class of stratospheric ozone DIAL provides
547 opportunities for NDACC deployment in remote areas, such as Antarctica, the Arctic, Asian or Africa providing the
548 opportunity to fill critical measurement gaps. NDACC continues to evaluate new measurement techniques and target
549 variables. For example, in 2020, the UV-VIS Working Group updated the instrument and validation protocols for
550 including MAX-DOAS-type instruments, several of which have been NDACC-certified since then. Wind lidar joins
551 microwave wind instruments to extend NDACC's meteorological observational capability. The Steering Committee is
552 also evaluating the addition of temperature data measured by microwave instruments.

553 **4.4.2 Migration towards central processing**

554 NDACC ensures a high standard of data quality as well as a high degree of homogenization and consistency across
555 instruments and platforms. Centralized data processing with network-wide scrutiny is a powerful tool to achieve quality,
556 consistency, and homogenization.

557 Several NDACC Instrument Working Groups made significant efforts towards the development of centralized data
558 processing. The Global Lidar Analysis Software Suite (GLASS) was initially developed to retrieve stratospheric ozone,
559 temperature, aerosol, tropospheric ozone, and water vapor for the four NASA/JPL lidars. It was then expanded to process
560 the raw data of more than a dozen lidar instruments contributing to NDACC, TOLNet and GRUAN (GCOS reference
561 Upper Air Network). GLASS is used to support several NDACC-contributing stations on a routine basis and has served
562 as a transfer standard during campaigns (e.g., the SCOOP and STOIC campaigns in 2016 and 2024 respectively). A
563 second centralized lidar data processor named LIDAR Ozone ACTRIS was also installed at ACTRIS for the analysis of
564 several European NDACC lidars. It has been integrated in the ACTRIS Centre for Reactive Trace Remote Sensing
565 Central (CREGARS).

566 Within the ESA FRM4DOAS consortium, a Centralised Data Processing System (CDPS) dedicated to the retrieval of
567 tropospheric and stratospheric trace gas data products from MAX-DOAS and zenith-sky light DOAS instruments has
568 been developed In BIRA-IASB (Van Roozendael et al., 2024). In its current demonstration, the FRM4DOAS system
569 generates total ozone, stratospheric NO₂ profiles, and tropospheric columns and profiles of NO₂ and HCHO from
570 approximately 20 stations. Retrieval algorithms are selected through community consensus, resulting in quality-
571 controlled data products being delivered daily to the NDACC rapid delivery (RD) repository and mirrored at the ESA
572 Validation Data Centre (EVDC) to serve as an FRM for satellite validation.

573 An FTIR CDPS has also been developed to ingest infrared spectral data from standard NDACC high-resolution, moderate
574 and low-resolution instruments to accommodate rapid delivery for Sentinel 5P and CAMS validation systems. Key
575 features are the easy integration of additional instruments and open source. For more than a dozen FTIR instruments, the
576 system provides NDACC retrievals for selected species and the capacity for both instruments and species is increasing.

577 The above systems for Lidar, DOAS and FTIR instruments demonstrate the advantages of the CDPS:

- 578 • High level of harmonization of retrieval results e.g. uncertainty budgets, regularization
- 579 • Traceability of processing: e.g. registration of retrieval strategy, spectroscopy data, ensures FAIR adherence
- 580 • Responsiveness to changes, e.g. prior data, spectroscopy, algorithm, reporting and guidelines (GEOMS or NDACC
581 DOI generation),
- 582 • Automated rapid delivery data to NDACC DHF or other destinations,
- 583 • Decreased operational workload for instrument PI, and
- 584 • Uniform quality assurance across all instruments and all data levels (L0 - L2).

585

586 The CDPS has created advanced visualization tools for L0, L1 and L2 data accessible to the public at ([https://actris-
587 ftir.aeronomie.be/actrisvisualizer?view=visualize](https://actris-ftir.aeronomie.be/actrisvisualizer?view=visualize)). The FRM4DOAS and FTIR CDPS are integrated into the ACTRIS
588 CREGARS FTIR facility (<https://actris-ftir.aeronomie.be/>) and used by ACTRIS National Facilities. The ACTRIS CDPS
589 are aligned with NDACC retrieval procedures to maintain consistency with NDACC.

590 **4.4.3 Data Handling Facility: GEOMS, versioning, licensing, DOIs**

591 The NDACC maintains a leading-edge Data Host Facility (DHF) designed to address the complex challenges of
592 managing large scale geophysical archives. Central to its mission is assurance of long-term measurement traceability and
593 stability via change management. The GEOMS metadata standard is used to enhance interoperability with partner
594 networks. Recent enhancements to GEOMS have improved data versioning capabilities allowing the identification of
595 data processed with distinct algorithms, with varying integration times, or linked to specific publications.

596

597 NDACC supports the FAIR principles: Findability, Accessibility, Interoperability, and Reusability through its use of
598 GEOMS metadata; the use of data protocols guiding public archive and general rules for use of data; and the
599 incorporation of Data Object Identifiers (DOI). Creation of DOIs, offered to NDACC data providers by EVDC, allows
600 direct citation of data records in scientific literature, a frequent requirement for many peer-review journals. The data
601 protocols stipulate details on the public accessibility of NDACC data. As well, GEOMS and NDACC recommend

602 Creative Commons licensing (creativecommons.org) which dictates how data can be used and reused. This transparency
603 ensures that the legal and technical requirements for data reuse are clearly communicated to the global research
604 community.

605
606 Beyond primary observational data, the DHF archives high-resolution atmospheric model output to provide broader
607 auxiliary context at the location of NDACC measurements. These include the Global Modeling Initiative (GMI),
608 chemical transport model (CTM) dating back to 1985 and GEOS-GMI replay simulations (Orbe et al, 2017) that
609 constrain the meteorology to the MERRA-2 reanalysis through 2023 (Gelaro et al., 2017, Duncan et al., 2007; Strahan
610 et al., 2013; Nielsen et al., 2017, Molod et al., 2015). The GEOS-GMI simulation, described in Fisher et al. (2024), has
611 higher horizontal resolution than the GMI CTM simulation. Additionally, Chemical Lagrangian Model of the
612 Stratosphere (ClAMS; e.g. Pommrich et al., 2014 and references therein) products, such as regional model tracers of
613 surface origin and age-of-air simulations (e.g. Ploeger et al., 2021; Graßl et al., 2024; Vogel
614 et al., 2025), are available to NDACC researchers for joint project studies. Physical locations of the NDACC DHF and
615 website are at NASA Langley Research Center (LaRC), ensuring continuity of infrastructure central to the network's
616 functioning. In addition, NILU provides a mirror of the NDACC DHF and a backup of the website content. The recent
617 move of the DHF from its NOAA (Maryland) home at NASA LaRC (Virginia) provided an opportunity for a full redesign
618 of the interface for both data providers and users. While preserving the integrity of data quality and interfaces with
619 partnering organizations, the data ingestion now allows for interactive and programmatic upload. The query of data using
620 the database tables is available to the public via an intuitive interface, allowing for data access with identification of
621 statistics on the data, e.g., number of files, submission dates and more.

622 **5 NDACC Challenges and opportunities**

623 The structure of NDACC and how it meets the principal goal of providing the highest quality atmospheric composition
624 data were detailed in Sections 2 and 3. Section 4 illustrates major discoveries and accomplishments focusing on NDACC
625 observations since 2018. The network is not without challenges (Section 5.1). At the same time, NDACC seeks to
626 expand measurements to address emerging areas that require high-quality ground-based observations (Section 5.2).

627 **5.1 Challenges**

628 **5.1.1 Technical challenges**

629 There are two general types of challenges facing NDACC. First, there are technical challenges (Section 5.1.1.1), i.e.,
630 incorporating new instruments, maintaining reference standards and consistent calibrations, and adapting to every-
631 changing archives and formats. Second, infrastructure challenges (Section 5.1.2) include sustained funding, adapting to
632 new scientific priorities while maintaining long-term measurements, changing expectations on data availability and re-
633 posting on an ever-growing population of secondary and tertiary data platforms.

634 **5.1.1.1 Instrument and IT issues**

635 NDACC researchers often push instruments to their limits, dedicated to collecting consistently high-quality data as
636 instruments age, spare parts dwindle, the cost of maintenance increases, and some instruments are replaced with newer
637 technology.

638

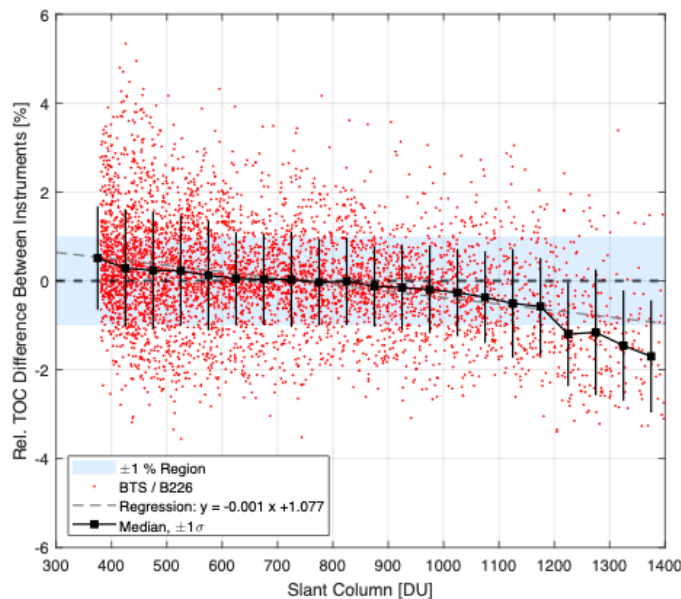
639 Total column ozone instruments, a mainstay of satellite calibration and cross calibration, have been deployed globally
640 for 6-7 decades. Many of the Dobson spectrophotometers used in NDACC are more than 50 years old. There are no
641 dedicated suppliers for replacement parts. Mechanical and optical properties are not well documented. Furthermore, the
642 manufacturer of the NDACC Brewer instruments has recently discontinued production.

643

644 Simpler, automated and less expensive instruments have been developed, e.g., Pandora or BTS array spectrometers for
645 total ozone and UV measurements (Herman et al., 2015; Zuber et al., 2021) or moderate spectral resolution mid-IR
646 interferometers (e.g., Sha et al., 2020). Some newer instruments are still being evaluated for accuracy and multi-decade
647 stability. An example (Fig. 14) compares total ozone columns measured by a new BTS spectrometer and an NDACC
648 Brewer. When slant ozone columns are large and the sun is lower in the sky, the BTS instrument reports lower values,
649 presumably due to straylight effects that will need to be corrected.

650

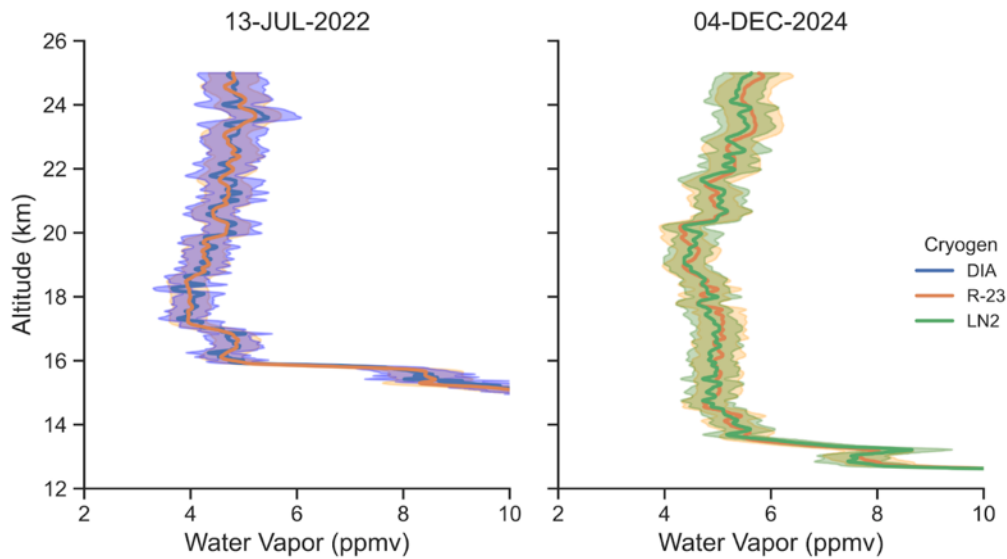
651 Other challenges include the scarcity and/or cost of supplies, e.g., helium for launching sondes, gases used in lasers, and
652 the phase-out of certain technologies. The latter case is illustrated by the need to replace the HFC coolant (R23) in
653 frostpoint water vapor sondes. R23, a powerful greenhouse gas, is banned in accordance with the Montreal Protocol
654 Kigali Amendment.



655

656 **Figure 14. Relative difference between total ozone columns (TOC) measured by a modern CCD-based spectrometer**
657 **(Gigahertz BTS) and the NDACC Brewer double-monochromator #226, shown as a function of slant TOC for observations at**
658 **Hohenpeißenberg from November 2021 to December 2025.**

659 Figure 15 shows profiles of water vapor from paired launches of NOAA frost point hygrometers (FPHs) using 1) dry ice
660 and ethanol (DIA) and 2) liquid nitrogen (LN2). Although significant progress has been made transitioning away from
661 R23, further intercomparisons with alternative cryogenes are ongoing.



662
663 **Figure 15. Near simultaneous launches from Boulder with NOAA R-23 and NOAA DIA FPHs on July 13, 2022 and with**
664 **NOAA R-23 and NOAA LN2 FPHs on December 4, 2024. Shown are the 1-second gaussian filtered water vapor data products**
665 **and total calculated uncertainties of each, derived using sources of error in the frost point temperature measurements and the**
666 **reported uncertainty of the iMet-54 radiosonde pressure.**

667 Many NDACC instruments come from small manufacturers with limited staff. This limitation makes it difficult to track
668 unintentional manufacturing changes in ozonesonde production, for example, that have contributed to inconsistencies in
669 ozone profile time series (Stauffer et al., 2022). The NDACC and WMO-sponsored Assessment of Standard Operating
670 Procedures for Ozonesondes (ASOPOS) activity is standardizing procedures for ozonesonde operations and data
671 processing (WMO Report 268; Smit et al. 2024) with the idea of homogenizing long-term records using an absolute
672 ozone standard.

673 Recent problems with Raman lidar water vapor measurements illustrate an unusual challenge. Their data in regions
674 affected by UT/LS biogenic aerosols from extreme wildfires (Khaykin et al., 2020a) are contaminated by aerosol
675 fluorescence (Chouza et al., 2022). The measurements can be corrected, but with reduced signal-to-noise ratio,
676 compromising reliable trend detection. Raman lidar observations performed at 532 nm are an alternative.

677 Ongoing changes in IT, lasers, spectrometric systems, components, etc., across 40 years or more is a challenge that
678 requires expertise and costly efforts to digitize historic data and to upgrade to new systems. To guarantee trend-worthy
679 data, parallel operation of old and new systems, sometimes over years, is essential and required by NDACC protocols.
680 Remote access to and/or automatic operation of instruments is increasingly available. This reduces staffing requirements
681 and cost, although in some cases internet security limits remote access.

682 **5.1.1.2 Traceability, fiducial reference measurements, changing calibration**

683 Validating satellite observations and numerical models has been a primary objective of NDACC since its inception. Over
684 the past 35 years, the fleet of satellites and their validation needs have evolved significantly. NDACC data meet many
685 of the requirements but not always all.

686 Challenges to the FRM process include outdated standards for uncertainty budgets, e.g., Basher (1982) for Dobsons. For
687 Brewers, calibration relies on several entities: International Ozone Services (IOS), the RBCC-E (Regional Brewer
688 Calibration Center - Europe), and Environment and Climate Change Canada. All three organizations participate in
689 calibration campaigns, publishing results in WMO/GAW reports. There is a high level of agreement, typically 0.5% to
690 1% or better (Zhao et al., 2023), but it is time-consuming to specify data and metadata to ensure reproducible calibrations
691 and efficient reprocessing. The methods developed for more reliable uncertainties (Redondas et al., 2024) are difficult to
692 implement but they represent an opportunity for data format transition, e.g., from NASA Ames to GEOMS-HDF.

693 Spectroscopic reference databases (e.g., HITRAN used in IRWG) are typically updated every 4 years. Instrument
694 Working Groups track the effect of changes on NDACC data records to decide on whether to reprocess historical records.
695 An example of ensuring accurate data comes from ozone absorption cross sections used to derive traceable ozone values
696 that have changed several times over ~60 years, i.e., over the lifetime of the Dobson network. NDACC and the larger
697 community have yet to complete the transition to new temperature-dependent cross sections (Serdyuchenko et al., 2014;
698 Weber et al. 2016), approved a decade ago by the International Ozone Commission (Orphal et al., 2016) because
699 implementation requires reprocessing of large archives (Voglmeier et al., 2024). NDACC and WMO/GAW are
700 coordinating the update at the World Ozone and UV Data Center (woudc.org).

701 **5.1.2 Programmatic and infrastructure challenge**

702 **5.1.2.1 Funding challenges**

703 Long-term consistency and continuity are emblematic of NDACC. However, "continue to do for the next five years
704 what was done over the last five years" is not attractive for funding organizations that are oriented toward innovation.
705 NDACC research is heavily driven by instrument PIs and staff who need to diversify their work while also maintaining
706 and expanding their NDACC activities. This is a challenge when funding decreases or when staff move on or retire.
707 Institutional priorities may change and a research group is disbanded. NDACC is proactive in overcoming obstacles.
708 NDACC engagement with WMO scientific advisory groups, expert teams and technical conferences, with satellite
709 groups, and with evolving observation strategies, provides support for projects that leverage NDACC measurements
710 as well as for helping individual stations. NDACC's letters to sponsors have prevented station closures. Instrument
711 working group meetings promote visibility of PIs and staff to program managers. NDACC's advances in creating and
712 promulgating standard operating procedures and processing and reprocessing software helps maintain operations as
713 personnel and instruments change.

714 **5.1.2.2 Enhancing network efficiency and expanding NDACC**

715 The focus of NDACC has been on general coordination, and scientific and technical support. Central processing, or very
716 rigid or intrusive requirements, have not been part of NDACC's strategy, although they might make some things more
717 efficient. Over the years, instruments and operating procedures have, however, become more standardized and simpler

718 to operate. NDACCs FTIR stations, for example, use nearly all the same instrument, as well as common traveling
719 calibration standards and operation procedures, which allows processing and species retrieval with a common software
720 and in a central facility for PIs interested in this option. Benefits are more cohesive network-wide data products (e.g.,
721 Hannigan et al., 2022), more timely deposits to data centers, more rapid data reprocessing, retrieval of an increased
722 number of species with greater efficiency, and a reduced burden on station PIs.

723 Another aspect, also from FTIR, is extension of the very high quality but sparse NDACC network to lower quality
724 stations to give better coverage. The standard NDACC high-resolution FTIR interferometers are expensive and require
725 substantial expertise. As a consequence, important portions of the globe are not monitored. Lower cost, moderate spectral
726 resolution (e.g., 2 to 4.5 cm OPD) mid-IR interferometers (Sha et al., 2020), that require little maintenance can provide
727 a solution, especially for tropospheric species or total column abundances (e.g., Zhou et al., 2023). Hardware and
728 software that enable autonomous operation are used. In Kolkata, India, a lower-resolution FTIR instrument provides
729 good quality data for species like HCHO.

730 A “tiered system” might be considered within the NDACC once the recently developed (and future) mobile observational
731 systems will be incorporated in the NDACC (i.e. SMOL, and compact FTIRs). The new set of requirements will be
732 designed for the short and long-term data obtained with these instruments. Depending on the outcomes of the ongoing
733 assessments of these mobile, more cost-effective instruments, they will be fully integrated into NDACC or integrated
734 along the concept of tiered system. NDACC is open to partner with other networks to discuss the needs for further
735 harmonization, integration and cost-effectiveness. Such efforts are initiated in the European CARGO-ACT project
736 (<https://www.cargo-act.eu/>) in which NDACC is represented.

737 A world-wide homogeneity among similar instruments within, but also outside NDACC, should be a high priority, e.g.,
738 for global satellite validation and long-term variability analyses. NDACC’s ozonesonde community, for example, seeks
739 to increase collaboration with China (e.g., Beijing and Hong Kong) and India (e.g., Pune and Trivandrum), stations that
740 collect a significant number of profiles. However, they use ozonesonde models for which instrumental errors are not
741 fully characterized, e.g. at the World Calibration Centre for Ozone Sondes in Jülich, Germany.

742 More challenging is a lack of homogeneity among different instrument types or networks, e.g., for column NO₂, O₃ and
743 HCHO data from NDACC DOAS UV-visible instruments, NDACC FTIRs, and the PGN (Pinaridi et al., 2025) or for
744 CH₄, N₂O and CO column data from NDACC FTIR and TCCON (e.g., Zhou et al., 2018; 2019).

745 Easy access to data remains a challenge. The NDACC Data Handling Facility provides access to all NDACC
746 measurements, but formats and versions change over time, and the granularity of data packaging is not always user-
747 friendly. Data archived in multiple centers, in various formats, and with various overlaps among the centers are difficult
748 to use. Examples include ozonesonde data, archived in eight archives (NDACC, WOUDC, SHADOZ, NOAA, EVDC,
749 AVDC, HEGIFTOM, CDS) in different data formats. This leads not only to inconsistencies in data and metadata stored
750 across archives, but also between stations in one archive, and even in the data record of one given site. It is expected that
751 transition to unified metadata and data formats, e.g., GEOMS-HDF, will facilitate better coordination among archives.
752 The goal is always to provide simple, friendly access to users, incorporating FAIR principles.

753 **5.2 Scientific opportunities and technical challenges**

754 Challenges and unexpected findings represent new opportunities for NDACC as the following examples illustrate.

755 **5.2.1 Ozone recovery and climate change**

756 Mandates based on the Vienna Convention for the Protection of the Ozone Layer and the associated Montreal Protocol
757 provided the scientific motivation for NDSC in the early 1990s. Following the success of the Montreal Protocol and its
758 subsequent amendments (WMO, 2014), there is a common perception that stratospheric ozone depletion is a "solved
759 problem". However, ozone depletion is still substantial and ozone layer recovery is more complex than a decade ago
760 (WMO, 2022), partially due to unexpected increases in very short-lived ODSs into the UT/LS from Asian emissions
761 (e.g., Adcock et al, 2021, Lauther et al., 2022, Pan et al, 2022). These species are only tracked from NDACC ground-
762 based instruments. The need for these data is greater than ever.

763 Related to the need to maintain ODS monitoring for ozone recovery is the impending loss of the MLS water vapor and
764 ClO coverage as well as reduced viewing of Arctic ozone depletion events, volcanic and/or wildfire injections of material
765 into the stratosphere. Springtime stratospheric ozone depletion in polar regions continues to be highly variable year to
766 year (e.g., Manney et al., 2020; Bogner et al., 2021; Pazmino et al., 2023; Shi et al., 2023), making long-term NDACC
767 measurements of ozone-related species important for tracking future changes.

768 **5.2.2 Unexpected events**

769 Unexpected events, such as recent extreme wildfires (Khaykin et al., 2020a; John et al. 2021; Wizenberg et al. 2023;
770 Tickl et al., 2024, Flood et al., 2025, Khaykin et al. 2025) and or the Hunga volcanic eruption (Nedoluha et al., 2023)
771 sharply modified stratospheric composition and perturbed predictions of future stratospheric composition (Strahan et al.,
772 2022; Solomon et al., 2023). Modeling is required to assess impacts of potential injected sulfate particles to the
773 stratosphere, an action designed to counteract global warming. Ongoing climate change has modified the trajectory of
774 ozone recovery (WMO, 2022). Whereas anthropogenic ODS defined NDACC's original measurement portfolio,
775 increasing emissions of GHGs like CO₂, CH₄ and N₂O are re-defining some NDACC priorities. Also relevant are changes
776 in air quality, atmospheric aerosol loading, and cloud cover, for example, affecting surface UV (Cordero et al., 2014;
777 Cordero et al., 2023). Extreme UV events still occur from Antarctic ozone loss, e.g. over Patagonia and the Antarctic
778 peninsula (de Laat et al., 2010; Cordero et al., 2022).

779 **5.2.3 Candidates for expanding NDACC measurements**

780 Generally, as some satellite capabilities decrease and others emerge, NDACC's ground-based measurements remain
781 vital. Examples of expansion opportunities follow.

782 **5.2.3.1 More species from FTIR**

783 NDACC FTIRs at nearly two dozen stations provide clear-sky high-resolution solar absorption measurements for 13 key
784 air quality, ozone, ozone precursors, and greenhouse gases. A strategic aim is to expand this list to more constituents
785 important in climate change, global pollution, and ozone depletion. Potential molecules, already retrieved and archived
786 on the DHF for some FTIR sites, include ammonia (NH₃), ethylene (C₂H₄), methanol (CH₃OH), peroxy-acetyl nitrate

787 (PAN), and hydrofluorocarbons (HFCs) that are regulated by the 2016 Kigali Amendment of the Montreal Protocol.
788 Retrieval of the two most abundant HFCs, HFC-134a and HFC-23, has been demonstrated at a few NDACC stations
789 (Pardo Cantos et al., 2024).

790 **5.2.3.2 Wind**

791 Wind data are vital for weather forecasting and for understanding global circulation, but upper air wind data are scarce.
792 For a short period, the space-based AEOLUS lidar provided global upper atmospheric wind data, greatly improving
793 weather forecasts (Rennie et al. 2021; Garret et al., 2022). Ground-based wind-lidars, a recent NDACC addition (Khaykin
794 et al., 2020b), were instrumental in validating AEOLUS (Ratynski et al., 2023). Microwave radiometers also measure
795 upper atmospheric winds (Hagen et al., 2018). A network of ground-based wind instruments could also validate a space-
796 based wind lidar.

797 **5.2.3.3 Water vapor**

798 Water vapor, the most important greenhouse gas, affects radiation and dynamics, cloud formation and atmospheric
799 chemistry. Climate models show a substantial moist bias in the lowermost stratosphere (Stenke et al, 2007; Charlesworth
800 et al, 2023), a sensitive climate-feedback region. NDACC profiles of water vapor are essential for improving models.
801 NDACC measures high resolution water vapor profiles with balloon-borne FPH and water vapor Raman lidars in the
802 troposphere and (lower) stratosphere (Vömel et al., 2016; Hall et al., 2016; Leblanc et al., 2012; Hicks-Jalali, 2020), as
803 well as coarse resolution profiles in the (upper) stratosphere and mesosphere with microwave radiometers (Nedoluha et
804 al., 2021; 2023). Water vapor measurements for stratospheric needs are usually adequate with monthly or bi-weekly
805 observations.

806 Natural stratospheric water vapor sources, i.e., CH₄ and H₂ oxidation, may be augmented by overshooting convection
807 and subtropical monsoonal circulations. Looking ahead, NDACC has created a water vapor strategy: (https://ndacc.org/under_sites/default/files/2024-01/NDACC_WaterVaporStrategy_20220119.pdf).

809 **5.2.3.4 Aerosols and climate interventions**

810 The stratospheric aerosol layer impacts radiation and chemistry, but stratospheric aerosol is variable, routinely perturbed
811 by small and moderate volcanic eruptions and increasingly by large wildfires (Solomon et al., 2022; Solomon et al, 2023;
812 Peterson et al., 2022). Typical stratospheric aerosol, concentrated between the tropopause and 25 km, is composed of
813 sulfuric acid particles from SO₂ and OCS oxidation, mixed organic sulfate particles that enter from the troposphere, and
814 meteoric particles (Murphy et al., 1998, 2014). Particles from rocket emissions (Katich et al., 2022) and satellite re-entry
815 (Murphy et al., 2023) are likely to increase in the coming decades. The Asian Tropopause Aerosol Layer (Vernier et al.,
816 2011), occurring during boreal summer, contributes up to 15% of Northern Hemisphere aerosol (Yu et al., 2017). Recent
817 NDACC aerosol measurements show that the Asian summer monsoon is a weak but a measurable source of stratospheric
818 aerosol even in the Arctic from late summer to early autumn (Graßl et al., 2024). Routine measurements of stratospheric
819 aerosol, a key capability of NDACC, are essential, particularly if climate intervention leads to enhanced particle
820 injections (Asher et al., 2023) and large wildfires (Asher et al., 2024). Because size distributions are not directly
821 observable from space, measurements of particle composition are frequently carried out during aircraft campaigns.
822 NDACC proposes to add routine balloon-borne measurements of aerosol size distributions with optical particle
823 spectrometers, e.g., the Portable Optical Particle Spectrometer (POPS; Todt et al., 2023) in the next 3-5 years.

824 **6 Outlook**

825 This article has reviewed the fundamentals of NDACC, its rationale, mission and the success of the highest quality
826 instruments in monitoring atmospheric composition and contributing to major assessments. NDACC's Working Groups
827 have been exemplary in promulgating standards and best practices. Similar approaches have been employed by
828 NDACC's 10 Cooperating Networks. NDACC has been active in research and scientific service programs, especially
829 within the European Union and North America, and within international satellite projects where its data are essential to
830 algorithm and model development and validation. NDACC is operating within the framework of the latest developments
831 in data distribution and management practices.

832 NDACC's impact on solving major problems in atmospheric composition and climate has been highlighted. For example,
833 long-term monitoring has been foundational in tracking the health of the stratospheric ozone layer and more recently, the
834 evolution of air quality and climate pollutants. Exceptional events, such as volcanic eruptions, are captured with NDACC
835 observations, which can measure impacts on a scale too small for satellites. With a decreasing satellite constellation for
836 stratospheric composition, the need for NDACC observations could not be greater. NDACC is at a crossroads as resource
837 pressures on ground-based monitoring programs increase. With data archiving and distribution activities diverting
838 resources from data collection in some networks, strategic planning is essential to strengthen NDACC and its
839 Cooperating Networks.

840 Based on specific recommendations in prior sections, NDACC is well-positioned to adopt a three-pronged strategy:
841 protect existing stations and data streams; promote greater usage of NDACC data; and expand NDACC's coverage
842 geographically and in species-parameter space.

843 **Protect Existing Stations and Data streams.** As described above, current NDACC observing infrastructure and
844 resources (instruments, data, and people) must be sustained. With many stations operating for three to four decades, their
845 records are increasingly indispensable as the value of a dataset increases with its longevity. NDACC and cooperating
846 partners are actively engaging a younger generation of scientists and technical professionals, with a specific focus on
847 expanding representations from underrepresented areas. The goal is to evolve infrastructure so that expertise and projects
848 are transferred, that capacity is built, and that innovative ideas and insights emerge. An important element of this effort
849 is the ongoing development of more cost-effective and automated instruments, with centralized data acquisition and
850 processing. Adding new observations at existing stations, leveraging infrastructure and personnel, is another approach to
851 strengthening the networks.

852 **Promote Greater Usage of NDACC Data:** It is important to advertise and promote the usage of the NDACC data with
853 network stakeholders and throughout the global scientific community. Due to its roots in stratospheric ozone research,
854 including development and validation of satellite products, there is a dedicated data user group worldwide that extends
855 to atmospheric dynamics and air quality. NDACC is currently extending data impact through cross-disciplinary
856 initiatives in climate and carbon cycle research, climate intervention, etc. The efforts of NDACC and cooperating
857 networks to distribute data more rapidly and more accessible, conforming to the latest data practices (e.g., FAIR), are
858 widening impact even more, as are data sharing initiatives with WMO and other organizations. The CAMS assimilation
859 system that relies on NDACC observations as an independent reference is another sign of network impact. The TOAR

860 II HEGIFTOM activity, with data reprocessing from four NDACC instrument types, marks a major milestone. The
861 HEGIFTOM homogenized dataset is moved to the NDACC DHF and other historical archives, and is now a gold
862 standard, supplying reference data for evaluation of satellite products and global model output. More active collaboration
863 with satellite and modeling communities will further promote applications of NDACC data.

864 **Expand NDACC's coverage in two ways:**

865 Geographical Coverage. NDACC's coverage is still poor in Africa, Asia, South America and the Mediterranean region,
866 partly due to shortage of resources for equipment and of skilled personnel or expertise. In other cases, high-quality data
867 are collected but they are not shared. The latter situation is expected to improve over time as more journals publish links
868 to data archives. NDACC needs to engage with organizations that have infrastructure and expertise. An NDACC
869 affiliation is a path to greater visibility and access to unique expertise and support.

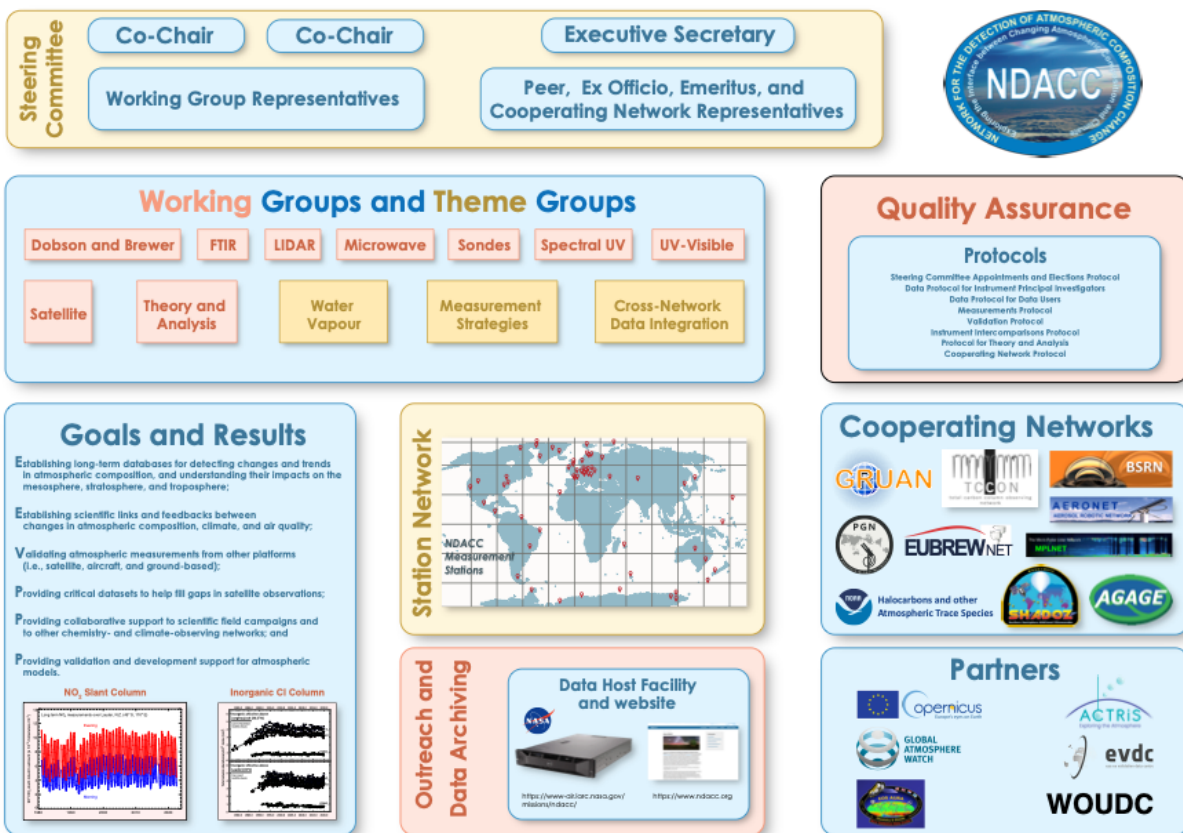
870 Collaborations within Cooperating Networks, WMO/GAW, and other agencies can be leveraged to augment NDACC
871 stations. Finding a means of incorporating data from environmental and air quality agencies is an approach to consider.
872 A compelling rationale for expanding NDACC to more urban stations is that researchers evaluating satellite products for
873 air quality and emissions estimates are a growing user community for our data.

874 Coverage of Species and Parameters (Variables Space). NDACC needs to add measurements of species that are coming
875 to greater prominence or that may not have existed or been measurable decades ago. Selection criteria must include the
876 added-value and complementarity with existing observations at a given station. NDACC instrument working groups,
877 laboratory spectroscopists, and instrument developers can support this work. With the advent of constellations of nadir-
878 looking satellites focusing on air quality pollutants and greenhouse gas observations, including those from geostationary
879 platforms, and the NRT assimilation of their data in forecast systems, we must ensure that observations are carried out
880 and assimilated as continuously as possible. The increasing automation and rapid distribution capacity of NDACC
881 observations is a must for these operations. NDACC is ready to face its future evolution and is confident that the network
882 will maintain and even strengthen its relevance provided that the required resources can be leveraged.

883 NDACC has faced, and will continue to face, challenges. However, the combined experience and substantial know-how
884 of NDACC's PIs, instrument working groups, and its associated networks should overcome these challenges, develop
885 new opportunities, and secure the continuation of the 35+ years of high-quality, long-term measurements that NDACC
886 is known for. Ground-based data remain irreplaceable for documenting key aspects of atmospheric composition in a
887 warming troposphere and a cooling stratosphere.

888 **Appendix A. NDACC Organizational structure.**

889 **Figure A1. Organizational structure of NDACC.**



890

891 **Appendix B. Spectral Range of NDACC observations.**

892 **Table B1. Definition of Solar spectral range used in the NDACC observations. See full instrument description at**
 893 **<https://ndacc.larc.nasa.gov/instruments>.**

Name & Spectral Range	Working Group & Cooperating Network	Instrumentation
UV (Ultra-Violet) 200 - 400 nm	Brewer, Dobson, UV Spectroradiometer, UV/Vis Spectrometer	Dobson, Brewer, SAOZ, MAX-DOAS, SUV-100, SUV-150B, JYHD10, Bentham (DTM300, DTMc300, DTM300V, DM150), UV (5, 6, 7), Lidar (DIAL, Rayleigh, Raman)
VIS (Visible) 400 - 700 nm	<i>AERONET</i> , <i>BSRN</i> , <i>EuBrewNet</i> , <i>MPLNet</i> , <i>PGN</i> , <i>TOLNet</i>	
NIR (Near IR) ~700 nm - 2 μm	<i>COCCON</i> , <i>TCCON</i> , <i>AERONET</i>	Bruker 120HR, Bruker EM-27
MIR (Middle Infra-Red) ~2.0 - 14.3 μm	IRWG	Bruker (120, 120M, 125M, 120HR, 125HR), JPL MkIV, Bomem (DA2, DA3, DA8), EOCOM, McMath FTS

MW (Microwave) 13.47 mm - 1.08 mm	MWWG	MIAWARA, MIAWARA-C, GROMOS, GROMOS-C, SOMORA, WIRA, WIRA-C
--------------------------------------	------	---

894 **Appendix C. List of satellite validation work and collaborative effort.**

895 **Table C1. recent and current satellite missions for which NDACC provides validation data and / or collaboration effort. Sect.**
896 **3.4 gives more details on present and upcoming missions.**

Satellite / Sensor	Product	NDACC Group	Reference paper
SAGE III / ISS	H ₂ O	Lidar, Ozonesonde	Davis et al., 2021 Wang et al., 2020
	O ₃	Lidar, Ozonesonde	Johnson et al., 2024, Mettig et al., 2022, Mettig et al., 2021
Terra/MOPITT	CO	IRWG	Gaubert et. al., 2023, 2024 ; Lutsch et. al., 2022 ; Buchholz et. al., 2017 ; Jalali et al., 2022
TEMPO	HCHO	IRWG	Ortega et al (Accepted to ESS)
	O ₃	Lidar	Johnson et al., 2018
TEMPO+GEMS	O ₃ (tot)	Brewer/Dobson	Zhao et al., 2025
GEMS	HCHO	IRWG, UV-VIS	Lee et al., 2024
NPP/CrIS	CH ₃ OH, C ₂ H ₂ , C ₂ H ₄ , C ₅ H ₈ , HCN	IRWG	Wells et al., 2022, Wells et al., 2024, Brewer et al., 2024 Wells et al. 2024
IASI	N ₂ O	IRWG	Barrret et al., 2021 Vandenbussche et. al., 2022
	CO	IRWG	Langerock et al., 2023
	HNO ₃	IRWG	Langerock et al., 2023
	CH ₄	IRWG	Dils et al., 2024
	PAN	IRWG	Mahieu et al., 2021; Wizenberg et al., 2022; Wizenberg et al., 2023
	HCOOH	IRWG	Franco et al., 2020; Franco et al., 2021
	H ₂ CO	IRWG	Kwon et al., 2023
Aura/MLS	T	Lidar; MWG	Chen et al., 2023; Navas-Guzman et al, 2017
	O ₃	MWG	Maillard Barras et al, 2020; Sauvageat et al, 2022
	ClO	MWG	Nedoluha et al., 2025
	H ₂ O	MWG	Nedoluha et al., 2022; Bell et al, 2025
		SWG, MWG	Livesey et al., 2021

SCISAT/ACE	N ₂ O	IRWG	Minganti et al, 2022
	inorganic fluorine	IRWG	Prignon et al., 2021
AURA /OMI	O ₃	SWG	Huang et al., 2017, Bak et al., 2024
	NO ₂	IRWG, UV-VIS	Souri et al., 2023
	HCHO	RWGI, UV-VIS	De Smedt et al. (2021); Ayazpour et al., 2025; Müller et al., 2024; Souri et al., 2023
SAGE III/ISS	O ₃ , WV	Lidar, O ₃ sonde	Wang et al., 2020
	Aerosol	Lidar	Knepp et al., 2020
	H ₂ O	SWG	Davis et al., 2021
GOME-2	OCIO	UV-VIS	Pinardi et al., 2022
FengYun- 3E/HIRAS-II	CO, HCOOH, PAN	IRWG	Hua et al., 2025
Copernicus S5P	H ₂ CO	IRWG, UV-VIS	De Smedt et al. (2021), Oomen et al., 2024, Müller et al., 2024, Vigouroux et al.2020
	CH ₄	IRWG	Sha et al (2020)
	O ₃	IRWG, SWG	Keppens et al., 2024
	NO ₂	UV-VIS	Verhoelst et al., 2021
GOSAT/TIR	CH ₄	IRWG	Olsen et al, 2017

899 **Data Availability**

900 The NDACC data used in this paper are archived at the Data Host Facility (DHF) that is hosted at NASA Langley
901 Research Center (LaRC). DHF is serving as a central archive and access point for atmospheric data, offering tools for
902 scientists to query and download datasets related to ozone, aerosols, and other atmospheric components: [https://www-
903 air.larc.nasa.gov/missions/ndacc/](https://www-air.larc.nasa.gov/missions/ndacc/)

904 **Author contributions**

905 MD, JCL, IP and JW conceptualized the paper. IP, MD, JW, AT, HS, JWH, RH, WS and JCL led the paper preparation.
906 All authors contributed to the writing of the paper and/or provided figures either from their published papers or updated
907 published figures.

908 **Competing interests**

909 The contact author has declared that none of the authors has any competing interests.

910 **Disclaimer**

911 The statements, findings, conclusions, and recommendations are those of the author(s) and do not necessarily reflect the
912 views of NOAA or the U.S. Department of Commerce.

913 **Acknowledgements**

914 This work has been supported in part by NOAA (grant no. NA19NES4320002; Cooperative Institute for Satellite Earth
915 System Studies – CISESS) at the University of Maryland/ESSIC and NOAA (grant no. NA22OAR4320151) for the
916 Cooperative Institute for Earth System Research and Data Science (CIESRDS). Emmanuel Mahieu is a research director
917 with F.R.S.-FNRS (Brussels, Belgium). Cloud and radiation measurements within NDACC are supported by DFG, which
918 funds the project "Cloud 3D Structure and Radiation (C3SAR). JWH & IO at the National Center for Atmospheric
919 Research are sponsored by the National Science Foundation. Part of this research was carried out at the Jet Propulsion
920 Laboratory, California Institute of Technology, under a contract with the National Aeronautics and Space Administration
921 (80NM0018D0004) The NCAR NDACC program is supported under contract by the National Aeronautics and Space
922 Administration (NASA).

923 **Financial support**

924 This research has been supported in part by NOAA (grant no. NA19NES4320002; Cooperative Institute for Satellite
925 Earth System Studies – CISESS) at the University of Maryland/ESSIC and NOAA (grant no. NA22OAR4320151) for
926 the Cooperative Institute for Earth System Research and Data Science (CIESRDS). GMI and the GEOS CCM were

927 supported by the NASA Modeling, Analysis, and Prediction program and the GEOS-GMI MINDS simulation was
928 supported by the NASA MEaSUREs program and computational resources from the NASA Center for Climate
929 Simulation.

930 **References**

- 931 Adcock, K. E., Fraser, P. J., Hall, B. D., Langenfelds, R. L., Lee, G., Montzka, S. A., Oram, D. E., Rockmann, T., Stroh,
932 F., Sturges, W. T., Vogel, B., and Laube, J. C. (2021). Aircraft-Based Observations of Ozone-Depleting Substances in
933 the Upper Troposphere and Lower Stratosphere in and Above the Asian Summer Monsoon. *J. Geophys. Res.*, **126**,
934 e2020JD033137. <https://doi.org/10.1029/2020JD033137>.
- 935 Asher E, Baron A, Yu P, Todt M, Smale P, Liley B, Querel R, Sakai T, Morino I, Jin Y, Nagai T, Uchino O, Hall E,
936 Cullis P, Johnson B, and Thornberry TD: Balloon baseline stratospheric aerosol profiles (B2SAP)—perturbations in the
937 southern hemisphere, 2019–2022, *J. Geophys. Res.-Atmos.*, **129**, e2024JD041581, 2024.
938 <https://doi.org/10.1029/2024JD041581>
- 939 Asher E, Todt M, Rosenlof K, Thornberry T, Gao R, Taha G, Walter P, Alvarez S, Flynn J, Davis S, Evan S, Brioude J,
940 Metzger J-M, Hurst DF, Hall E, and Xiong K (2023), Unexpectedly rapid aerosol formation in the Hunga Tonga plume,
941 *Proc. Natl. Acad. Sci.*, **120**, e2219547120, <https://doi.org/10.1073/pnas.2219547120>
- 942 Agustí-Panareda, A., Barré, J., Massart, S., Inness, A., Aben, I., Ades, M., Baier, B. C., Balsamo, G., Borsdorff, T.,
943 Bousserez, N., Boussetta, S., Buchwitz, M., Cantarello, L., Crevoisier, C., Engelen, R., Eskes, H., Flemming, J.,
944 Garrigues, S., Hasekamp, O., Huijnen, V., Jones, L., Kipling, Z., Langerock, B., McNorton, J., Meilhac, N., Noël, S.,
945 Parrington, M., Peuch, V.-H., Ramonet, M., Razinger, M., Reuter, M., Ribas, R., Suttie, M., Sweeney, C., Tarniewicz,
946 J., and Wu, L.: Technical note: The CAMS greenhouse gas reanalysis from 2003 to 2020, *Atmos. Chem. Phys.*, **23**,
947 3829–3859, <https://doi.org/10.5194/acp-23-3829-2023>, 2023.
- 948 Ayazpour, Z., González Abad, G., Nowlan, C. R., Sun, K., Kwon, H.-A., Chan Miller, C., et al. (2025). Aura ozone
949 monitoring instrument (OMI) Collection 4 formaldehyde products. *Earth and Space Science*, **12**, e2024EA003792.
950 <https://doi.org/10.1029/2024EA003792>
- 951 Bak, J., Liu, X., Yang, K., Gonzalez Abad, G., O'Sullivan, E., Chance, K., and Kim, C.-H.: An improved OMI ozone
952 profile research product version 2.0 with collection 4 L1b data and algorithm updates, *Atmos. Meas. Tech.*, **17**, 1891–
953 1911, <https://doi.org/10.5194/amt-17-1891-2024>, 2024.
- 954 Ball, WT, Krivošova N, Rozanov E V., et al. (2018). The Upper Troposphere and Lower Stratosphere as a key region
955 for future tropical ozone, *Atmos. Chem. Phys.*, **18**, 1379–1392, <https://doi.org/10.5194/acp-18-1379-2018>
- 956 Baron, A., Chazette, P., Khaykin, S., Payen, G., Marquestaut, N., Bègue, N., and Dufлот, V. (2023). Early evolution of
957 the stratospheric aerosol plume following the 2022 Hunga Tonga-Hunga Ha'apai eruption: Lidar observations from
958 Reunion (21°S, 55°E). *Geophysical Research Letters*, **50**, e2022GL101751.
- 959 Barret B, Gouzenes Y, Le Flochmoen E, Ferrant S. Retrieval of Metop-A/IASI N2O Profiles and Validation with
960 NDACC FTIR Data. *Atmosphere*. 2021; 12(2):219. <https://doi.org/10.3390/atmos12020219>
- 961 Basher, R. E. (1982): “Review of the Dobson spectrophotometer and its accuracy”, WMO Global Ozone Research and
962 Monitoring, Report No. 13, Geneva, Switzerland. <https://gml.noaa.gov/ozwv/dobson/papers/report13/report13.html> (last
963 access: 11 April 2024).
- 964 Bell, A., Sauvageat, E., Stober, G., Hocke, K., and Murk, A.: Developments on a 22 GHz microwave radiometer and
965 reprocessing of 13-year time series for water vapour studies, *Atmos. Meas. Tech.*, **18**, 555–567,
966 <https://doi.org/10.5194/amt-18-555-2025>, 2025.
- 967 Bernhard, G., & Stierle, S. (2020). Trends of UV radiation in Antarctica. *Atmosphere*, **11**(8), 795.
- 968 Bernhard, G.H., Bais, A.F., Aucamp, P.J. et al. Stratospheric ozone, UV radiation, and climate interactions. *Photochem*
969 *Photobiol Sci* **22**, 937–989 (2023). <https://doi.org/10.1007/s43630-023-00371-y>
- 970 Bjorklund, R., Vigouroux, C., Effertz, P., García, O. E., Geddes, A., Hannigan, J., Miyagawa, K., Kotkamp, M.,
971 Langerock, B., Nedoluha, G., Ortega, I., Petropavlovskikh, I., Poyraz, D., Querel, R., Robinson, J., Shiona, H., Smale,

- 972 D., Smale, P., Van Malderen, R., and De Maziere, M. (2024). Intercomparison of long-term ground-based measurements
973 of total, tropospheric, and stratospheric ozone at Lauder, New Zealand. *Atmos. Meas. Tech.*, **17**, 6819–6849.
974 <https://doi.org/10.5194/amt-17-6819-2024>.
- 975 Bogner, K., Alwarda, R., Strong, K., Chipperfield, M. P., Dhomse, S. S., Drummond, J. R., et al. (2021). Unprecedented
976 spring 2020 ozone depletion in the context of 20 years of measurements at Eureka, Canada. *Journal of Geophysical*
977 *Research: Atmospheres*, 126, e2020JD034365. <https://doi.org/10.1029/2020JD034365>
- 978 Boone, C. D., Bernath, P. F., and Fromm, M. D. (2020). Pyrocumulonimbus stratospheric plume injections measured by
979 the ACE-FTS. *Geophysical Research Letters*, **47**(15), e2020GL088442.
- 980 Brewer, J.F., Millet, D.B., Wells, K.C. et al. Space-based observations of tropospheric ethane map emissions from fossil
981 fuel extraction. *Nat Commun* 15, 7829 (2024). <https://doi.org/10.1038/s41467-024-52247-z>
- 982 Broderick, A. J., and T. M. Hard. (1974). Proceedings of the Third Conference on the Climatic Impact Assessment
983 Program, February 26-March 1, 1974. U. S. Dept. of Transportation, Cambridge, MA, 672 pp.
984 <https://ntrl.ntis.gov/NTRL/dashboard/searchResults/titleDetail/ADA003846.xhtml#>.
- 985 Brogniez, C., Doré, J. F., Auriol, F., Cesarini, P., Minvielle, F., Deroo, C., & Da Conceicao, P. (2021). Erythematous and
986 vitamin D weighted solar UV dose-rates and doses estimated from measurements in mainland France and on Reunion
987 Island. *Journal of Photochemistry and Photobiology B: Biology*, **225**, 112330.
- 988 Buchholz, J., Querner, P., Paredes, D. et al. Soil biota in vineyards are more influenced by plants and soil quality than by
989 tillage intensity or the surrounding landscape. *Sci Rep* 7, 17445 (2017). <https://doi.org/10.1038/s41598-017-17601-w>
- 990 Charlesworth, E., Ploger, F., Birner, T., Baikhadzhaev, R., Abalos, M., Abraham, N. L., Akiyoshi, H., Bekki, S.,
991 Dennison, F., Jockel, P., Keeble, J., Kinnison, D., Morgenstern, O., Plummer, D., Rozanov, E., Strode, S., Zeng, G.,
992 Egorova, T. & Riese, M. (2023). Stratospheric water vapor affecting atmospheric circulation. *Nat Commun* **14**, 3925.
- 993 Chen, Z., Schwartz, M. J., Bhartia, P. K., Schoeberl, M., Kramarova, N., Jaross, G., and DeLand, M. (2023). Mesospheric
994 and upper stratospheric temperatures from OMPS-LP. *Earth and Space Science*, **10**(5):e2022EA002763.
- 995 Chipperfield, M. P., Hegglin, M. I., A., M. S., Newman, P. A., Park, S., Reimann, S., Rigby, M., Stohl, A., Velders, G.
996 J. M., Walter-Terrinoni, H. and Yao, B. (2021). **Report on the Unexpected Emissions of CFC-11**.
- 997 Chipperfield, M. P., Liang, Q., Rigby, M., Hossaini, R., Montzka, S. A., Dhomse, S., Feng, W., Prinn, R. G., Weiss, R.
998 F., Harth, C. M., Salameh, P. K., Muhle, J., O'Doherty, S., Young, D., Simmonds, P. G., Krummel, P. B., Fraser, P. J.,
999 Steele, L. P., Happell, J. D., Rhew, R. C., Butler, J., Yvon-Lewis, S. A., Hall, B., Nance, D., Moore, F., Miller, B. R.,
1000 Elkins, J. W., Harrison, J. J., Boone, C. D., Atlas, E. L. and Mahieu, E. (2016). Model sensitivity studies of the decrease
1001 in atmospheric carbon tetrachloride. *Atmos. Chem. Phys.*, **16**(24), 15741–15754. doi:10.5194/acp-16-15741-2016.
- 1002 Chouza, F., Leblanc, T., Brewer, M., Wang, P., Martucci, G., Haeefe, A., Vèrèmes, H., Duflo, V., Payen, G., and
1003 Keckhut, P.: The impact of aerosol fluorescence on long-term water vapor monitoring by Raman lidar and evaluation of
1004 a potential correction method, *Atmos. Meas. Tech.*, **15**, 4241–4256, <https://doi.org/10.5194/amt-15-4241-2022>, 2022.
- 1005 Chouza, F., Leblanc, T., Wang, P., Brown, S. S., Zuraski, K., Chace, W., Womack, C. C., Peischl, J., Hair, J., Shingler,
1006 T., and Sullivan, J.: The Small Mobile Ozone Lidar (SMOL): instrument description and first results, *Atmos. Meas.*
1007 *Tech.*, **18**, 405–419, <https://doi.org/10.5194/amt-18-405-2025>, 2025.
- 1008 Compernelle, S., A. Argyrouli, R. Lutz, M. Sneep, J.-C. Lambert, A. M. Fjaeraa, D. Hubert, A. Keppens, D. Loyola, E.
1009 O'Connor, F. Romahn, P. Stammes, T. Verhoelst, and P. Wang, Validation of the Sentinel-5 Precursor TROPOMI cloud
1010 data with Cloudnet, Suomi-NPP VIIRS and OMI O2-O2 (2021). *Atmos. Meas. Tech.*, Vol. **14**, 2451–2476,
1011 <https://doi.org/10.5194/amt-14-2451-2021>
- 1012 Cordero R. R., Feron S., Damiani A., Sepúlveda E., Jorquera J., Redondas A., Seckmeyer G., Carrasco J., Rowe P.,
1013 Ouyang Z. (2023). Surface Solar Extremes in the Most Irradiated Region on Earth, Altiplano. *Bulletin of the American*
1014 *Meteorological Society (BAMS)*. DOI 10.1175/BAMS-D-22-0215.1.
- 1015 Cordero, R. R., Feron, S., Damiani, A., Redondas, A., Carrasco, J., Sepúlveda, E., & Seckmeyer, G. (2022). Persistent
1016 extreme ultraviolet irradiance in Antarctica despite the ozone recovery onset. *Scientific reports*, **12**(1), 1266.
1017 <https://doi.org/10.1038/s41598-022-05449-8>.
- 1018 Cordero, R.R., Seckmeyer, G., Damiani, A. et al. (2014). The world's highest levels of surface UV. *Photochem Photobiol*
1019 *Sci* **13**, 70-81. <https://doi.org/10.1039/c3pp50221j>.

- 1020 Dammers, E., Vigouroux, C., Palm, M., Mahieu, E., Warneke, T., Smale, D., Langerock, B., Franco, B., Van Damme,
1021 M., Schaap, M., Notholt, J., and Erisman, J. W.: Retrieval of ammonia from ground-based FTIR solar spectra, *Atmos.*
1022 *Chem. Phys.*, **15**, 12789–12803, <https://doi.org/10.5194/acp-15-12789-2015>, 2015.
- 1023 Davis, S. M., Damadeo, R., Flittner, D., Rosenlof, K. H., Park, M., Randel, W. J., et al. (2021). Validation of SAGE
1024 III/ISS solar water vapor data with correlative satellite and balloon-borne measurements. *Journal of Geophysical*
1025 *Research: Atmospheres*, **126**, e2020JD033803. <https://doi.org/10.1029/2020JD033803>
- 1026 De Mazière, et al. (2018). The Network for the Detection of Atmospheric Composition Change (NDACC): history, status
1027 and perspectives. *Atmos. Chem. Phys.*, **18**, 4935. <https://doi.org/10.5194/acp-18-4935-2018>.
- 1028 de Laat, A. T. J., R. J. van der A, M. A. F. Allaart, M. van Weele, G. C. Benitez, C. Casiccia, N. M. Paes Leme, E. Quel,
1029 J. Salvador, and E. Wolfram (2010), Extreme sunbathing: Three weeks of small total O₃ columns and high UV radiation
1030 over the southern tip of South America during the 2009 Antarctic O₃ hole season. *Geophys. Res. Lett.*, **37**, L14805.
1031 doi:10.1029/2010GL043699.
- 1032 De Smedt, I., Pinardi, G., Vigouroux, C., Compornolle, S., Bais, A., Benavent, N., Boersma, F., Chan, K.-L., Donner,
1033 S., Eichmann, K.-U., Hedelt, P., Hendrick, F., Irie, H., Kumar, V., Lambert, J.-C., Langerock, B., Lerot, C., Liu, C.,
1034 Loyola, D., PETERS, A., Richter, A., Rivera Cárdenas, C., Romahn, F., Ryan, R. G., Sinha, V., Theys, N., Vlietinck, J.,
1035 Wagner, T., Wang, T., Yu, H., and Van Roozendaal, M.: Comparative assessment of TROPOMI and OMI formaldehyde
1036 observations and validation against MAX-DOAS network column measurements, *Atmos. Chem. Phys.*, **21**, 12561–
1037 12593, <https://doi.org/10.5194/acp-21-12561-2021>, 2021.
- 1038 Dils, B., Zhou, M., Camy-Peyret, C., De Mazière, M., Kangah, Y., Langerock, B., Prunet, P., Serio, C., Siddans, R., and
1039 Kerridge, B.: Independent validation of IASI/MetOp-A LMD and RAL CH₄ products using CAMS model, in situ
1040 profiles, and ground-based FTIR measurements, *Atmos. Meas. Tech.*, **17**, 5491–5524, [https://doi.org/10.5194/amt-17-](https://doi.org/10.5194/amt-17-5491-2024)
1041 [5491-2024](https://doi.org/10.5194/amt-17-5491-2024), 2024.
- 1042 Duncan, B. N., Strahan, S. E., Yoshida, Y., Steenrod, S. D., and Livesey, N. (2007). Model study of the cross-tropopause
1043 transport of biomass burning pollution. *Atmos. Chem. Phys.*, **7**, 3713–3736. <https://doi.org/10.5194/acp-7-3713-2007>.
- 1044 Evan, S., et al. (2023). Rapid ozone depletion after humidification of the stratosphere by the Hunga Tonga eruption.
1045 *Science*, **382**, 282. <https://doi.org/10.1126/science.adg2551>.
- 1046 Fisher, B.L., Lamsal, L.N., Fasnacht, Z., Oman, L.D., Joiner, J., Krotkov, N.A., Choi, S., Qin, W. and Yang, E.S. (2024).
1047 Revised estimates of NO₂ reductions during the COVID-19 lockdowns using updated TROPOMI NO₂ retrievals and
1048 model simulations. *Atmospheric Environment*, **326**, 120459.
- 1049 Flood et al., 2025. <https://doi.org/10.1029/2024JD042254>.
- 1050 Franco, B., Clarisse, L., Stavrakou, T., Müller, J.-F., Taraborrelli, D., Hadji-Lazaro, J., et al. (2020). Spaceborne
1051 measurements of formic and acetic acids: A global view of the regional sources. *Geophysical Research Letters*, **47**,
1052 e2019GL086239. <https://doi.org/10.1029/2019GL086239>.
- 1053 Franco B., Blumenstock T., Cho C., Clarisse L., Clerbaux C., Coheur P.F., De Mazière M., De Smedt I., Dorn H.P.,
1054 Emmerichs T., Fuchs H., Gkatzelis G., Griffith D.W.T., Hannigan J.W., Hase F., Jones N., Kerkweg A., Kiendler-Scharr
1055 A., Mahieu E., Novelli A., Ortega I., Paton-Walsh C., Pommier M., Pozzer A., Reimer D., Rosanka S., Sander R.,
1056 Schneider M., Strong K., Tillmann R., Van Roozendaal M., Vereecken L., Vigouroux C., Wahner A., Taraborrelli D.
1057 (2021). Ubiquitous atmospheric production of organic acids mediated by cloud droplets. *Nature*, **593**(7858), 233–237.
1058 doi:10.1038/s41586-021-03462-x.
- 1059 Garane, K., Koukouli, M.-E., Verhoelst, T., Fioletov, V., Lerot, C., Heue, K.-P., Bais, A., Balis, D., Bazureau, A., Dehn,
1060 A., Goutail, F., Granville, J., Griffin, D., Hubert, D., Keppens, A., Lambert, J.-C., Loyola, D., McLinden, C., Pazmino,
1061 A., Pommereau, J.-P., Redondas, A., Romahn, F., Valks, P., Van Roozendaal, M., Xu, J., Zehner, C., Zerefos, C., and
1062 Zimmer, W. (2019). TROPOMI/S5P total ozone column data: global ground-based validation & consistency with other
1063 satellite missions, *Atmos. Meas. Tech.*, <https://doi.org/10.5194/amt-2019-147>
- 1064 Garrett, K., Liu, H., Ide, K., Hoffman, R.N. & Lukens, K.E. (2022). Optimization and impact assessment of Aeolus
1065 HLOS wind assimilation in NOAA's global forecast system. *Quarterly Journal of the Royal Meteorological Society*,
1066 **148**(747), 2703–2716. <https://doi.org/10.1002/qj.4331>.

- 1067 Gaubert, B., Stephens, B. B., Baker, D. F., Basu, S., Bertolacci, M., Bowman, K. W., et al. (2023). Neutral tropical
1068 African CO₂ exchange estimated from aircraft and satellite observations. *Global Biogeochemical Cycles*, 37,
1069 e2023GB007804. <https://doi.org/10.1029/2023GB007804>
- 1070 Gaudel, A., O. R. Cooper, et al. (2018). Tropospheric Ozone Assessment Report: Present-day distribution and trends of
1071 tropospheric ozone relevant to climate and global atmospheric chemistry model evaluation. *Elem. Sci. Anth.*, 6(1):39.
1072 doi: <https://doi.org/10.1525/elementa.291>.
- 1073 Gaudel, A, Bourgeois, I, Li, M, Chang KL et al: Tropical tropospheric ozone distribution and trends from in situ and
1074 satellite data, *Atmos. Chem. Phys.*, <https://doi.org/10.5194/acp-24-9975-2024>
- 1075 Gelaro, R., McCarty, W., Suárez, M.J., Todling, R., Molod, A., Takacs, L., Randles, C.A., Darmenov, A., Bosilovich,
1076 M.G., Reichle, R. and Wargan, K. (2017). The modern-era retrospective analysis for research and applications, version
1077 2 (MERRA-2). *Journal of Climate*, 30(14), 5419-5454.
- 1078 Godin-Beekmann, S., Azouz, N., Sofieva, V. F., Hubert, D., Petropavlovskikh, I., Effertz, P., Ancellet, G., Degenstein,
1079 D. A., Zawada, D., Froidevaux, L., Frith, S., Wild, J., Davis, S., Steinbrecht, W., Leblanc, T., Querel, R., Tourpali, K.,
1080 Damadeo, R., Maillard Barras, E., Stübi, R., Vigouroux, C., Arosio, C., Nedoluha, G., Boyd, I., Van Malderen, R.,
1081 Mahieu, E., Smale, D., and Sussmann, R.: Updated trends of the stratospheric ozone vertical distribution in the 60° S–
1082 60° N latitude range based on the LOTUS regression model , *Atmos. Chem. Phys.*, 22, 11657–11673,
1083 <https://doi.org/10.5194/acp-22-11657-2022>, 2022.
- 1084 Goldman, A., Paton-Walsh, C., Bell, W., Toon, G., Blavier, J., Sen, B., Coffey, M., Hannigan, J., and Mankin, W. (1999).
1085 Network for the Detection of Stratospheric Change Fourier Transform Infrared Intercomparison at Table Mountain
1086 Facility, November 1996. *Journal of Geophysical Research-Atmospheres*, 104(D23):30481–30503.
- 1087 Goryl, P.; Fox, N.; Donlon, C.; Castracane, P. (2023). Fiducial Reference Measurements (FRMs): What Are They?
1088 *Remote Sensing*, 15(20), 5017. <https://doi.org/10.3390/rs15205017>.
- 1089 Graßl, S., Ritter, C., Tritscher, I., and Vogel, B.: Does the Asian summer monsoon play a role in the stratospheric aerosol
1090 budget of the Arctic?, *Atmos. Chem. Phys.*, 24, 7535–7557, <https://doi.org/10.5194/acp-24-7535-2024>, URL
1091 <https://acp.copernicus.org/articles/24/7535/2024/>, 2024.
- 1092 Groöß, J.-U., Müller, R., Crowley, J. N., & Hegglin, M. I. (2025). Chlorine peroxide reaction explains observed
1093 wintertime hydrogen chloride in the antarctic vortex. *Communications Earth & Environment*, 6(1), 1–8.
- 1094 Hagen, J., Murk, A., Rüfenacht, R., Khaykin, S., Hauchecorne, A., and Kämpfer, N. (2018). WIRA-C: a compact 142-
1095 GHz-radiometer for continuous middle-atmospheric wind measurements. *Atmos. Meas. Tech.*, 11, 5007–5024.
1096 <https://doi.org/10.5194/amt-11-5007-2018>.
- 1097 Hall, E. G., Jordan, A. F., Hurst, D. F., Oltmans, S. J., Vömel, H., Kühnreich, B., and Ebert, V.: Advancements,
1098 measurement uncertainties, and recent comparisons of the NOAA frost point hygrometer, *Atmos. Meas. Tech.*, 9, 4295–
1099 4310, <https://doi.org/10.5194/amt-9-4295-2016>, 2016.
- 1100 Hannigan, J. W., Ortega, I., Shams, S. B., Blumenstock, T., Campbell, J. E., Conway, S., et al. (2022). Global atmospheric
1101 OCS trend analysis from 22 NDACC stations. *Journal of Geophysical Research: Atmospheres*, 127, e2021JD035764.
1102 <https://doi.org/10.1029/2021JD035764>.
- 1103 Herman, J., Evans, R., Cede, A., Abuhassan, N., Petropavlovskikh, I., and McConville, G. (2015). Comparison of ozone
1104 retrievals from the Pandora spectrometer system and Dobson spectrophotometer in Boulder, Colorado. *Atmos. Meas.*
1105 *Tech.*, 8, 3407–3418. <https://doi.org/10.5194/amt-8-3407-2015>.
- 1106 Herrera, B., Bezanilla, A., Blumenstock, T., Dammers, E., Hase, F., Clarisse, L., Magaldi, A., Rivera, C., Stremme, W.,
1107 Strong, K., Viatte, C., Van Damme, M., and Grutter, M.: Measurement report: Evolution and distribution of NH₃ over
1108 Mexico City from ground-based and satellite infrared spectroscopic measurements, *Atmos. Chem. Phys.*, 22, 14119–
1109 14132, <https://doi.org/10.5194/acp-22-14119-2022>, 2022.
- 1110 Hicks-Jalali, S., R. J. Sica, G. Martucci, E. Maillard Barras, J. Voirin, and A. Haefele (2020). A Raman lidar tropospheric
1111 water vapour climatology and height-resolved trend analysis over Payerne, Switzerland. *Atmos. Chem. Phys.*, 20(16),
1112 9619-9640.
- 1113 Huang, G., Liu, X., Chance, K., Yang, K., Bhartia, P. K., Cai, Z., Allaart, M., Ancellet, G., Calpini, B., Coetzee, G. J.
1114 R., Cuevas-Agulló, E., Cupeiro, M., De Backer, H., Dubey, M. K., Fuelberg, H. E., Fujiwara, M., Godin-Beekmann, S.,
1115 Hall, T. J., Johnson, B., Joseph, E., Kivi, R., Kois, B., Komala, N., König-Langlo, G., Laneve, G., Leblanc, T., Marchand,

1116 M., Minschwaner, K. R., Morris, G., Newchurch, M. J., Ogino, S.-Y., Ohkawara, N., Piters, A. J. M., Posny, F., Querel,
1117 R., Scheele, R., Schmidlin, F. J., Schnell, R. C., Schrems, O., Selkirk, H., Shiotani, M., Skrivánková, P., Stübi, R., Taha,
1118 G., Tarasick, D. W., Thompson, A. M., Thouret, V., Tully, M. B., Van Malderen, R., Vömel, H., von der Gathen, P.,
1119 Witte, J. C., and Yela, M.: Validation of 10-year SAO OMI Ozone Profile (PROFOZ) product using ozonesonde
1120 observations, *Atmos. Meas. Tech.*, **10**, 2455–2475, <https://doi.org/10.5194/amt-10-2455-2017>, 2017.

1121 Hubert, D., K.-P. Heue, J.-C. Lambert, T. Verhoelst, M. Allaart, S. Compernelle, P. D. Cullis, A. Dehn, C. Félix, B. J.
1122 Johnson, A. Keppens, D. E. Kollonige, C. Lerot, D. Loyola, M. Mohamad, M. Paulete Pereira Martins, A. J. M. Piters,
1123 Selkirk, H. B., A. M. Thompson, P. Veefkind, H. Vömel, J. C. Witte, and C. Zehner (2021). TROPOMI tropospheric
1124 ozone column data : Geophysical assessment and comparison to ozonesondes, GOME-2B and OMI, *Atmos. Meas. Tech.*,
1125 **14**, 7405–7433, <https://doi.org/10.5194/amt-14-7405-2021>

1126 Hubert, D., Miyazaki, K., Dufour, G., Pennington, E. A., Sofieva, V., Arosio, C., Barret, B., Boynard, A., Coldewey-
1127 Egbers, M., Cuesta, J., Heue, K.-P., Keppens, A., Kramarova, N. A., Lambert, J.-C., Loyola, D., Orfanoz-Cheuquela,
1128 A. P., Siddans, R., Van Malderen, R., Veefkind, P., Wespes, C., and Ziemke, J. R.: Tropospheric Ozone Assessment
1129 Report II: Past and present tropospheric ozone using satellite observations, *Phil. Trans. R. Soc. A* (in review), 2026.

1130 Jalali, A., Walker, K. A., Strong, K., Buchholz, R. R., Deeter, M. N., Wunch, D., Roche, S., Wizenberg, T., Lutsch, E.,
1131 McGee, E., Worden, H. M., Fogal, P., and Drummond, J. R.: A comparison of carbon monoxide retrievals between the
1132 MOPITT satellite and Canadian high-Arctic ground-based NDACC and TCCON FTIR measurements, *Atmos. Meas.*
1133 *Tech.*, **15**, 6837–6863, <https://doi.org/10.5194/amt-15-6837-2022>, 2022.

1134 Johnson, M. S., Philip, S., Meech, S., Kumar, R., Sorek-Hamer, M., Shiga, Y. P., and Jung, J.: Insights into the long-
1135 term (2005–2021) spatiotemporal evolution of summer ozone production sensitivity in the Northern Hemisphere derived
1136 with the Ozone Monitoring Instrument (OMI), *Atmos. Chem. Phys.*, **24**, 10363–10384, [https://doi.org/10.5194/acp-24-](https://doi.org/10.5194/acp-24-10363-2024)
1137 [10363-2024](https://doi.org/10.5194/acp-24-10363-2024), 2024.

1138 John SS, Deutscher NM, Paton-Walsh C, Velazco VA, Jones NB, Griffith DWT. 2019–20 Australian Bushfires and
1139 Anomalies in Carbon Monoxide Surface and Column Measurements. *Atmosphere*. 2021; 12(6):755.
1140 <https://doi.org/10.3390/atmos12060755>

1141 Johnson, M. S., Liu, X., Zoogman, P., Sullivan, J., Newchurch, M. J., Kuang, S., Leblanc, T., and McGee, T.: Evaluation
1142 of potential sources of a priori ozone profiles for TEMPO tropospheric ozone retrievals, *Atmos. Meas. Tech.*, **11**, 3457–
1143 3477, <https://doi.org/10.5194/amt-11-3457-2018>, 2018.

1144 Keppens, A., Di Pede, S., Hubert, D., Lambert, J.-C., Veefkind, P., Sneep, M., De Haan, J., ter Linden, M., Leblanc, T.,
1145 Compernelle, S., Verhoelst, T., Granville, J., Nath, O., Fjaeraa, A. M., Boyd, I., Niemeijer, S., Van Malderen, R., Smit,
1146 H. G. J., Duflo, V., Godin-Beekmann, S., Johnson, B. J., Steinbrecht, W., Tarasick, D. W., Kollonige, D. E., Stauffer,
1147 R. M., Thompson, A. M., Dehn, A., and Zehner, C. (2024). Five years of Sentinel-5p TROPOMI operational ozone
1148 profiling and geophysical validation using ozonesonde and lidar ground-based networks, *Atmos. Meas. Tech.*, **17**, 3969–
1149 3993, <https://doi.org/10.5194/amt-2023-264>

1150 Khaykin, S., Bekki, S., Godin-Beekmann, S., Fromm, M. D., Goloub, P., Hu, Q., Josse, B., Laeng, A., Meziane, M.,
1151 Peterson, D. A., Pelletier, S., and Thouret, V. (2025). Stratospheric impact of the anomalous 2023 Canadian wildfires:
1152 the two vertical pathways of smoke. *Atmos. Chem. Phys.*, **25**, 14551–14571. <https://doi.org/10.5194/acp-25-14551-2025>.

1153 Khaykin, S., Legras, B., Bucci, S. et al. (2020). The 2019/20 Australian wildfires generated a persistent smoke-charged
1154 vortex rising up to 35 km altitude. *Commun Earth Environ* **1**, 22. <https://doi.org/10.1038/s43247-020-00022-5>.

1155 Khaykin, S., Podglajen, A., Ploeger, F. et al. (2022). Global perturbation of stratospheric water and aerosol burden by
1156 Hunga eruption. *Commun Earth Environ* **3**, 316. <https://doi.org/10.1038/s43247-022-00652-x>.

1157 Khaykin, S. M., et al. (2017). Variability and evolution of the midlatitude stratospheric aerosol budget from 22 years of
1158 ground-based lidar and satellite observations. *Atmos. Chem. Phys.*, **17**(3), 1829–1845.

1159 Khaykin, S. M., Hauchecorne, A., Wing, R., Keckhut, P., Godin-Beekmann, S., Porteneuve, J., Mariscal, J.-F., and
1160 Schmitt, J (2020). Doppler lidar at Observatoire de Haute-Provence for wind profiling up to 75 km altitude: performance
1161 evaluation and observations. *Atmos. Meas. Tech.*, **13**, 1501–1516. <https://doi.org/10.5194/amt-13-1501-2020>.

1162 Knepp, T. N., Thomason, L., Roell, M., Damadeo, R., Leavor, K., Leblanc, T., Chouza, F., Khaykin, S., Godin-
1163 Beekmann, S., and Flittner, D.: Evaluation of a method for converting Stratospheric Aerosol and Gas Experiment
1164 (SAGE) extinction coefficients to backscatter coefficients for intercomparison with lidar observations, *Atmos. Meas.*
1165 *Tech.*, **13**, 4261–4276, <https://doi.org/10.5194/amt-13-4261-2020>, 2020.

1166 Kurylo, M. J., Thompson, A. M., and De Mazière, M.: The Network for the Detection of Atmospheric Composition
1167 Change: 25 Years Old and Going Strong, *The Earth Observer*, 28, 4–15, 2016.

1168 Kwon, H.-A., González Abad, G., Nowlan, C. R., Chong, H., Souri, A. H., Vigouroux, C., Röhling, A., Kivi, R.,
1169 Makarova, M., Notholt, J., Palm, M., Winkler, H., Té, Y., Sussmann, R., Rettinger, M., Mahieu, E., Strong, K., Lutsch,
1170 E., Yamanouchi, S., Nagahama, T., Hannigan, J. W., Zhou, M., Murata, I., Grutter, M., Stremme, W., De Mazière, M.,
1171 Jones, N., Smale, D., Morino, I. (2023). Validation of OMPS Suomi NPP and OMPS NOAA-20 Formaldehyde Total
1172 Columns with NDACC FTIR Observations. *Earth and Space Science*, **10**(5). <https://doi.org/10.1029/2022EA002778>.

1173 Laj, P., and Coauthors, 2024: Aerosol, Clouds and Trace Gases Research Infrastructure (ACTRIS): The European
1174 Research Infrastructure Supporting Atmospheric Science. *Bull. Amer. Meteor. Soc.*, **105**, E1098–E1136,
1175 <https://doi.org/10.1175/BAMS-D-23-0064.1>.

1176 Langerock, B. et al., (2023): Validation Report IASI, CO, CDR, Nov 2025.
1177 https://acsaf.org/docs/vr/Validation_Report_IASI_CO_CDR_Nov_2023.pdf

1178 Langerock, B., et al., (2023): Validation Report IASI HNO3 April 2022,
1179 https://acsaf.org/docs/vr/Validation_Report_IASI_HNO3_Apr_2022.pdf

1180 Laube, J. C., Tegtmeier, S., Fernandez, R. P., Harrison, J., Hu, L., Krummel, P., Mahieu, E., Park, S. and Western, L.
1181 (2022). Update on Ozone-Depleting Substances (ODSs) and Other Gases of Interest to the Montreal Protocol, in
1182 *Scientific Assessment of Ozone Depletion: 2022*, World Meteorological Organization.

1183 Lauther, V., Vogel, B., Wintel, J., Rau, A., Hoor, P., Bense, V., Müller, R., and Volk, C. M. (2022). In situ observations
1184 of CH₂Cl₂ and CHCl₃ show efficient transport pathways for very short-lived species into the lower stratosphere via the
1185 Asian and the North American summer monsoon. *Atmos. Chem. Phys.*, **22**, 2049–2077. [https://doi.org/10.5194/acp-22-](https://doi.org/10.5194/acp-22-2049-2022)
1186 [2049-2022](https://doi.org/10.5194/acp-22-2049-2022).

1187 Leblanc, T., I. S. McDermid, and T. D. Walsh (2012). Ground-based water vapor raman lidar measurements up to the
1188 upper troposphere and lower stratosphere for long-term monitoring. *Atmos. Meas. Tech.*, **5**(1), 17–36.

1189 Lee, G. T., Park, R. J., Kwon, H.-A., Ha, E. S., Lee, S. D., Shin, S., Ahn, M.-H., Kang, M., Choi, Y.-S., Kim, G., Lee,
1190 D.-W., Kim, D.-R., Hong, H., Langerock, B., Vigouroux, C., Lerot, C., Hendrick, F., Pinardi, G., De Smedt, I., Van
1191 Roozendaal, M., Wang, P., Chong, H., Cho, Y., and Kim, J. (2024). First evaluation of the GEMS formaldehyde product
1192 against TROPOMI and ground-based column measurements during the in-orbit test period. *Atmos. Chem. Phys.*, **24**,
1193 4733–4749. <https://doi.org/10.5194/acp-24-4733-2024>.

1194 Livesey, N. J., Read, W. G., Froidevaux, L., Lambert, A., Santee, M. L., Schwartz, M. J., Millán, L. F., Jarnot, R. F.,
1195 Wagner, P. A., Hurst, D. F., Walker, K. A., Sheese, P. E., and Nedoluha, G. E.: Investigation and amelioration of long-
1196 term instrumental drifts in water vapor and nitrous oxide measurements from the Aura Microwave Limb Sounder (MLS)
1197 and their implications for studies of variability and trends, *Atmos. Chem. Phys.*, 21, 15409–15430,
1198 <https://doi.org/10.5194/acp-21-15409-2021>, 2021.

1199 Lutsch, E., Strong, K., Jones, D. B., Ortega, I., Hannigan, J. W., Dammers, E., et al. (2019). Unprecedented atmospheric
1200 ammonia concentrations detected in the high Arctic from the 2017 Canadian wildfires. *Journal of Geophysical Research:*
1201 *Atmospheres*, 124(14), 8178–8202. <https://doi.org/10.1029/2019jd030419>

1202 Lutsch, E., Wunch, D., Jones, D.B.A., et al. (2022), Can the data assimilation of CO from MOPITT or IASI constrain
1203 high-latitude wildfire emissions? A Case Study of the 2017 Canadian Wildfires. ESS Open Archive, DOI:
1204 10.1002/essoar.10510875.1

1205 Maillard Barras, E., Haeferle, A., Stübi, R., Jouberton, A., Schill, H., Petropavlovskikh, I., Miyagawa, K., Stanek, M.,
1206 and Froidevaux, L.: Dynamical linear modeling estimates of long-term ozone trends from homogenized Dobson Umkehr
1207 profiles at Arosa/Davos, Switzerland, *Atmos. Chem. Phys.*, 22, 14283–14302, [https://doi.org/10.5194/acp-22-14283-](https://doi.org/10.5194/acp-22-14283-2022)
1208 [2022](https://doi.org/10.5194/acp-22-14283-2022), 2022.

1209 Mahieu, E., Chipperfield, M. P., Notholt, J., Reddman, T., Anderson, J., Bernath, P. F., Blumenstock, T., Coffey, M.
1210 T., Dhomse, S. S., Feng, W., Franco, B., Froidevaux, L., Griffith, D. W. T., Hannigan, J. W., Hase, F., Hossaini, R.,
1211 Jones, N. B., Morino, I., Murata, I., Nakajima, H., Palm, M., Paton-Walsh, C., Russell, J. M., Schneider, M., Servais, C.,
1212 Smale, D. and Walker, K. A. (2014). Recent Northern Hemisphere stratospheric HCl increase due to atmospheric
1213 circulation changes. *Nature*, **515**(7525), 104–107. doi:10.1038/nature13857.

1214 Mahieu, E., Fischer, E. V., Franco, B., Palm, M., Wizenberg, T., Smale, D., Clarisse, L., Clerbaux, C., Coheur, P.-F.,
1215 Hannigan, J. W., Lutsch, E., Notholt, J., Cantos, I. P., Prignon, M., Servais, C., and Strong, K. (2021). First retrievals of
1216 peroxyacetyl nitrate (PAN) from ground-based FTIR solar spectra recorded at remote sites, comparison with model and
1217 satellite data. *Elementa: Science of the Anthropocene*, **9**(1), 00027.

1218 Manney, G. L., Livesey, N. J., Santee, M. L., Froidevaux, L., Lambert, A., & Lawrence, Z. D., et al. (2020). Record-low
1219 Arctic stratospheric ozone in 2020: MLS observations of chemical processes and comparisons with previous extreme
1220 winters. *Geophysical Research Letters*, **47**, e2020GL089063. <https://doi.org/10.1029/2020GL089063>

1221 McKenzie, R., Liley, B., Kotkamp, M., Geddes, A., Querel, R., Stierle, S., & Madronich, S. (2022). Relationship between
1222 ozone and biologically relevant UV at 4 NDACC sites. *Photochemical & Photobiological Sciences*, **21**(12), 2095-2114.

1223 McKenzie, R.L., Lucas, R.M. (2018). Reassessing Impacts of Extended Daily Exposure to Low Level Solar UV
1224 Radiation. *Sci Rep* **8**, 13805.

1225 Mettig, N., Weber, M., Rozanov, A., Arosio, C., Burrows, J. P., Veefkind, P., Thompson, A. M., Querel, R., Leblanc,
1226 T., Godin-Beekmann, S., Kivi, R., and Tully, M. B.: Ozone profile retrieval from nadir TROPOMI measurements in the
1227 UV range, *Atmos. Meas. Tech.*, **14**, 6057–6082, <https://doi.org/10.5194/amt-14-6057-2021>, 2021.

1228 Mettig, N., Weber, M., Rozanov, A., Burrows, J. P., Veefkind, P., Thompson, A. M., Stauffer, R. M., Leblanc, T.,
1229 Ancellet, G., Newchurch, M. J., Kuang, S., Kivi, R., Tully, M. B., Van Malderen, R., Piders, A., Kois, B., Stübi, R., and
1230 Skrivankova, P.: Combined UV and IR ozone profile retrieval from TROPOMI and CrIS measurements, *Atmos. Meas.*
1231 *Tech.*, **15**, 2955–2978, <https://doi.org/10.5194/amt-15-2955-2022>, 2022.

1232 Millán, L., Hoor, P., Hegglin, M. I., Manney, G. L., Jeffery, P. S., Weyland, F. M., et al. (2025). Ozone trends in the
1233 upper troposphere-lower stratosphere using equivalent latitude-potential temperature coordinates. *Geophysical Research*
1234 *Letters*, **52**, e2025GL118651. <https://doi.org/10.1029/2025GL118651>

1235 Millán, L. F., Santee, M. L., Lambert, A., Livesey, N. J., Werner, F., Schwartz, M. J., Pumphrey, H. C., Manney, G. L.,
1236 Wang, Y., Su, H., Wu, L., Read, W. G., and Froidevaux, L. (2022). The Hunga-Tonga Ha'apai hydration of the
1237 stratosphere. *Geophys. Res. Lett.*, **49**, e2022GL099381. <https://doi.org/10.1029/2022GL099381>.

1238 Millán, L. F., Manney, G. L., Boenisch, H., Hegglin, M. I., Hoor, P., Kunkel, D., Leblanc, T., Petropavlovskikh, I.,
1239 Walker, K., Wargan, K., and Zahn, A. (2023). Multi-parameter dynamical diagnostics for upper tropospheric and lower
1240 stratospheric studies. *Atmos. Meas. Tech.*, **16**, 2957–2988. <https://doi.org/10.5194/amt-16-2957-2023>.

1241 Minganti, D., Chabrilat, S., Errera, Q., Prignon, M., Schneider, M., Smale, D., Jones, N. and Mahieu, E. (2022).
1242 Evaluation of the N2O Rate of Change to Understand the Stratospheric Brewer-Dobson Circulation in a Chemistry-
1243 Climate Model. *J. Geophys. Res. Atmos.*, **127**, 1–22. doi:10.1029/2021JD036390.

1244 Molod, A., Takacs, L., Suarez, M., and Bacmeister, J. (2015). Development of the GEOS-5 atmospheric general
1245 circulation model: Evolution from MERRA to MERRA2. *Geoscientific Model Development*, **8**, 1339–1356.
1246 <https://doi.org/10.5194/gmd-8-1339-2015>.

1247 Montzka, S.A., Dutton, G.S., Yu, P. et al. An unexpected and persistent increase in global emissions of ozone-depleting
1248 CFC-11. *Nature* **557**, 413–417 (2018). <https://doi.org/10.1038/s41586-018-0106-2>

1249 Müller, J.-F., Stavrakou, T., Oomen, G.-M., Opacka, B., De Smedt, I., Guenther, A., Vigouroux, C., Langerock, B.,
1250 Aquino, C. A. B., Grutter, M., Hannigan, J., Hase, F., Kivi, R., Lutsch, E., Mahieu, E., Makarova, M., Metzger, J.-M.,
1251 Morino, I., Murata, I., Nagahama, T., Notholt, J., Ortega, I., Palm, M., Röhling, A., Stremme, W., Strong, K., Sussmann,
1252 R., Té, Y., and Fried, A. (2024). Bias correction of OMI HCHO columns based on FTIR and aircraft measurements and
1253 impact on top-down emission estimates. *Atmos. Chem. Phys.*, **24**, 2207–2237. <https://doi.org/10.5194/acp-24-2207-2024>.

1254 Navas-Guzmán, F., Kämpfer, N., Schranz, F., Steinbrecht, W., and Haefele, A.: Intercomparison of stratospheric
1255 temperature profiles from a ground-based microwave radiometer with other techniques, *Atmos. Chem. Phys.*, **17**, 14085–
1256 14104, <https://doi.org/10.5194/acp-17-14085-2017>, 2017.

1257 Nedoluha, G. E., Gomez, R. M., Boyd, I., Neal, H., Allen, D. R., and Lambert, A. (2024). The spread of the Hunga Tonga
1258 H₂O plume in the middle atmosphere over the first two years since eruption. *Journal of Geophysical Research:*
1259 *Atmospheres*, **129**(11):e2024JD040907.

1260 Nedoluha, G. E., Gomez, R. M., Boyd, I., Neal, H., Allen, D. R., Lambert, A., and Livesey, N. J. (2023). Mesospheric
1261 Water Vapor in 2022. *Journal of Geophysical Research: Atmospheres*, **128**(18):e2023JD039196.

- 1262 Nedoluha, G. E., Gomez, R. M., Boyd, I., Neal, H., Allen, D. R., Lambert, A., and Livesey, N. J. (2023). Measurements
1263 of Stratospheric Water Vapor at Mauna Loa and the Effect of the Hunga Tonga Eruption. *Journal of Geophysical*
1264 *Research: Atmospheres*, **128**(8):e2022JD038100.
- 1265 Nedoluha, G. E., Kiefer, M., Lossow, S., Gomez, R. M., Kämpfer, N., Lainer, M., Forkman, P., Christensen, O. M., Oh,
1266 J. J., Hartogh, P., Anderson, J., Bramstedt, K., Dinelli, B. M., Garcia-Comas, M., Hervig, M., Murtagh, D., Raspollini,
1267 P., Read, W. G., Rosenlof, K., Stiller, G. P., and Walker, K. A. (2017). The Sparc water vapor assessment ii:
1268 intercomparison of satellite and ground-based microwave measurements. *Atmospheric Chemistry and Physics*,
1269 **17**(23):14543–14558.
- 1270 Nielsen, J. E., Pawson, S., Molod, A., Auer, B., da Silva, A. M., Douglass, A. R., et al. (2017). Chemical mechanisms
1271 and their applications in the Goddard Earth Observing System (GEOS) earth system model. *Journal of Advances in*
1272 *Modeling Earth Systems*, **9**, 3019–3044. <https://doi.org/10.1002/2017MS001011>.
- 1273 Oomen, G.-M., Müller, J.-F., Stavrou, T., De Smedt, I., Blumenstock, T., Kivi, R., Makarova, M., Palm, M., Röhling,
1274 A., Té, Y., Vigouroux, C., Friedrich, M. M., Frieß, U., Hendrick, F., Merlaud, A., Piters, A., Richter, A., Van Roozendael,
1275 M., and Wagner, T. (2024). Weekly derived top-down volatile-organic-compound fluxes over Europe from TROPOMI
1276 HCHO data from 2018 to 2021. *Atmos. Chem. Phys.*, **24**, 449–474. <https://doi.org/10.5194/acp-24-449-2024>.
- 1277 Orbe, C., Oman, L. D., Strahan, S. E., Waugh, D. W., Pawson, S., Takacs, L. L., & Molod, A. M. (2017). Large-scale
1278 atmospheric transport in GEOS replay simulations. *Journal of Advances in Modeling Earth Systems*, **9**, 2545–2560.
1279 <https://doi.org/10.1002/2017MS001053>.
- 1280 Orbe, C., Plummer, D. A., Waugh, D. W., Yang, H., Jöckel, P., Kinnison, D. E., Josse, B., Marecal, V., Deushi, M.,
1281 Abraham, N. L., Archibald, A. T., Chipperfield, M. P., Dhomse, S., Feng, W., and Bekki, S.: Description and Evaluation
1282 of the specified-dynamics experiment in the Chemistry-Climate Model Initiative, *Atmos. Chem. Phys.*, **20**, 3809–3840,
1283 <https://doi.org/10.5194/acp-20-3809-2020>, 2020.
- 1284 Orphal, J., Staehelin, J., Tamminen, J., Braathen, G., De Backer, M.-R., Bais, A., Balis, D., Barbe, A., Bhartia, P. K.,
1285 Birk, M., Burkholder, J. B., Chance, K., von Clarmann, T., Cox, A., Degenstein, D., Evans, R., Flaud, J.-M., Flittner, D.,
1286 Godin-Beekmann, S., Gorschelev, V., Gratien, A., Hare, E., Janssen, C., Kyrölä, E., McElroy, T., McPeters, R., Pastel,
1287 M., Petersen, M., Petropavlovskikh, I., Picquet-Varrault, B., Pitts, M., Labow, G., Rotger-Languereau, M., Leblanc, T.,
1288 Lerot, C., Liu, X., Moussay, P., Redondas, A., Van Roozendael, M., Sander, S. P., Schneider, M., Serdyuchenko, A.,
1289 Veefkind, P., Viallon, J., Viatte, C., Wagner, G., Weber, M., Wielgosz, R. I., and Zehner, C. (2016). Absorption cross-
1290 sections of ozone in the ultraviolet and visible spectral regions: Status report 2015. *J. Mol. Spectrosc.*, **327**, 105–121.
1291 <https://doi.org/10.1016/j.jms.2016.07.007>.
- 1292 Pan, L. L. (Corresponding author) ; Atlas, E. L. ; Honomichl, S. B. ; Smith, W. P. ; Kinnison, D. E. ; Solomon, S. ;
1293 Santee, M. L. ; Saiz-Lopez, A. ; Laube, J. C. ; Wang, B. ; Ueyama, R. ; Bresch, J. F. ; Hornbrook, R. S. ; Apel, E. C. ;
1294 Hills, A. J. ; Treadaway, V. ; Smith, K. ; Schauffler, S. ; Donnelly, S. ; Hendershot, R. ; Lueb, R. ; Campos, T. ; Viciani,
1295 S. ; D’Amato, F. ; Bianchini, G. ; Barucci, M. ; Podolske, J. R. ; Iraci, L. T. ; Gurganus, C. ; Bui, P. ; Dean-Day, J. M. ;
1296 Millán, L. ; Ryoo, J.-M. ; Barletta, B. ; Koo, J.-H. ; Kim, J. ; Liang, Q. ; Randel, W. J. ; Thornberry, T. ; Newman, P. A.
1297 (2022): East Asian summer monsoon delivers large abundances of very short-lived organic chlorine substances to the
1298 lower stratosphere, *P. Natl. Acad. Sci.*, **119**(25), e2117325119, 2022.
- 1299 Pardo Cantos, I., Mahieu, E., Chipperfield, M. P., Smale, D., Hannigan, J. W., Friedrich, M., Fraser, P., Krummel, P.,
1300 Prignon, M., Makkor, J., Servais, C. and Robinson, J. (2022). Determination and analysis of time series of CFC-11
1301 (CCl₃F) from FTIR solar spectra, in situ observations, and model data in the past 20 years above Jungfraujoch (46°N),
1302 Lauder (45°S), and Cape Grim (40°S) stations. *Environ. Sci. Atmos.*, doi:10.1039/D2EA00060A.
- 1303 Pardo Cantos, I., Mahieu, E., Chipperfield, M.P., Servais, C., Reimann, S., Vollmer, M.K. (2024). First HFC-134a
1304 retrievals from ground-based FTIR solar absorption spectra, comparison with TOMCAT model simulations, in-situ
1305 AGAGE observations, and ACE-FTS satellite data for the Jungfraujoch station. *Journal of Quantitative Spectroscopy*
1306 *and Radiative Transfer*, **318**, 108938. <https://doi.org/10.1016/j.jqsrt.2024.108938>.
- 1307 Pazmiño, A., Goutail, F., Godin-Beekmann, S., Hauchecorne, A., Pommereau, J.-P., Chipperfield, M. P., Feng, W.,
1308 Lefèvre, F., Lecouffe, A., Van Roozendael, M., Jepsen, N., Hansen, G., Kivi, R., Strong, K., and Walker, K. A.: Trends
1309 in polar ozone loss since 1989: potential sign of recovery in the Arctic ozone column, *Atmos. Chem. Phys.*, **23**, 15655–
1310 15670, <https://doi.org/10.5194/acp-23-15655-2023>, 2023.
- 1311 Peterson, D. A., and Coauthors, 2022: Measurements from inside a Thunderstorm Driven by Wildfire: The 2019 FIREX-
1312 AQ Field Experiment. *Bull. Amer. Meteor. Soc.*, **103**, E2140–E2167, <https://doi.org/10.1175/BAMS-D-21-0049.1>.

1313 Petropavlovskikh, I., Wild, J. D., Abromitis, K., Effertz, P., Miyagawa, K., Flynn, L. E., Maillard Barras, E., Damadeo,
1314 R., McConville, G., Johnson, B., Cullis, P., Godin-Beekmann, S., Ancellet, G., Querel, R., Van Malderen, R., and
1315 Zawada, D.: Ozone trends in homogenized Umkehr, ozonesonde, and COH overpass records, *Atmos. Chem. Phys.*, 25,
1316 2895–2936, <https://doi.org/10.5194/acp-25-2895-2025>, 2025.

1317 Ortega, I., J. W Hannigan, D. Edwards, et al. Evaluating TEMPO formaldehyde retrievals with co-located ground-based
1318 FTIR and Pandora observations. *ESS Open Archive* . February 06, 2026, DOI: 10.22541/essoar.177038422.25114803/v1

1319 Pinardi, G., Van Roozendael, M., Hendrick, F., Richter, A., Valks, P., Alwarda, R., Bogner, K., Frieß, U., Granville, J.,
1320 Gu, M., Johnston, P., Prados-Roman, C., Querel, R., Strong, K., Wagner, T., Wittrock, F., and Yela Gonzalez, M.:
1321 Ground-based validation of the MetOp-A and MetOp-B GOME-2 OCIO measurements, *Atmos. Meas. Tech.*, 15, 3439–
1322 3463, <https://doi.org/10.5194/amt-15-3439-2022>, 2022.

1323 Pinardi, G., Friedrich, M. M., Vigouroux, C., Langerock, B., De Smedt, I., Fayt, C., Hermans, C., Beirle, S., Wagner, T.,
1324 Zhou, M., Wang, T., Wang, P., De Mazière, M., and Van Roozendael, M.: Intercomparison of MAX-DOAS, FTIR and
1325 direct sun HCHO vertical columns at Xianghe, China, *EGUsphere* [preprint], [https://doi.org/10.5194/egusphere-2025-](https://doi.org/10.5194/egusphere-2025-3320)
1326 3320, 2025.

1327 Ploeger, F., Diallo, M., Charlesworth, E., Konopka, P., Legras, B., Laube, J. C., Groöß, J.-U., Günther, G., Engel, A.,
1328 and Riese, M.: The stratospheric Brewer–Dobson circulation inferred from age of air in the ERA5 reanalysis, *Atmos.*
1329 *Chem. Phys.*, 21, 8393–8412, <https://doi.org/10.5194/acp-21-8393-2021>, 2021.

1330 Polyakov, A., Poberovsky, A., Makarova, M., Virolainen, Y., Timofeyev, Y., and Nikulina, A. (2021). Measurements of
1331 CFC-11, CFC-12, and HCFC-22 total columns in the atmosphere at the St. Petersburg site in 2009–2019. *Atmospheric*
1332 *Measurement Techniques*, 14(8):5349–5368.

1333 Pommrich, R., Müller, R., Groöß, J.-U., Konopka, P., Ploeger, F., Vogel, B., Tao, M., Hoppe, C. M., Günther, G.,
1334 Spelten, N., Hoffmann, L., Pumphrey, H.-C., Viciani, S., D’Amato, F., Volk, C. M., Hoor, P., Schlager, H., and Riese,
1335 M.: Tropical troposphere to stratosphere transport of carbon monoxide and long-lived trace species in the Chemical
1336 Lagrangian Model of the Stratosphere (CLaMS), *Geosci. Model Dev.*, 7, 2895–2916,
1337 <https://doi.org/10.5194/gmd-7-2895-2014>, 2014.

1338 Prignon, M., Chabrillat, S., Friedrich, M., Smale, D., Strahan, S. E., Bernath, P. F., Chipperfield, M. P., Dhomse, S. S.,
1339 Feng, W., Minganti, D., Servais, C. and Mahieu, E. (2021). Stratospheric fluorine as a tracer of circulation changes:
1340 comparison between infrared remote-sensing observations and simulations with five modern reanalyses. *J. Geophys.*
1341 *Res. Atmos.*, doi:10.1029/2021JD034995.

1342 Ratynski, M., Khaykin, S., Hauchecorne, A., Wing, R., Cammas, J.-P., Hello, Y., and Keckhut, P. (2023). Validation of
1343 Aeolus wind profiles using ground-based lidar and radiosonde observations at Réunion island and the Observatoire de
1344 Haute-Provence. *Atmos. Meas. Tech.*, 16, 997–1016. <https://doi.org/10.5194/amt-16-997-2023>.

1345 Read, W. G., Stiller, G., Lossow, S., Kiefer, M., Khosrawi, F., Hurst, D., Vömel, H., Rosenlof, K., Dinelli, B. M.,
1346 Raspollini, P., Nedoluha, G. E., Gille, J. C., Kasai, Y., Eriksson, P., Sioris, C. E., Walker, K. A., Weigel, K., Burrows,
1347 J. P., and Rozanov, A.: The SPARC Water Vapor Assessment II: assessment of satellite measurements of upper
1348 tropospheric humidity, *Atmos. Meas. Tech.*, 15, 3377–3400, <https://doi.org/10.5194/amt-15-3377-2022>, 2022.

1349 Redondas, A. et al (2024), WMO (World Meteorological Organization) (2024): Eighteenth Intercomparison Campaign
1350 of the Regional Brewer Calibration Centre Europe, El Arenosillo Atmospheric Sounding Station, Huelva, Spain, 4–15
1351 September 2023, GAW Report No. 302, 81 pp., WMO, Geneva, <https://doi.org/10.31978/666-20-018-3>

1352 Rennie, M.P., Isaksen, L., Weiler, F., de Kloe, J., Kanitz, T. & Reitebuch, O. (2021). The impact of Aeolus wind retrievals
1353 on ECMWF global weather forecasts. *Q J R Meteorol Soc*, 147(740), 3555–3586. <https://doi.org/10.1002/qj.4142>.

1354 Salawitch, R. J., J. B. Smith, H. B. Selkirk, K. Wargan, M. Chipperfield, R. Hossaini, P. Levelt, N. Livesey, L. McBride,
1355 L. Millán, E. Moyer, M. Santee, M. R. Schoeberl, S. Solomon, K. Stone and H. Worden (2025). The Imminent Data
1356 Desert: The future of stratospheric monitoring in a rapidly changing world. *Bull. Amer. Meteor. Soc.*
1357 <https://doi.org/10.1175/BAMS-D-23-0281.1>.

1358 Santee, M. L., Lambert, A., Manney, G. L., Livesey, N. J., Froidevaux, L., Neu, J. L., et al. (2022). Prolonged and
1359 pervasive perturbations in the composition of the Southern Hemisphere midlatitude lower stratosphere from the
1360 Australian New Year's fires. *Geophysical Research Letters*, 49, e2021GL096270.
1361 <https://doi.org/10.1029/2021GL096270>.

1362 Sauvageat, E., Maillard Barras, E., Hocke, K., Haeferle, A., and Murk, A.: Harmonized retrieval of middle atmospheric
1363 ozone from two microwave radiometers in Switzerland, *Atmos. Meas. Tech.*, **15**, 6395–6417,
1364 <https://doi.org/10.5194/amt-15-6395-2022>, 2022.

1365 Serdyuchenko, A., Gorshchev, V., Weber, M., Chehade, W., and Burrows, J. P. (2014). High spectral resolution ozone
1366 absorption cross-sections – Part 2: Temperature dependence. *Atmos. Meas. Tech.*, **7**, 625–636.
1367 <https://doi.org/10.5194/amt-7-625-2014> (data available at: [https://www.iup.uni-](https://www.iup.uni-bremen.de/gruppen/molspec/databases/referencespectra/o3spectra2011/index.html)
1368 [bremen.de/gruppen/molspec/databases/referencespectra/o3spectra2011/index.html](https://www.iup.uni-bremen.de/gruppen/molspec/databases/referencespectra/o3spectra2011/index.html)), last access: 11 April 2024).

1369 Sha, M. K., De Mazière, M., Notholt, J., Blumenstock, T., Chen, H., Dehn, A., Griffith, D. W. T., Hase, F., Heikkinen,
1370 P., Hermans, C., Hoffmann, A., Huebner, M., Jones, N., Kivi, R., Langerock, B., Petri, C., Scolas, F., Tu, Q., and
1371 Weidmann, D. (2020). Intercomparison of low- and high-resolution infrared spectrometers for ground-based solar remote
1372 sensing measurements of total column concentrations of CO₂, CH₄, and CO. *Atmos. Meas. Tech.*, **13**, 4791–4839.
1373 <https://doi.org/10.5194/amt-13-4791-2020>.

1374 Shi, G., Krochin, W., Sauvageat, E., and Stober, G.: Ozone and water vapor variability in the polar middle atmosphere
1375 observed with ground-based microwave radiometers, *Atmos. Chem. Phys.*, **23**, 9137–9159, [https://doi.org/10.5194/acp-](https://doi.org/10.5194/acp-23-9137-2023)
1376 [23-9137-2023](https://doi.org/10.5194/acp-23-9137-2023), 2023

1377 Smit, H. G. J., Poyraz, D., Van Malderen, R., Thompson, A. M., Tarasick, D. W., Stauffer, R. M., Johnson, B. J., and
1378 Kollonige, D. E. (2024). New insights from the Jülich Ozone Sonde Intercomparison Experiment: calibration functions
1379 traceable to one ozone reference instrument. *Atmos. Meas. Tech.*, **17**, 73–112. <https://doi.org/10.5194/amt-17-73-2024>.

1380 Smit, H.G.J., Thompson, A. M., and ASOPOS panel. (2021): Ozonesonde Measurement Principles and Best Operational
1381 Practices, ASOPOS (Assessment of Standard Operating Procedures for Ozonesondes) 2.0, WMO Global Atmosphere
1382 Watch report series, No. 268, World Meteorological Organization, Geneva.
1383 [https://library.wmo.int/index.php?lvl=notice](https://library.wmo.int/index.php?lvl=notice_display&id=21986#.YaFNSbpOlc8) display&id=21986#.YaFNSbpOlc8.

1384 Solomon, S., K. Dube, K. Stone, D. Degenstein (2022). On the stratospheric chemistry of midlatitude wildfire smoke.
1385 *Pro. Nat. Acad. Sci.*, **119**, e2117325119. <https://doi.org/10.1073/pnas.2117325119>.

1386 Solomon, S., Stone, K., Yu, P. et al. (2023). Chlorine activation and enhanced ozone depletion induced by wildfire
1387 aerosol. *Nature* **615**, 259–264. <https://doi.org/10.1038/s41586-022-05683-0>.

1388 Souri, A. H., Johnson, M. S., Wolfe, G. M., Crawford, J. H., Fried, A., Wisthaler, A., Brune, W. H., Blake, D. R.,
1389 Weinheimer, A. J., Verhoelst, T., Comperolle, S., Pinardi, G., Vigouroux, C., Langerock, B., Choi, S., Lamsal, L., Zhu,
1390 L., Sun, S., Cohen, R. C., Min, K.-E., Cho, C., Philip, S., Liu, X., and Chance, K. (2023). Characterization of Errors in
1391 Satellite-based HCHO / NO₂ Tropospheric Column Ratios with Respect to Chemistry, Column to PBL Translation,
1392 Spatial Representation, and Retrieval Uncertainties. *Atmos. Chem. Phys.*, **23**, 1963–1986. [https://doi.org/10.5194/acp-](https://doi.org/10.5194/acp-23-1963-2023)
1393 [23-1963-2023](https://doi.org/10.5194/acp-23-1963-2023).

1394 SPARC Report on the Mystery of Carbon Tetrachloride. Q. Liang, P.A. Newman, S. Reimann (Eds.). (2016). SPARC
1395 Report No. 7, WCRP-13/2016. doi: 10.3929/ethz-a-010690647.

1396 Stauffer, R. M., Thompson, A. M., Kollonige, D. E., Witte, J. C., Tarasick, D. W., Davies, J. M., Vömel, H., Morris,
1397 GA, Van Malderen, R., Johnson, B. J., Querel, R. R., Selkirk, H. B., Stübi, R., and Smit, HGJ: A post-2013 drop-off in
1398 total ozone at third of global ozonesonde stations: ECC Instrument Artifacts?, *Geophys. Res. Lett.*, doi:
1399 [10.1029/2019/GL086791](https://doi.org/10.1029/2019/GL086791), 2020.

1400 Stauffer, R. M., Thompson, A. M., Kollonige, D. E., Tarasick, D. W., Van Malderen, R., Smit, H. G. J., et al. (2022). An
1401 examination of the recent stability of ozonesonde global network data. *Earth and Space Science*, **9**, e2022EA002459.
1402 <https://doi.org/10.1029/2022EA002459>.

1403 Stenke, A., Grewe, V. & Ponater, M. (2007). Lagrangian transport of water vapor and cloud water in the ECHAM4 GCM
1404 and its impact on the cold bias. *Clim. Dyn.* **31**, 491–506.

1405 Strahan, S. E., A. R. Douglass, and P. A. Newman (2013). The contributions of chemistry and transport to low arctic
1406 ozone in March 2011 derived from Aura MLS observations. *J. Geophys. Res. Atmos.*, **118**, 1563–1576.
1407 doi:10.1002/jgrd.50181.

1408 Strahan, S. E., Smale, D., Douglass, A. R., Blumenstock, T., Hannigan, J. W., Hase, F., et al. (2020). Observed
1409 hemispheric asymmetry in stratospheric transport trends from 1994 to 2018. *Geophysical Research Letters*, **47**,
1410 e2020GL088567. <https://doi.org/10.1029/2020GL088567>

- 1411 Strahan, S. E., Smale, D., Solomon, S., Taha, G., Damon, M. R., Steenrod, S. D., et al. (2022). Unexpected repartitioning
1412 of stratospheric inorganic chlorine after the 2020 Australian wildfires. *Geophysical Research Letters*, **49**,
1413 e2022GL098290. <https://doi.org/10.1029/2022GL098290>.
- 1414 Takeda, M., Nakajima, H., Murata, I., Nagahama, T., Morino, I., Toon, G. C., Weiss, R. F., Mühle, J., Krummel, P. B.,
1415 Fraser, P. J., and Wang, H.-J.: First ground-based Fourier transform infrared (FTIR) spectrometer observations of HFC-
1416 23 at Rikubetsu, Japan, and Syowa Station, Antarctica, *Atmos. Meas. Tech.*, **14**, 5955–5976, <https://doi.org/10.5194/amt-14-5955-2021>, 2021.
- 1418 Tarasick, D., I.E. Galbally, et al. (2019). Tropospheric Ozone Assessment Report: Tropospheric ozone from 1877 to
1419 2016, observed levels, trends and uncertainties. *Elem. Sci. Anth.*, **7**:39. doi: <https://doi.org/10.1525/elementa.376>.
- 1420 Thompson, A.M., Smit, H. G. J., Witte, J. C., Stauffer, R. M. et al: Ozonesonde Quality Assurance: The JOSIE-SHADOZ
1421 (2017) Experience, *Bull. Am. Meteor. Society*, doi.org/10.1175/BAMS-D-17-0311.1, 2019
- 1422 Thompson, A. M., Stauffer, R. M., Kollonige, D. E., Ziemke, J. R., Johnson, B. J., Morris, G. A., Cullis P., Cazorla, M.,
1423 Diaz, J. A., Piters, A., Nedeljkovic, I., Warsidikromo, T., Silva, F. R., Northam, E. T., Benjamin, P., Mkololo, T.,
1424 Machinini, T., Félix, C., Romanens, G., Nyadida, S., Brioude, J., Evan, S., Metzger, J.-M., Dindang, A., Mahat, Y. B.,
1425 Sammathuria, M. K., Zakaria, N. B., Komala, N., Ogino, S.-Y., Quyen, N. T., Mani, F. S., Vuiyasawa, M., Nardini, D.,
1426 Martinsen, M., Kuniyuki, D. T., Müller, K., Wolff, P., Sauvage, B.: Tropical tropospheric ozone trends (1998 to 2023):
1427 New perspectives from SHADOZ, IAGOS and OMI/MLS observations, *Atmos. Chem. Phys.*, **25**, 18475–18507, 2025
- 1428 Trickl, T., Vogelmann, H., Fromm, M. D., Jäger, H., Perfahl, M., and Steinbrecht, W.: Measurement report: Violent
1429 biomass burning and volcanic eruptions – a new period of elevated stratospheric aerosol over central Europe (2017 to
1430 2023) in a long series of observations, *Atmos. Chem. Phys.*, **24**, 1997–2021, <https://doi.org/10.5194/acp-24-1997-2024>,
1431 2024.
- 1432 Van Malderen, R., Thompson, A. M., Kollonige, D. E., Stauffer, R. M., Smit, H. G. J., Maillard Barras, E., Vigouroux,
1433 C., Petropavlovskikh, I., Leblanc, T., Thouret, V., Wolff, P., Effertz, P., Tarasick, D. W., Poyraz, D., Ancellet, G., De
1434 Backer, M.-R., Evan, S., Flood, V., Frey, M. M., Hannigan, J. W., Hernandez, J. L., Iarlori, M., Johnson, B. J., Jones,
1435 N., Kivi, R., Mahieu, E., McConville, G., Müller, K., Nagahama, T., Notholt, J., Piters, A., Prats, N., Querel, R., Smale,
1436 D., Steinbrecht, W., Strong, K., and Sussmann, R. (2025a). Global ground-based tropospheric ozone measurements:
1437 reference data and individual site trends (2000–2022) from the TOAR-II/HEGIFTOM project. *Atmos. Chem. Phys.*, **25**,
1438 7187–7225. <https://doi.org/10.5194/acp-25-7187-2025>.
- 1439 Van Malderen, R., Zang, Z., Chang, K.-L., Björklund, R., Cooper, O. R., Liu, J., Maillard Barras, E., Vigouroux, C.,
1440 Petropavlovskikh, I., Leblanc, T., Thouret, V., Wolff, P., Effertz, P., Gaudel, A., Tarasick, D. W., Smit, H. G. J.,
1441 Thompson, A. M., Stauffer, R. M., Kollonige, D. E., Poyraz, D., Ancellet, G., De Backer, M.-R., Frey, M. M., Hannigan,
1442 J. W., Hernandez, J. L., Johnson, B. J., Jones, N., Kivi, R., Mahieu, E., Morino, I., McConville, G., Müller, K., Murata,
1443 I., Notholt, J., Piters, A., Prignon, M., Querel, R., Rizi, V., Smale, D., Steinbrecht, W., Strong, K., and Sussmann, R.
1444 (2025b). Ground-based tropospheric ozone measurements: regional tropospheric ozone column trends from the TOAR-
1445 II/HEGIFTOM homogenized datasets. *Atmos. Chem. Phys.*, **25**, 9905–9935. <https://doi.org/10.5194/acp-25-9905-2025>.
- 1446 Van Roozendaal, M.; Hendrick, F.; Friedrich, M.M.; Fayt, C.; Bais, A.; Beirle, S.; Bösch, T.; Navarro Comas, M.; Friess,
1447 U.; Karagkiozidis, D.; et al. Fiducial Reference Measurements for Air Quality Monitoring Using Ground-Based MAX-
1448 DOAS Instruments (FRM4DOAS). *Remote Sens.* **2024**, *16*, 4523. <https://doi.org/10.3390/rs16234523>
- 1449 Vandembussche, S.; Langerock, B.; Vigouroux, C.; Buschmann, M.; Deutscher, N.M.; Feist, D.G.; Garcia, O.; Hannigan,
1450 J.W.; Hase, F.; Kivi, R.; Kumps, N.; Makarova, M.; Millet, D.B.; Morino, I.; Nagahama, T.; Notholt, J.; Ohshima, H.;
1451 Ortega, I.; Petri, C.; Rettinger, M.; Schneider, M.; Servais, C.P.; Sha, M.K.; Shiomi, K.; Smale, D.; Strong, K.; Sussmann,
1452 R.; Té, Y.; Velasco, V.A.; Vrekoussis, M.; Warneke, T.; Wells, K.C.; Wunch, D.; Zhou, M.; De Mazière, M. (2022).
1453 Nitrous Oxide Profiling from Infrared Radiances (NOPIR): Algorithm Description, Application to 10 Years of IASI
1454 Observations and Quality Assessment. *Remote Sens.*, **14**, 1810. <https://doi.org/10.3390/rs14081810>.
- 1455 Verhoelst, T., Compernelle, S., Pinardi, G., Lambert, J.-C., Eskes, H. J., Eichmann, K.-U., Fjærraa, A. M., Granville, J.,
1456 Niemeijer, S., Cede, A., Tiefenbrunner, M., Hendrick, F., Pazmiño, A., Bais, A., Bazureau, A., Boersma, K. F., Bogner,
1457 K., Dehn, A., Donner, S., Elohov, A., Gebetsberger, M., Goutail, F., Grutter de la Mora, M., Gruzdev, A., Gratsea, M.,
1458 Hansen, G. H., Irie, H., Jepsen, N., Kanaya, Y., Karagkiozidis, D., Kivi, R., Kreher, K., Levelt, P. F., Liu, C., Müller,
1459 M., Navarro Comas, M., Piters, A. J. M., Pommereau, J.-P., Portafaix, T., Prados-Roman, C., Puentedura, O., Querel,
1460 R., Remmers, J., Richter, A., Rimmer, J., Rivera Cárdenas, C., Saavedra de Miguel, L., Sinyakov, V. P., Stremme, W.,
1461 Strong, K., Van Roozendaal, M., Veeffkind, J. P., Wagner, T., Wittrock, F., Yela González, M., and Zehner, C. (2021).
1462 Ground-based validation of the Copernicus Sentinel-5P TROPOMI NO₂ measurements with the NDACC ZSL-DOAS,

- 1463 MAX-DOAS and Pandonia global networks. *Atmos. Meas. Tech.*, **14**, 481–510. [https://doi.org/10.5194/amt-14-481-](https://doi.org/10.5194/amt-14-481-1464)
1464 [2021](https://doi.org/10.5194/amt-14-481-2021).
- 1465 Vigouroux, C., C. A. B. Aquino, M. Bauwens, C. Becker, T. Blumenstock, M. D. Mazière, O. García, M. Grutter, C.
1466 Guarin, J. W. Hannigan, F. Hase, N. Jones, R. Kivi, D. Koshelev, B. Langerock, E. Lutsch, M. Makarova, J.-M. Metzger,
1467 J.-F. Müller, J. Notholt, I. Ortega, M. Palm, C. Paton-Walsh, A. Poberovskii, M. Rettinger, J. Robinson, D. Smale, T.
1468 Stavrakou, W. Stremme, K. Strong, R. Sussmann, Y. T´e, and G. Toon. (2018). NDACC harmonized formaldehyde
1469 time-series from 21 FTIR stations covering a wide range of column abundances. *Atmospheric Measurement Techniques*,
1470 **11**(9):5049–5073.
- 1471 Vigouroux, C., B. Langerock, C. A. Bauer Aquino, T. Blumenstock, Z. Cheng, M. De Mazière, I. De Smedt, M. Grutter,
1472 J. W. Hannigan, N. Jones, R. Kivi, D. Loyola, E. Lutsch, E. Mahieu, M. Makarova, J.-M. Metzger, I. Morino, I. Murata,
1473 T. Nagahama, J. Notholt, I. Ortega, M. Palm, G. Pinardi, A. Röhling, D. Smale, W. Stremme, K. Strong, R. Sussmann,
1474 Y. T´e, M. van Roozendaal, P. Wang, and H. Winkler. (2020). Tropomi–sentinel-5 precursor formaldehyde validation
1475 using an extensive network of ground-based fourier-transform infrared stations. *Atmospheric Measurement Techniques*,
1476 **13**(7):3751–3767.
- 1477 Vigouroux, C., Langerock, B., and De Mazière, M. and the FTIR observation Team: Validation of all S5P ozone products
1478 (total columns, tropospheric columns and profiles) with a single reference network. EGU General Assembly 2025,
1479 Vienna, Austria, 27 Apr–2 May 2025, EGU25-20500, <https://doi.org/10.5194/egusphere-egu25-20500>, 2025.
- 1480 Vogel, B., Lauther, V., Köllner, F., Ekinci, F., Rolf, C., Strobel, J., van Luijt, R., Volk, M. C., Borrmann, S., Dragoneas,
1481 A., Eppers, O., Molleker, S., Hoor, P., Ort, L., Weyland, F., Zahn, A., Clemens, J., Günther, G., Kachula, O., Müller, R.,
1482 Ploeger, F., and Riese, M.: Continental and marine source regions contributing to the out- flow of the Asian summer
1483 monsoon anticyclone during the PHILEAS campaign in summer 2023, EGU sphere, 2025, 1–49, [https://doi.org/10.](https://doi.org/10.5194/egusphere-2025-5609)
1484 [5194/egusphere-2025-5609](https://doi.org/10.5194/egusphere-2025-5609), URL [https://egusphere.copernicus.org/](https://egusphere.copernicus.org/preprints/2025/egusphere-2025-5609/) preprints/2025/egusphere-2025-5609/, 2025
- 1485 Voglmeier, K., Velazco, V. A., Egli, L., Gröbner, J., Redondas, A., and Steinbrecht, W. (2024). The transition to new
1486 ozone absorption cross sections for Dobson and Brewer total ozone measurements. *Atmos. Meas. Tech.*, **17**, 2277–2294.
1487 <https://doi.org/10.5194/amt-17-2277-2024>.
- 1488 Vömel, H., Evan, S., and Tully, M. (2022). Water vapor injection into the stratosphere by Hunga Tonga-Hunga Ha’apai.
1489 *Science*, **377**(6613):1444–1447. doi:10.1126/science.abq2299.
- 1490 Vömel, H., Naebert, T., Dirksen, R., and Sommer, M. (2016). An update on the uncertainties of water vapor
1491 measurements using cryogenic frost point hygrometers. *Atmos. Meas. Tech.*, **9**, 3755–3768. [https://doi.org/10.5194/amt-](https://doi.org/10.5194/amt-9-3755-2016)
1492 [9-3755-2016](https://doi.org/10.5194/amt-9-3755-2016).
- 1493 Wang J, Zhou M, Langerock B, Nan W, Wang T, Wang P. (2024). Optimizing the Atmospheric CO2 Retrieval Based
1494 on the NDACC-Type FTIR Mid-Infrared Spectra at Xianghe, China. *Remote Sensing*. **16**(5):900.
1495 <https://doi.org/10.3390/rs16050900>.
- 1496 Wang, H. J. R., Damadeo, R., Flittner, D., Kramarova, N., Taha, G., Davis, S., et al. (2020). Validation of SAGE III/ISS
1497 solar occultation ozone products with correlative satellite and ground based measurements. *Journal of Geophysical*
1498 *Research: Atmospheres*, **125**, e2020JD032430. <https://doi.org/10.1029/2020JD032430>.
- 1499 Annette Wagner, Y. Bennouna, A.-M. Blechschmidt, G. Brasseur, S. Chabrillat, Y. Christophe, Q. Errera, H. Eskes, J.
1500 Flemming, K. M. Hansen, A. Inness, J. Kapsomenakis, B. Langerock, A. Richter, N. Sudarchikova, V. Thouret, C.
1501 Zerefos; Comprehensive evaluation of the Copernicus Atmosphere Monitoring Service (CAMS) reanalysis against
1502 independent observations: Reactive gases. *Elementa: Science of the Anthropocene* 21 January 2021; **9** (1): 00171. doi:
1503 <https://doi.org/10.1525/elementa.2020.00171>
- 1504 Weber, M., Gorshchev, V., and Serdyuchenko, A. (2016). Uncertainty budgets of major ozone absorption cross sections
1505 used in UV remote sensing applications. *Atmos. Meas. Tech.*, **9**, 4459–4470. <https://doi.org/10.5194/amt-9-4459-2016>
1506 (data available at: <https://www.iup.uni-bremen.de/UVSAT/data/xsectionuncertainty/>, last access: 11 April 2024).
- 1507 Wells, K. C., Millet, D. B., Payne, V. H., Vigouroux, C., Aquino, C. A. B., De Mazière, M., et al. (2022). Next-generation
1508 isoprene measurements from space: Detecting daily variability at high resolution. *Journal of Geophysical Research:*
1509 *Atmospheres*, **127**, e2021JD036181. <https://doi.org/10.1029/2021JD036181>.
- 1510 Wells, K., Millet, D., Brewer, J., Payne, V., Cady-Pereira, K., Pernak, R., Kulawick, S., Vigouroux, C., Jones, N.,
1511 Mahieu, E., Makarova, M., Nagahama, T., Ortega, I., Palm, M., Strong, K., Schneider, M., Smale, D., Sussmann, R., and

1512 Zhou, M. (2024). Long-term global measurements of methanol, ethene, ethyne, and HCN from the Cross-track Infrared
1513 Sounder. *EGUsphere* [preprint]. <https://doi.org/10.5194/egusphere-2024-1551>.

1514 Wizenberg, T., Strong, K., Jones, D., Lutsch, E., Mahieu, E., Franco, B., & Clarisse, L. (2022). Replication data for:
1515 Exceptional wildfire enhancements of PAN, C₂H₄, CH₃OH, and HCOOH over the Canadian high Arctic during August
1516 2017 [Dataset]. Borealis. <https://doi.org/10.5683/SP3/6PBAHK>

1517 Wizenberg, T., Strong, K., Jones, D. B. A., Lutsch, E., Mahieu, E., Franco, B., & Clarisse, L. (2023). Exceptional wildfire
1518 enhancements of PAN, C₂H₄, CH₃OH, and HCOOH over the Canadian high Arctic during August 2017. *Journal of*
1519 *Geophysical Research: Atmospheres*, **128**, e2022JD038052. <https://doi.org/10.1029/2022JD038052>.

1520 WMO (World Meteorological Organization). (2014). **Scientific Assessment of Ozone Depletion: 2014**. Global Ozone
1521 Research and Monitoring Project-Report No. 55, 416 pp., Geneva, Switzerland.
1522 <https://www.csl.noaa.gov/assessments/ozone/2014/>.

1523 WMO (World Meteorological Organization). (2022). **Scientific Assessment of Ozone Depletion: 2022**. GAW Report
1524 No. 278, 509 pp., WMO, Geneva, Switzerland. [https://www.unep.org/resources/publication/scientific-assessment-](https://www.unep.org/resources/publication/scientific-assessment-ozone-layer-depletion-2022)
1525 [ozone-layer-depletion-2022](https://www.unep.org/resources/publication/scientific-assessment-ozone-layer-depletion-2022).

1526 Yamanouchi, S., Viatte, C., Strong, K., Lutsch, E., Jones, D. B. A., Clerbaux, C., Van Damme, M., Clarisse, L., and
1527 Coheur, P.-F.: Multiscale observations of NH₃ around Toronto, Canada, *Atmos. Meas. Tech.*, **14**, 905–921,
1528 <https://doi.org/10.5194/amt-14-905-2021>, 2021.

1529 Zhao, X., Fioletov, V., Redondas, A., Gröbner, J., Egli, L., Zeilinger, F., López-Solano, J., Arroyo, A. B., Kerr, J.,
1530 Maillard Barras, E., Smit, H., Brohart, M., Sit, R., Ogyu, A., Abboud, I., and Lee, S. C. (2023). The site-specific primary
1531 calibration conditions for the Brewer spectrophotometer. *Atmos. Meas. Tech.*, **16**, 2273–2295.
1532 <https://doi.org/10.5194/amt-16-2273-2023>.

1533 Zhou, M., Langerock, B., Vigouroux, C., Sha, M. K., Ramonet, M., Delmotte, M., Mahieu, E., Bader, W., Hermans, C.,
1534 Kumps, N., Metzger, J.-M., Dufлот, V., Wang, Z., Palm, M., and De Mazière, M.: Atmospheric CO and CH₄ time series
1535 and seasonal variations on Reunion Island from ground-based in situ and FTIR (NDACC and TCCON) measurements,
1536 *Atmos. Chem. Phys.*, **18**, 13881–13901, <https://doi.org/10.5194/acp-18-13881-2018>, 2018.

1537 Zhou, M., Langerock, B., Wells, K. C., Millet, D. B., Vigouroux, C., Sha, M. K., Hermans, C., Metzger, J.-M., Kivi, R.,
1538 Heikkinen, P., Smale, D., Pollard, D. F., Jones, N., Deutscher, N. M., Blumenstock, T., Schneider, M., Palm, M., Notholt,
1539 J., Hannigan, J. W., and De Mazière, M.: An intercomparison of total column-averaged nitrous oxide between ground-
1540 based FTIR TCCON and NDACC measurements at seven sites and comparisons with the GEOS-Chem model, *Atmos.*
1541 *Meas. Tech.*, **12**, 1393–1408, <https://doi.org/10.5194/amt-12-1393-2019>, 2019.

1542 Zhou, M., Langerock, B., Vigouroux, C., Sha, M. K., Hermans, C., Metzger, J.-M., Chen, H., Ramonet, M., Kivi, R.,
1543 Heikkinen, P., Smale, D., Pollard, D. F., Jones, N., Velazco, V. A., García, O. E., Schneider, M., Palm, M., Warneke, T.,
1544 and De Mazière, M.: TCCON and NDACC XCO measurements: difference, discussion and application, *Atmos. Meas.*
1545 *Tech.*, **12**, 5979–5995, <https://doi.org/10.5194/amt-12-5979-2019>, 2019.

1546 Zhou, M., Langerock, B., Sha, M. K., Hermans, C., Kumps, N., Kivi, R., Heikkinen, P., Petri, C., Notholt, J., Chen, H.,
1547 and De Mazière, M. (2023). Atmospheric N₂O and CH₄ total columns retrieved from low-resolution Fourier transform
1548 infrared (FTIR) spectra (Bruker VERTEX 70) in the mid-infrared region. *Atmos. Meas. Tech.*, **16**, 5593–5608.
1549 <https://doi.org/10.5194/amt-16-5593-2023>.

1550 Zhou, M., Langerock, B., Vigouroux, C., Smale, D., Toon, G., Polyakov, A., Hannigan, J. W., Mellqvist, J., Robinson,
1551 J., Notholt, K., Strong, E., Mahieu, M., Palm, M., Prignon, N., Jones, O., Garc'ia, I., Morino, I., Murata, I., Ortega, T.,
1552 Nagahama, T., Wizenberg, V., Flood, K., Walker, and M. De Mazi`ere. (2024). Recent decreases in the growth rate of
1553 atmospheric HCFC-22 column derived from the ground-based ftir harmonized retrievals at 16 NDACC sites.
1554 *Geophysical Research Letters*, **51**(22):e2024GL112470. <https://doi.org/10.1029/2024GL112470>.

1555 Zuber, R., Köhler, U., Egli, L., Ribnitzky, M., Steinbrecht, W., and Gröbner, J.: Total ozone column intercomparison of
1556 Brewers, Dobsons, and BTS-Solar at Hohenpeißenberg and Davos in 2019/2020, *Atmos. Meas. Tech.*, **14**, 4915–4928,
1557 <https://doi.org/10.5194/amt-14-4915-2021>, 2021.

1558 Zumkehr, A., Hilton, T. W., Whelan, M., Smith, S., Kuai, L., Worden, J., and Campbell, J. E. (2018). Global gridded
1559 anthropogenic emissions inventory of carbonyl sulfide. *Atmospheric Environment*, **183**:11